INTERNATIONAL ATOMIC ENERGY AGENCY
UNITED NATIONS EDUCATIONAL, SCIENTIFIC AND CULTURAL ORGANIZATION

INTERNATIONAL CENTRE FOR THEORETICAL PHYSICS
34100 TRIESTE (ITALY) - P.O.B. 586 - MIRAMARE - STRADA COSTIERA 11 - TELEPHONE: 2240-1
CABLE: CENTRATOM - TELEX 460392-1

H4.SMR/381-11

COLLEGE ON ATOMIC AND MOLECULAR PHYSICS: PHOTON ASSISTED COLLISIONS IN ATOMS AND MOLECULES

(30 January - 24 February 1989)

ENERGY POOLING REACTIONS

M. ALLEGRINI

Dipartimento di Fisica
Università di Pisa
Pisa

ICTP WINTER COLLEGE ON

ATOMIC AND MOLECULAR PHYSICS : PHOTON ASSISTED COLLISIONS IN ATOMS AND MOLECULES

(January 30 - February 24 / 1989)

ENERGY POOLING REACTIONS

Lecturer : M. ALLEGRINI
Dipartimento di Fisica, Universita' di Pisa
Piazza Torricelli, 2 - PISA, ITALY

INTRODUCTION

In classical spectroscopy the properties of isolated atoms are investigated through their interaction with the light, while the interactions with other particles (atoms, molecules, electrons, etc.) are the domain of classical scattering. Before the advent of the laser, excited atoms were obtained by means of spectral lamps that can not give densities of excited states high enough to allow the observation of collisions between excited reactants. Others excitation methods, like discharges or electron impact, although more efficient than spectral lamps, are not very selective. It is only with the advent of tunable laser sources that both selective excitation and high density of excited states became possible. Thus in the last two decades, thanks to the laser sources, the observation of collisions involving excited atoms became possible and we have witnessed the interplay of the two research tools of spectroscopy and scattering. The interatomic distances where inelastic collisions are efficient are generally in the range 5-30Å; at these distances the atoms are not yet bound to form a stable molecule, nevertheless they can not be considered completly free. The usual picture in this case is that the two atoms constitute a *quasi-molecule* system, well described by molecular adiabatic potentials. Obviously there are several of these potential curves connecting the entrance and the exit channels of the collision processes, with the transfer occuring at the "avoided crossing" points. The study of these interactions give complementary information to those provided by spectroscopy for free atoms and many new phenomena have been discovered. This new field of research has rapidly grown; useful references can be found in the proceedings of a series of recent workshops :

- *Photon-Assisted Collisions and Related Topics* - N.K. Rahman and C. Guidotti Eds., (Harwood Academic Publishers,1982)
- *Collisions and Half-Collisions with Lasers* - N.K. Rahman and C. Guidotti Eds., (Harwood Academic Publishers, 1984)
- *Atomic and Molecular Collisions in a Laser Field* - J.L. Picque', G. Spiess and F.J. Wuilleumier Eds., Journal de Physique Colloque C1, (Les Editions de Physique, 1985)
- *Photons and Continuum States of Atoms and Molecules* - N.K. Rahman, C. Guidotti and M. Allegrini Eds., (Springer - Verlag, 1987)

When an atomic vapor is irradiated with laser light there are several phenomena which take place simultaneously. Here we are interested in experiments performed with resonant radiation, i.e. with lasers tuned to a specific atomic transition, while all phenomena induced by irradiation with lasers not in resonance with any particular transition are outside the topics considered in these lectures. Generally speaking this second class of experiments requires laser intensities which exceed 10^4 Wcm^{-2} and are usually obtained by pulsed lasers. Resonant excitation, on the contrary, gives interesting phenomena also with cw lasers of low power density, even a few mWatts per cm^2.

In these lectures a few of the many collision processes involving laser excited reactants are presented, namely the inelastic collisions between two atoms, both excited to the first resonant level. Most of the experiments have been performed in alkali vapors because of their simple atomic structure (only one external electron), for which the first excited state is of the type nP_j, however interesting results have been obtained also in atoms with two external electrons (like Barium or Strontium). So far three exit channels have been identified for inelastic collisions between two alkali atoms excited to the first P-level, namely :

1.	energy transfer	$A^* + A^* \longrightarrow A^{**} + A$
2.	excited molecule formation	$A^* + A^* \longrightarrow A_2^{**}$
3.	associative ionization	$A^* + A^* \longrightarrow A_2^+ + e$

In process (1) the electronic excitation of both atoms A^* is transferred completly to only one of them, which is then found in a very excited state A^{**}, while the other is left by the collision in the ground state A. The first observation of this process was reported in 1976 (M. Allegrini, G. Alzetta, A. Kopystynska, L. Moi and G. Orriols - Opt. Commun. 19, 96 (1976)). In process (2) the initial system evolves to an excited state A_2^{**} of the diatomic molecule, which can also be a triplet state (M. Allegrini, G. Alzetta, A. Kopystynska, L. Moi and G. Orriols - Opt. Commun. 22, 329 (1977)). This fact is very important because the triplet ground state of alkali dimers is repulsive and can not be easily studied by absorption spectroscopy or laser induced fluorescence technique. Process (2) instead populates triplet excited levels which then radiate to other lower triplet states and eventually to the ground triplet state. Moreover population inversion is naturally achieved in a eximer-like scheme, that can be used for laser action. In process (3) the two colliding atoms are bound to form the molecular ion A_2^+, as reported by Bearman and Leventhal in Sodium vapor (Phys. Rev. Lett. 41, 1227 (1978)).

A common characteristic of all three processes is that the excitation energy of the reactants is shared in the collision to give one very excited product. For this reason Leventhal has suggested the denomination *ENERGY POOLING COLLISIONS* to describe all above mentioned processes, independently from the final product. However, in the recent literature the term "energy pooling" is more often restricted to designate the energy transfer process (1) in contrast to the usual term "excitation transfer", used for energy transfer in collisions between one excited and one ground state atom. The fundamental parameter of energy pooling reaction is the energy defect ΔE (positive or negative) between the entrance and exit channels. Since these collisions are thermal, the energy balance between the reactants and the products is provided by their kinetics energy and therefore these reactions are efficient only for energy defects which have values of few kT. Two other important parameters are the atom density N and the laser power density I. The range of these two parameters has been widely varied in the experiments; however, the interest here is for those experimental conditions which make the energy pooling collisions dominant over all other possible processes. Thus we refer only to experiments where N is restricted to the range 10^{11}-$10^{13}$$cm^{-3}$ in order to avoid secondary collisions and I to less than $\approx 10^3$$Wcm^{-2}$ in order to avoid multiphoton ionization and all laser-induced effects. In particular, if N and I exceed these values, the slow electrons created in the associative ionization may gain energy through the collisions with the laser excited atoms (superelastic collisions). The presence of fast electrons in the vapor easily produce avalanche processes which lead to a complete ionization, as it has been observed for the first time in Lithium vapor (T.B. Lucatorto and T.J. McIlrath - Phys. Rev. Lett. 37, 428 (1976)). For pulsed experiments, the laser pulse duration $\Delta\tau$ also become an important parameter (M. Allegrini, W.P. Garver, V.S. Kushawaha and J.J. Leventhal - Phys. Rev. A28, 199 (1983)), and very different results are obtained.

LECTURE I

- INTRODUCTION
- ENERGY TRANSFER COLLISIONS IN HOMONUCLEAR ALKALI VAPORS

ENERGY POOLING REACTIONS

- WHAT IS AN ENERGY TRANSFER COLLISION ?

CONSIDER ALKALI ATOMS : simple structure
strong dipole transitions
laser available for excitation

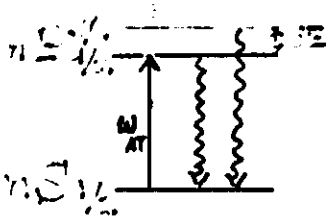

		$\Delta E\ (cm^{-1})$
2	Li	0.34
3	Na	17.2
4	K	57.9
5	Rb	237.6
6	Cs	554

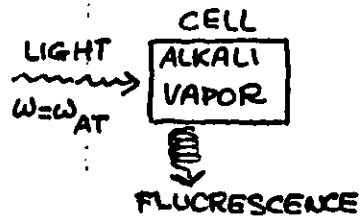

FLUORESCENCE SPECTRUM

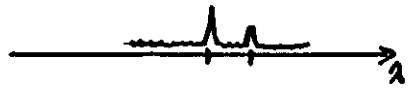

TWO ATOMS : A and B

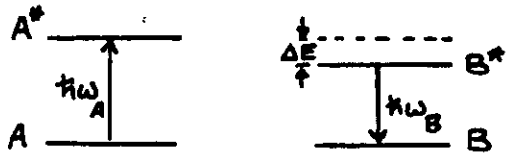

$\Delta E \approx kT$

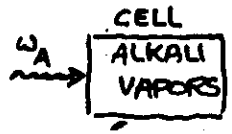

$A + \hbar\omega_A \longrightarrow A^*$

$A^* + B \xrightarrow{K,\sigma} A + B^*$

RATE EQUATIONS are easy

$$\begin{cases} \dfrac{dN_{A^*}}{dt} = S - \dfrac{N_{A^*}}{\tau_A} - K N_{A^*} N_B \\ \dfrac{dN_{B^*}}{dt} = K N_{A^*} N_B - \dfrac{N_{B^*}}{\tau_B} \end{cases}$$

S = number of atoms excited from A to A^* per second

τ = radiative lifetime

K = rate constant

FOR THERMAL COLLISIONS K is simply related to cross section σ

$$K = \langle \sigma v \rangle = \sigma \bar{v} \quad \text{with} \quad \bar{v} = \sqrt{\frac{8kT}{\pi \mu}}$$

Steady state solution of second equation gives

$$K = \frac{1}{N_B N_{A^*}} \frac{N_{B^*}}{\tau_B}$$

In actual experiments the intensity of the fluorescence lines is measured. For a transition from level i to level k

$$I_{i \to k} = \varepsilon \frac{V}{4\pi} A_{i \to k} N_i \hbar \omega_{i \to k}$$

ε factor for response of detecting apparatus

V fluorescence volume

$A_{i \to k} = \frac{1}{\tau}$ spontaneous transition probability

N_i excited atom density

$\omega_{i \to k}$ transition frequency

Therefore $K \propto \dfrac{1}{N_B \tau_A} \dfrac{I_B}{I_A}$ → measurements of K depend upon the determination of $\int N_B$

WHAT IS NEW WITH LASER EXCITATION ?

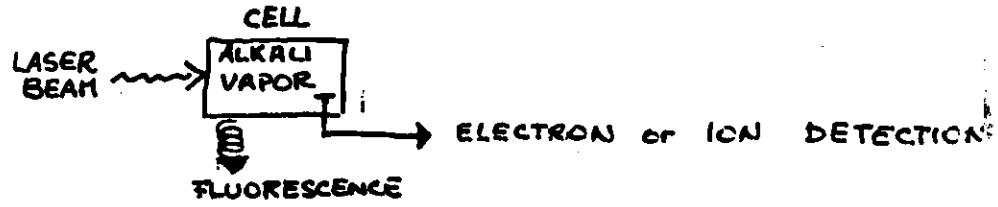

① LASER not necessarily resonant with atomic (or molecular) transitions → several effects (no treated here)

② LASER resonant $\boxed{\omega_L = \omega_{AT}}$ →

DENSITY of EXCITED ATOMS so high that COLLISIONS BETWEEN TWO EXCITED ATOMS occur.

ENERGY POOLING COLLISIONS

$A^* + A^* \longrightarrow A^{**} + A$		ENERGY TRANSFER
$\longrightarrow A_2^+ + e^-$		ASSOCIATIVE IONIZATION
$\longrightarrow A_2^{**}$		EXCITED MOLECULE FORMATIO
$\longrightarrow ? \ldots\ldots$		other processes ?

How to investigate and understand these processes ?

INVESTIGATION

EXPERIMENTS

1. FLUORESCENCE – SPECTRAL ANALYSIS
2. ION YIELD – MASS ANALYSIS
3. ELECTRON YIELD – ELECTRON SPECTROMETR.

IMPORTANT PARAMETERS

N	ATOM DENSITY (no superelastic collisions)		$\simeq 10^{13}$ – 10^{14} cm^{-3}
I	LASER POWER DENSITY (no multiphoton ionization or laser-induced effects		$\simeq 10^{3}$ W/cm^2
Δt	LASER PULSE DURATION	< cw	
		< pulsed	10 nsec ÷ 1 μsec
$\Delta\nu$	LASER BANDWIDTH		~ 40 GHz multimode ~ 1 MHz single mod
λ	LASER WAVELENGTH		RESONANT

SUPERELASTIC COLLISIONS may heat the e^-

$$e^-(\text{slow}) + X^* \xrightarrow[\sigma_1]{} e^-(\text{fast}) + X$$

Condition for the superelastic collisions to occur is: d mean free path of the e^- < cell dimensions

$$d = \frac{1}{\sigma_1 N_0}$$

σ_1 indirectly known from σ of the inverse process

$$e^-(\text{fast}) + X \xrightarrow[\sigma]{} e^-(\text{slow}) + X^*$$

N_0 atom density

HEATED – e^- cause impact-ionization ⇒ more e^-

IN POTASSIUM at $T \simeq 200\,^\circ C$

$d \simeq 0.18$ cm $\quad \mathcal{E} = 0.18$ eV
0.17 cm $\quad \mathcal{E} = 0.38$ eV

with σ taken from Massey - Burhop and σ_1 calculated from σ

CELL DIMENSIONS $\simeq \varnothing$ 36 mm
6 cm length

STRONG LASERS : – MULTIPHOTON IONIZATION $\quad A + 3\hbar\omega \rightarrow A^+ + e^-$

– TWO-PHOTON IONIZATION of RESONANT LEVEL $\quad A^* + 2\hbar\omega \rightarrow A^+ + e^-$

– LASER INDUCED PENNING $\quad A^* + A^* + \hbar\omega \rightarrow$

cw irradiation : excited species can be continuously produced so there is a steady-state concentration of potential reactants

pulsed irradiation : either

Δt_L (pulse duration) or τ (lifetime of excited state)

become key parameters

$\Delta t_L < \tau$ ⇝ τ determines the time dependence of the potential reactants

$\Delta t_L > \tau$ ⇝ Δt_L is important

In order to observe the effects of interactions involving excited reactants either the excited state lifetime or the laser pulse duration should be comparable or longer than the average time between collisions.

UNDERSTANDING

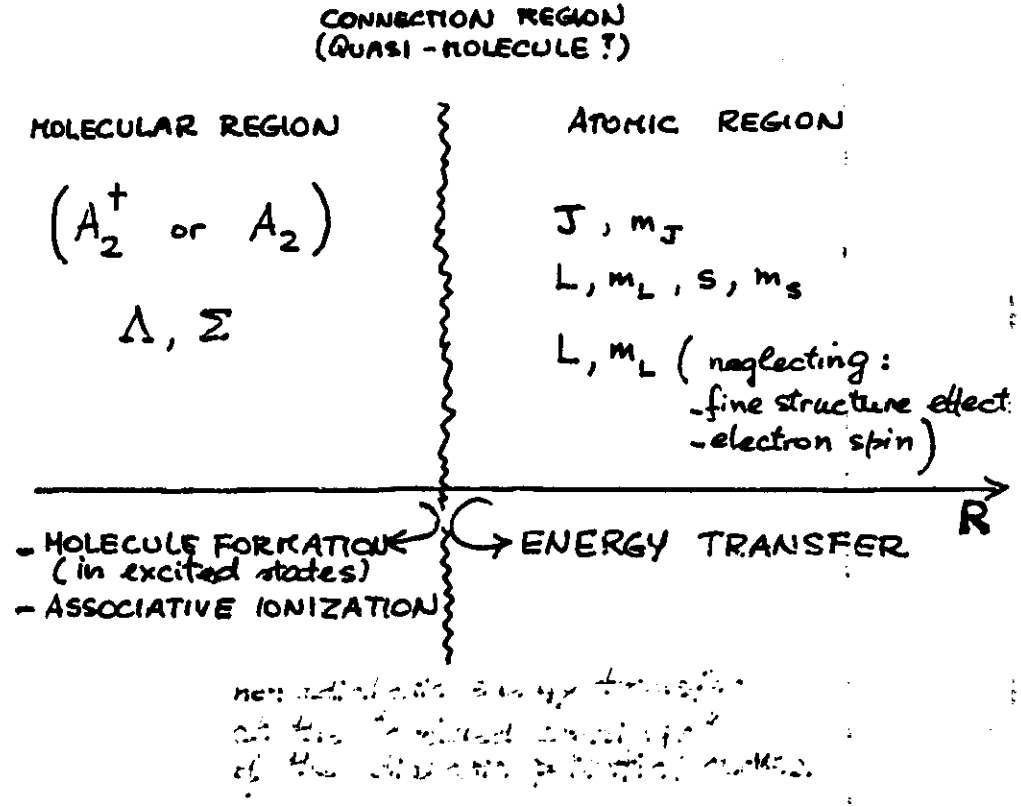

Difficult theoretical problem because of the number of potential curves involved (for example 12 curves correlate to 3P+3P two sodium atoms)

⇝ approximations, simplifications are necessa

THERMAL COLLISIONS

- $\Delta E \approx$ few kT
- COLLISION DURATION $\approx \frac{\text{ATOM DIMENSION}}{\text{THERMAL VELOCITY}} \approx 10^{-12} \div 10^{-13}$ sec
- RATE COEFFICIENTS $\propto$ CROSS SECTIONS $K = \bar{v}\sigma$ $\bar{v} = \sqrt{\frac{8kT}{\pi\mu}}$

from experiments : RATE EQUATIONS APPROACH

from theory : NONADIABATIC ENERGY TRANSFER AT AVOIDED CROSSINGS OF MOLECULAR ADIABATIC POTENTIALS

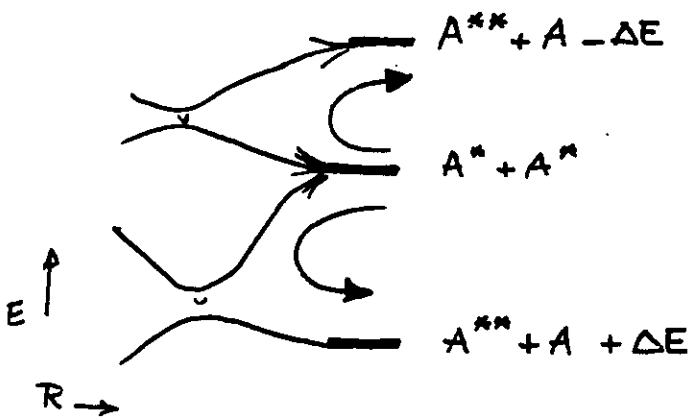

COLLISIONS BETWEEN EXCITED ATOMS

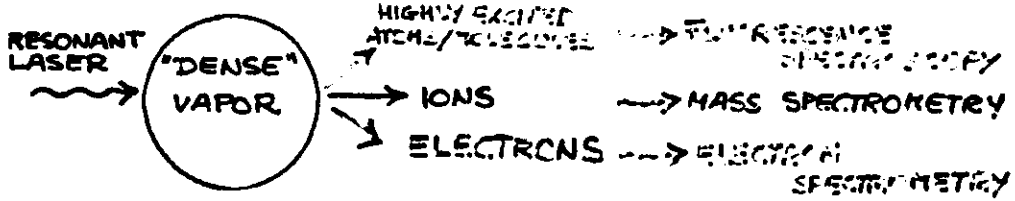

- ATOM DENSITY $N \approx 10^{12} \div 10^{13}$ cm^{-3}
- LASER ON RESONANCE I_L low

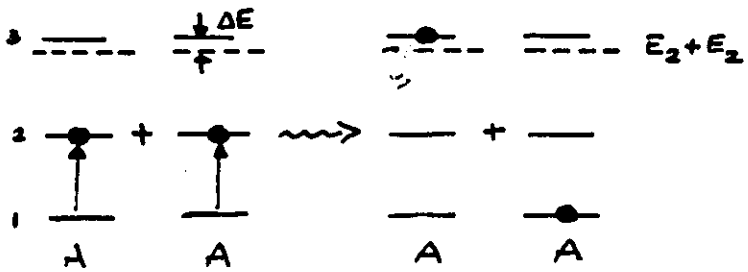

$$A^* + A^* \xrightarrow{K,\sigma} A^{**} + A$$

DETECTION THROUGH FLUORESCENCE SPECTRUM

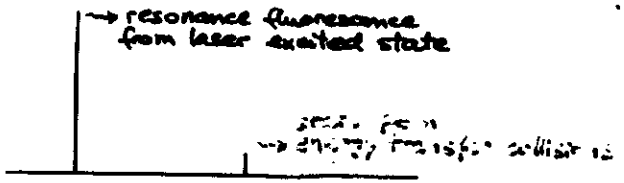

$$I_{ET} \propto \left[I_L^2 , N^2 \right]$$

$$I_{ET} \approx 10^{-3} \div 10^{-8} \, I_{RF}$$

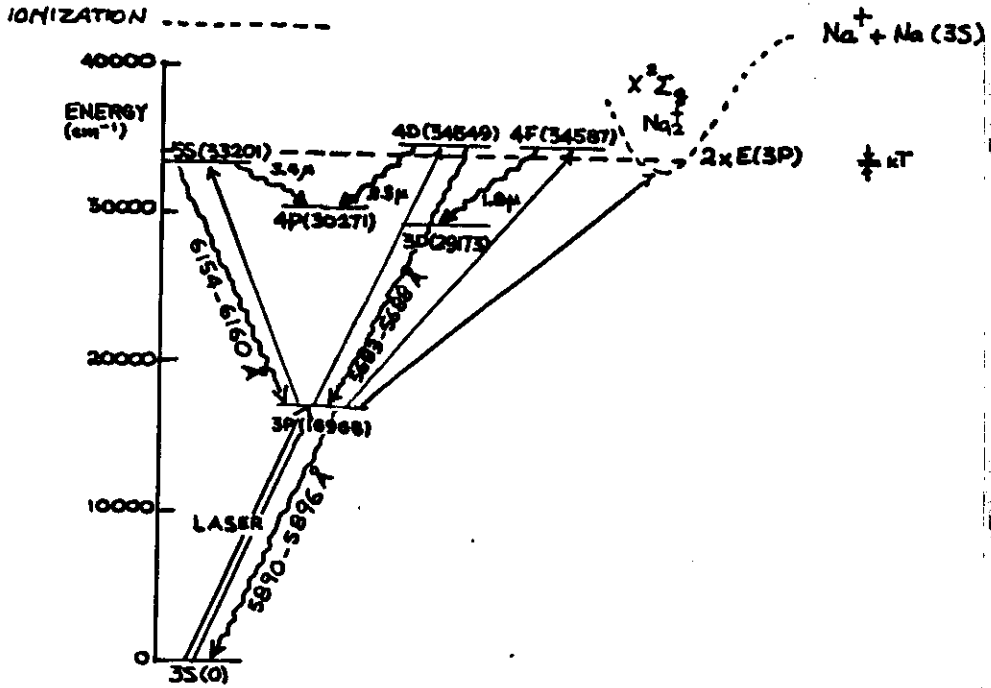

$$Na(3P) + Na(3P) \begin{cases} \xrightarrow{k_{AI}} Na_2^+ + e^- \\ \xrightarrow{k_{nL}} Na(nL) + Na(3S) \end{cases}$$

$nL = 5S, 4D, 4F$

APPARATUS

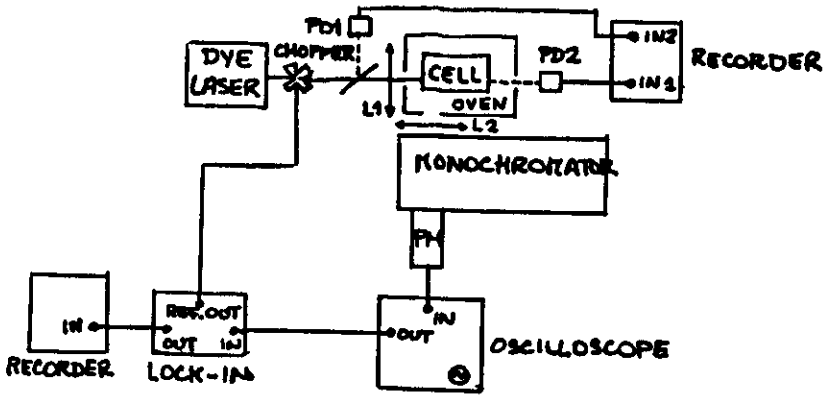

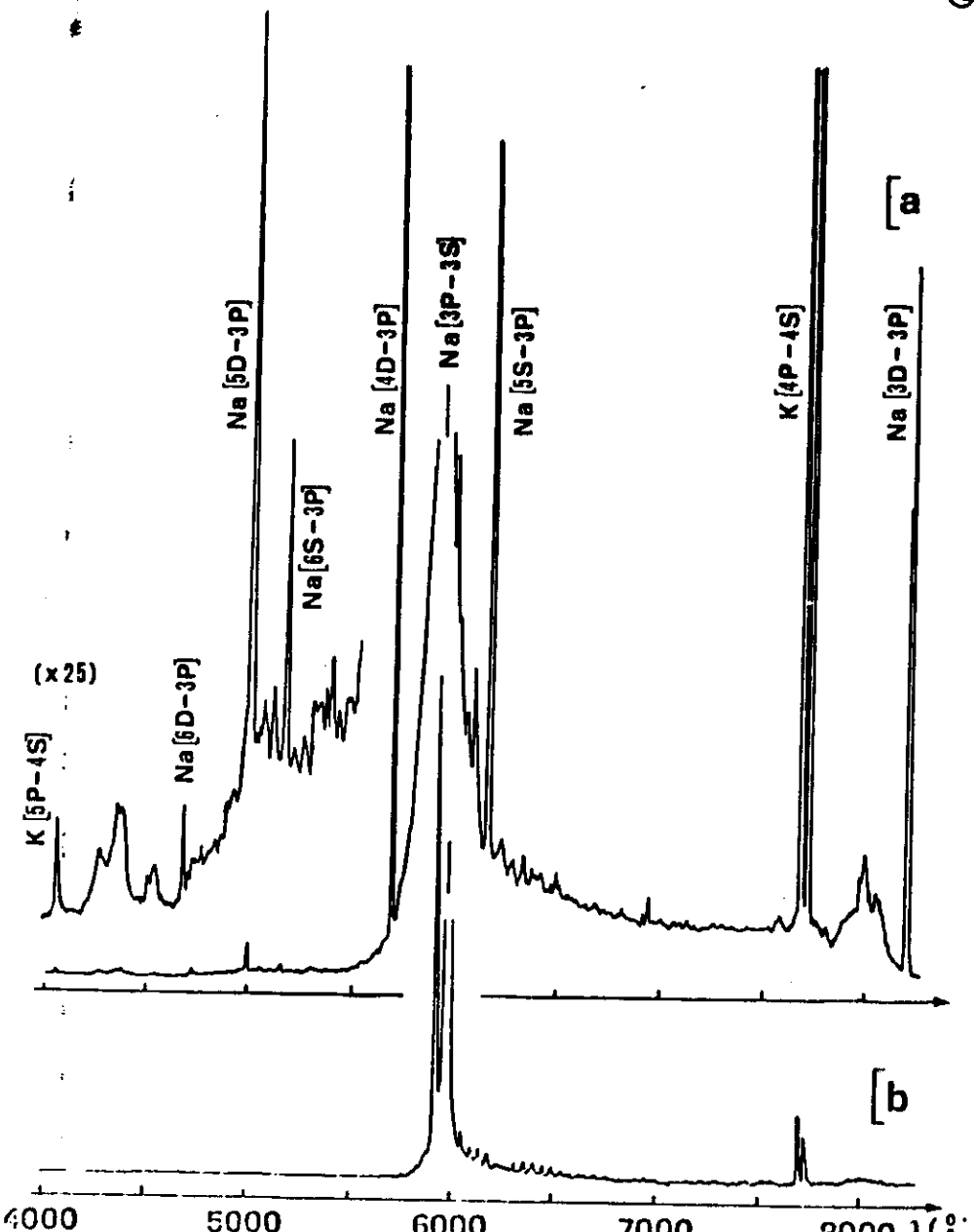

a) LASER tuned to $3S_{1/2} \rightarrow 3P_{1/2}$ transition of atomic Na

b) $\lambda_{LASER} = 5940$ Å resonant with $X^1\Sigma^+ \rightarrow B^1\Sigma^+$ and $X^1\Sigma^+ \rightarrow B^1\Pi$ transition of NaK molecule. Atomic Na and K lines are from energy transfer

FLUORESCENCE OF THE UNCORRECTED SPECTRUM

CELL : K + 5 Torr A
T = 170 °C
I_L = 100 mW
λ_L = 766.5 Å

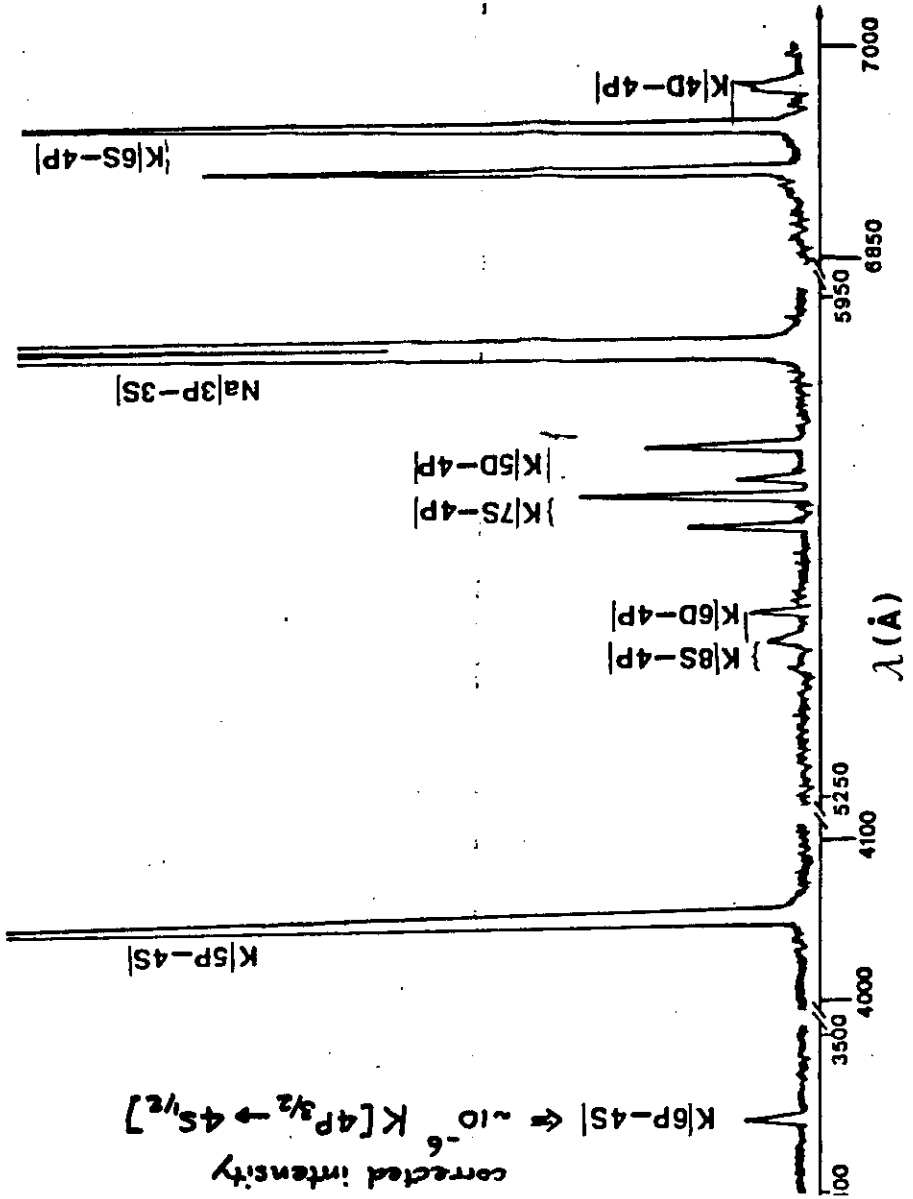

CROSS SECTION DETERMINATION

$$\frac{dN_{nL}}{dt} = KN_{3P}^2 - N_{nL} \sum_{n'L'} A_{nL \to n'L'}$$

STEADY-STATE SOLUTION $\rightsquigarrow$ $K_{nL} = \sigma_{nL} \bar{v} \dfrac{N_{nL}}{N_{3P}^2} \sum_{n'L'} A_{nL \to n'L'}$

$$K_{nL} = \frac{N_{nL}}{N_{3P}^2} A_{nL \to 3P} \underbrace{\left[1 + \sum_{n'L' \neq 3P} \frac{A_{nL \to n'L'}}{A_{nL \to 3P}}\right]}_{\gamma_{nL} \,=\, 1/[B.R.]} = \gamma_{nL} \frac{N_{nL}}{N_{3P}} \frac{A_{nL \to 3P}}{N_{3P}}$$

In terms of fluorescence intensities : $I_{i \to k} = \dfrac{V}{4\pi} A_{i \to k} N_i \hbar\omega_{i \to k} \varepsilon$

$$K_{nL} = \gamma_{nL} \frac{\omega_{3P \to 3S}}{\omega_{nL \to 3P}} \frac{I_{nL \to 3P}}{I_{3P \to 3S}} \frac{1}{N_{3P} \tau^*} \varepsilon$$

$\dfrac{1}{A} = \tau_{\text{spontaneous}}$ in presence of trapping has to be substituted by

$\tau^* = \tau_{\text{efficace}}$

K depends upon N_{3P}, τ^*, FLUORESCENCE VOLUME V

EXPERIMENT

- Volume problem solved by "CAPILLARY CELL".

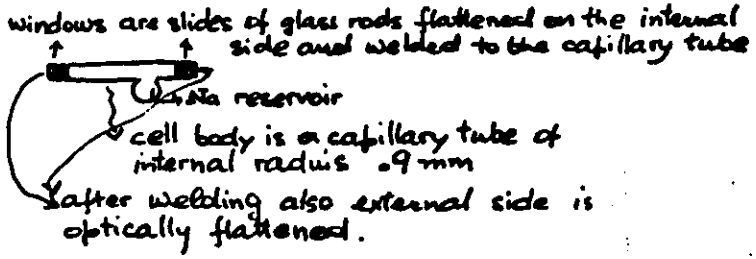

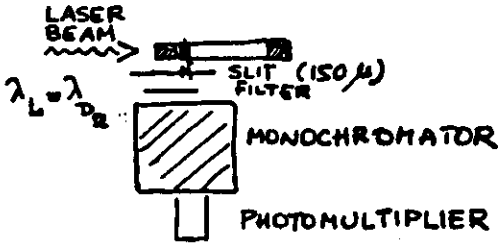

Laser is focused to the diameter of the cell window and illuminates the entire volume of the cell. The slit accepts radiation only for 150 μ from the entrance window ⇒ the resulting volume of laser-vapor interaction is well defined and is insensitive to variation in the optical absorption path. The fluorescence is taken from a region which is constant and uniformly illuminated.

- N_{3P} density determined by a novel calibration method based on the saturation of the resonance fluorescence at low temperature.

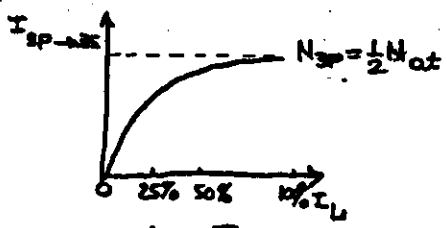

Low T

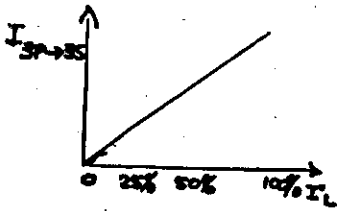

High T

$$\begin{cases} N_{at} = N_{3S} + N_{3P} \\ \frac{N_{3P}}{N_{3S}} = \frac{g_{3P}}{g_{3S}} = \frac{2}{2} \end{cases}$$

Solution gives $N_{3P} = \frac{1}{2} N_{at}$

N_{at} measured from T (Nesmeyanov tables)

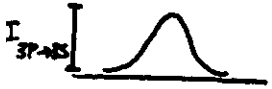

low $T = T_0$

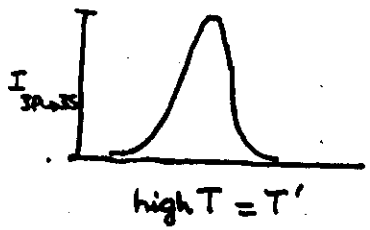

high $T = T'$

$$I(T_0) = \alpha \frac{N_{3P}(T_0)}{\tau_{nat}}$$

$$I(T') = \alpha \frac{N_{3P}(T')}{\tau^*}$$

$$\rightsquigarrow N_{3P}(T') = \frac{I(T')}{I(T_0)} N_{3P}(T_0) \frac{\tau^*}{\tau_{nat}}$$

Variation of the line intensity with laser intensity is

$$\frac{I_L/I_S}{\sqrt{1+I_L/I_S}} = A(I_L) \quad \text{and} \quad \frac{I_L/I_S}{1+I_L/I_S} = B(I_L)$$

for inhomogeneously broadened line

for homogeneously broadened line

I_S saturation parameter.

Our data are well fitted by a linear combination

$$I_{3P\to 3S} = \underbrace{e^{-\xi I_L} A(I_L)}_{\text{predominates for } I_L \to 0} + \underbrace{(1-e^{-\xi I_L})\, B(I_L)}_{\text{predominates for } I_L \to \infty}$$

ξ adjustable parameter ; $A(I_L)$ and $B(I_L)$ independently normalized

Line is homogeneous for $\Delta\nu_{\text{power broadening}} \simeq \delta\nu_{\text{mode spacing}}$ ~290MHz

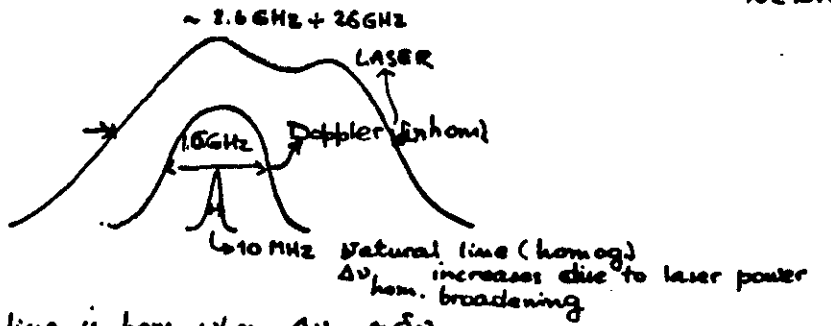

$\Delta\nu_{hom.}$ increases due to laser power broadening

All line is hom. when $\Delta\nu_{hom} \simeq \delta\nu_{\text{mode spacing}}$

no need to arrive at $\Delta\nu_{hom} = \Delta\nu_{DOPPLER}$

because of multimode laser

- τ^* is taken from Milne theory which is valid in the optical thin region of our experiment. A simple test is that Milne theory gives τ_{NET} in the limit of no-trapping - Other theories, valid in the optical thick limit, fail this test. Milne theory is also supported by the experiments.

However we have a test also from our data:

$$K_{nl} = \underbrace{\alpha_{nl}\,\gamma_{nl}}_{\text{detection apparatus efficiency}}\ \frac{\omega_{3P\to 3S}}{\omega_{nl\to 3P}}\ \frac{I_{nl\to 3P}}{I_{3P\to 3S}}\ \frac{1}{N_{3P}\,\tau^*}$$

$$K_{nl} \propto \frac{I_{nl\to 3P}}{I_{3P\to 3S}}\ \frac{\tau}{(\tau^*)^2}$$

$\left(K_{nl}\,\tau^{*2}\right)$ as function of T

K_{nl} does not vary over a small temperature range since the colliding Na (3P) atoms have thermal energy $\propto$ their relative energy remains ~ constant as does the collision frequency. The dependence upon T of that product is due to τ^*. Our data are well fitted by the Milne theory.

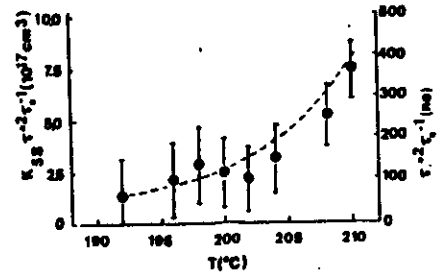

FIG. 4. Plot of $k_{5S}(\tau^{*2}/\tau_0)$ values versus T. The dashed curve represents τ^{*2}/τ_0 with τ^* calculated from Milne's theory for an optical depth $d=0.35$ mm.

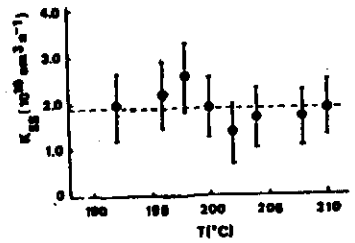

FIG. 5. Rate constant values versus T of the process (2) for the level 5S.

RATE EQUATIONS

$$\dot{N}_{4d} = -\underbrace{\sum_{nl} A(4d,nl)\,N_{4d}}_{\text{radiative decay } nl = 3p,4d} + \underbrace{K_{4d} N_{3p}^2}_{\text{energy-transfer } 3p+3p} - \underbrace{K N N_{4d} + K' N N_{4f}}_{\text{energy-transfer } 4d+3s,\ 4f+3s} +$$

$$+ \underbrace{K_{R,4d} N_e^2}_{\text{ion recombination } (N_e \approx N_i)} + \underbrace{\sum_{n'l'} A(n'l',4d)\,N_{n'l'}}_{\text{cascade from higher levels}} - \underbrace{K_{e,4d} N_e N_{4d}}_{\text{electron-impact ionization}} -$$

$$- \underbrace{B_i N_{4d} I_L}_{\text{photoionization}} - \underbrace{K_{3p,4d} N_{3p} N_{4d}}_{\text{Penning ionization } 3p,\,4d} - \underbrace{K_{3s,4d} N_{3s} N_{4d}}_{\text{associative ionization } 3s,\,4d}$$

$$\dot{N}_{4f} = -A(4f,3d)\,N_{4f} + K_{4f} N_{3p}^2 + K N N_{4d} - K' N N_{4f} + K_{R,4f} N_e^2 +$$

$$+ \sum_{n'l'} A(n'l',4f) N'_{n'l'} - K_{e,4f} N_e N_{4f} - B_i N_{4f} I_L -$$

$$- K_{3p,4f} N_{3p} N_{4f} - K_{3s,4f} N_{3s} N_{4f}$$

$N = N_{AT}$ or $N_{gas} \times (N_{gas} + N_{at})$ — cell with Na / cell with Na + buffer gas

$$\frac{K}{K'} = \frac{g_{4f}}{g_{4d}} e^{-\Delta E/kT} = 1.26$$

$$K_{ej} \sim \frac{2.7\times10^{-6}}{(E_i-E_j)\sqrt{kT_e}}\, e^{-(E_i-E_j)/kT} \quad cm^3\,sec^{-1}$$

$3kT = E_j + h\nu_L - E_i$

$K_{e,4d} \sim K_{e,4f} \sim 4\times10^{-7}\ cm^3\,sec^{-1}$

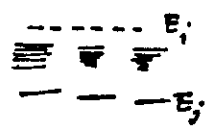

$$B_i = \frac{\sigma_{ph}}{h\nu_L}$$

$\sigma_{ph}(4d) = 1.5\times10^{-17}\ cm^2$ (A. Smith, et al., 1980)

$\sigma_{ph}(4f)$?

SOLUTION: RATIO EQUATIONS

CONSIDER ONLY FIRST 4 TERMS ⟶ SIMPLE SOLUTION

$$\frac{N_H}{N_{4d}} = \frac{[A(4d,3p)+A(4d,4p)+kN]\,K_{4f} + KNK_{4d}}{[A(4f,3d)+K'N]\,K_{4d} + K'NK_{4f}}$$

Data have been fitted with this expression taking K and K_{4f} as parameters and $K_{4d} = (3.0 \pm 0.9)\times10^{-10}\ cm^3\,sec^{-1}$

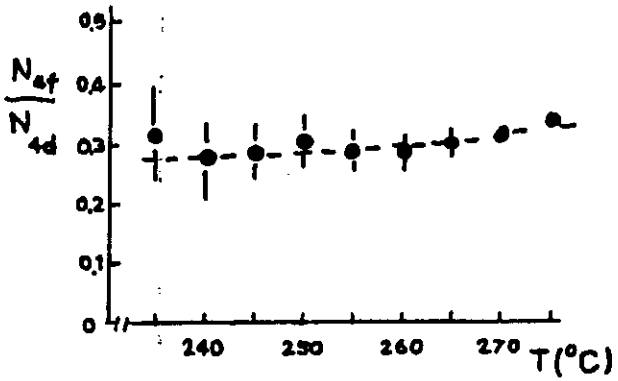

dots represent data, line represents best fit curve.

$K_{4f} = (5.6 \pm 2.2)\times10^{-11}\ cm^3\,sec^{-1}$

$K = (9.8 \pm 4.9)\times10^{-9}\ cm^3\,sec^{-1}$

Radiative 4d-4f energy transfer : $K_{..} = (6.0 \pm 2.4)\times10^{-11}\ cm^3\,sec^{-1}$

CROSS SECTION DETERMINATION — THEORY

- EXPERIMENTS provide TOTAL AVERAGED σ. Only initial and final set of atomic states is known; no other information about collision process is available.

- To compare σ_{exp} to σ_{th} one should <u>in principle</u> include all possible electronic states connected to the atomic products and solve the complete set of coupled equations for each possible value of relative velocity and total angular momentum. Then one should average cross sections with statistical weigths, according to the distribution of the atomic fragments among the initial states.

- However, possible states are so many (for example 12 states have 3P + 3P dissociation limit
16 states " 4F + 3S " ") and almost each pair of states with appropriate g/u and +/− simmetry is coupled by some terms in the Hamiltonian that <u>WE NEED SOME APPROXIMATIONS.</u>

- ONLY ONE ENTRY CHANNEL, THAT REPRESENTED BY THE $^1\Sigma_g^+$ MOLECULAR STATES.

i) Neglect centrifugal coupling with Π states (collisions are thermal and at large interatomic distances)

ii) Neglect spin orbit coupling with triplet states

1. CONSTRUCT ELECTRONIC WAVE FUNCTIONS
2. CALCULATE POTENTIAL ENERGY CURVES
3. CALCULATE COUPLING MATRIX ELEMENTS BETWEEN W.F.
4. EVALUATE $\sigma_{th.}$ and COMPARE TO $\sigma_{exp.}$

- Two separated atomic fragments
- Construct a set of Hartree-Fock orbitals, separately optimized for the various states.
- Then construct valence bond wavefunctions having $^1\Sigma_g^+$ symmetry and corresponding to various dissociation limits.
- Wavefunctions are orthogonal at infinite interatomic distances. Going to finite distances, allow free overlap between the two valence orbitals while orthogonalizing them to the core orbitals. Contribution from so called ionic structures (ion-pair) are then taken into account. No basis superposition errors.
- For each R, electronic wf. are weakly dependent on R, maintain a well defined atomic character, are coupled only by the electronic Hamiltonian and cross each other at finite R.
  They represent the <u>diabatic</u> reference states.

Diabatic potential energy curves vs. internuclear distance

Diabatic terms and w.f. to locate transition points between various surfaces and to evaluate transition probabilities at R ≥ 20 a.u.

$^1\Sigma_g^+$ terms

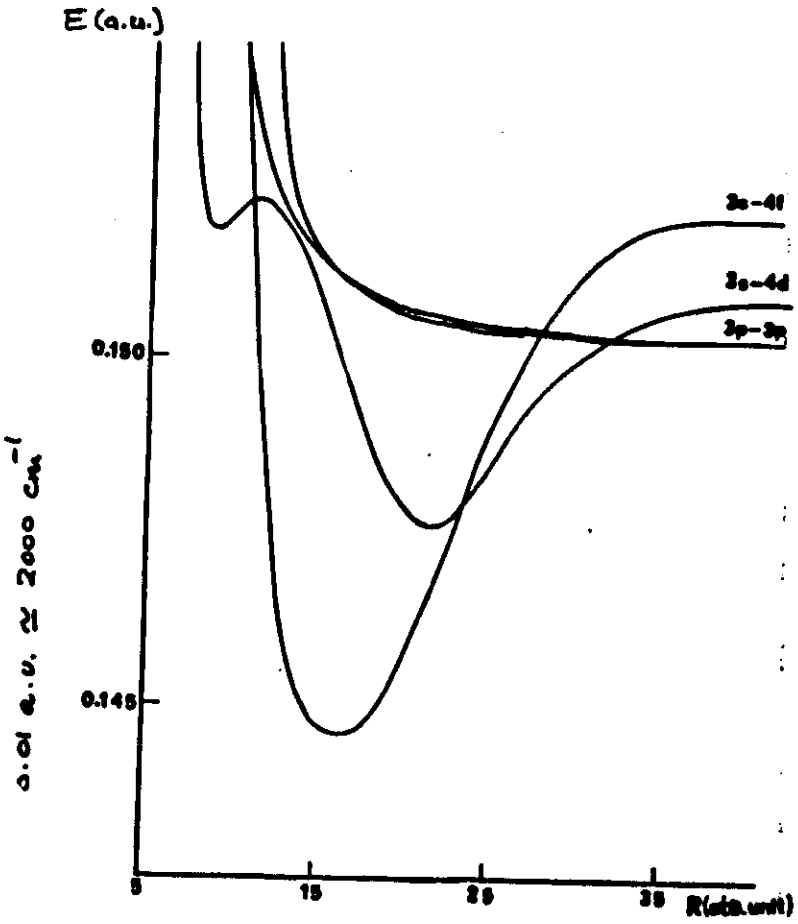

"DIABATIC" potential energy curves, from orthogonalized wavefunct., physical meaning at large R (≳ 20 a.u.).
For R ≤ 20 a.u. adiabatic representation is more appropriate.
"ADIABATIC" energy curves obtained by diagonalizing the matrix representative of the electronic Hamiltonian in the diabatic basis

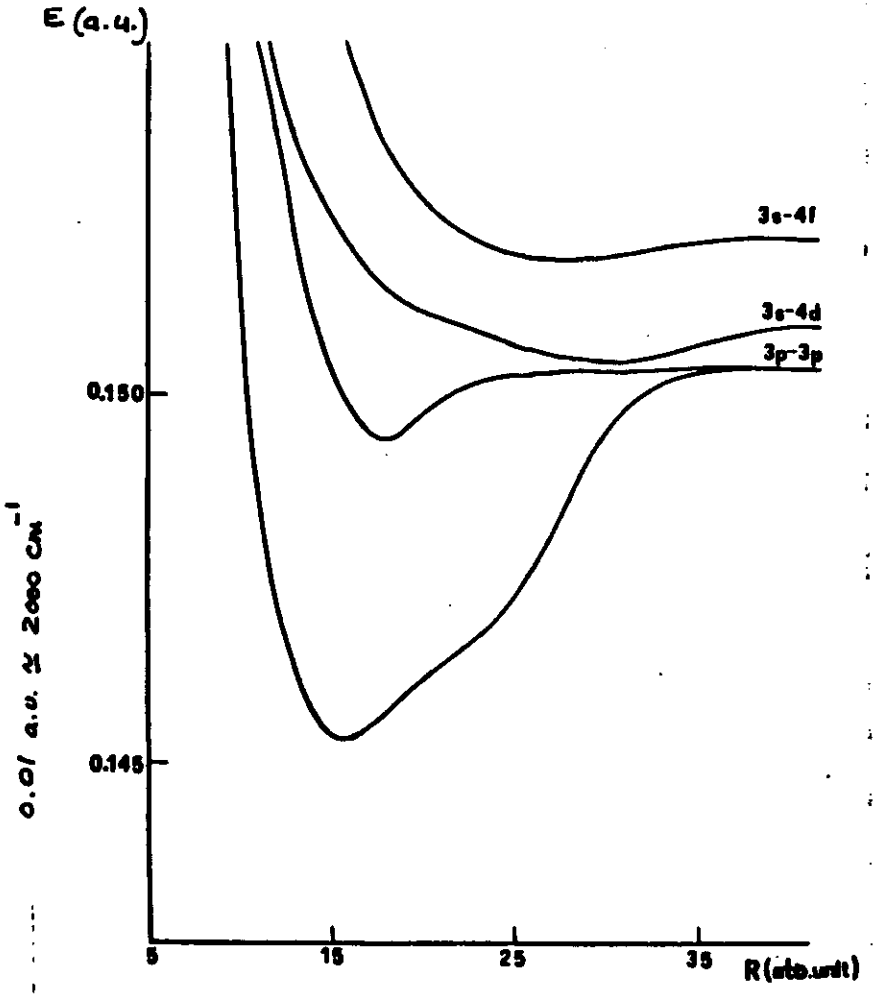

From: FUNDAMENTAL PROCESSES IN ATOMIC COLLISION PHYSICS
Edited by H. Kleinpoppen, J.S. Briggs and H.O. Lutz
(Plenum Publishing Corporation, 1986)

COLLISIONAL SPECTROSCOPY OF LASER EXCITED ATOMS

Maria Allegrini

Istituto di Fisica Atomica e Molecolare del C.N.R.
Via del Giardino, 7 - 56100 Pisa, Italy

INTRODUCTION

This lecture will be devoted to the study of collisions between two atoms, both in an excited state. For their simple structure (only one external electron) and strong interaction with the light, we will consider here only experiments involving alkali atoms. Recently a great deal of work has been done also on more complex atoms such as calcium, strontium and barium[1]. Collisions between two excited atoms were first observed using powerful discharge lamps as excitation sources, (for a review see for example ref./2/), but it is with the laser that high concentrations of excited reactants have been normally obtained. The study of collisions in a laser field is now a rapidly growing field of research[3-5]. The simplest case of collisions between laser excited alkali atoms regards two atoms both in the first P state. A near resonance, of the order of few kT, between the colliding atoms and the final products of the collision is required. Indeed the observed effects have been:

i) excitation transfer to higher atomic levels nL, with energy close to the sum energy of the two nP atoms;
ii) formation of the molecular ion which is energetically achievable from two atoms in the lowest P state in all the alkalis, but lithium.

Thus we are considering the binary inelastic collisions

$$A(nP) + A(nP) \longrightarrow A(nL) + A(nS) \qquad (1)$$

$$A(nP) + A(nP) \longrightarrow A_2^+ + e \qquad (2)$$

Many other phenomena are also produced in a dense vapor excited by

resonant laser radiation. For their understanding it is important to identify in the experiment the parameters determining the dominant effects. These parameters are the laser power density W, the atom density N and the temporal characteristics of the laser. We are interested in experiments where the laser provides a sufficient concentration of excited atoms to enable the observation of their collisions but it is not powerful enough to give direct multiphoton ionization or other processes induced by the strong electromagnetic field associated with the laser. With a laser power density $\lesssim 10^3 W/cm^2$ this aim is certainly achieved and an atom density of $\lesssim 10^{13} cm^{-3}$ usually assures that secondary collisional processes, either with other atoms or ions and electrons produced in the experiments, are negligible. Attention has to be paid also to the concentration of alkali dimer which may obscure the results of the atomic collisions we wish to study[6-8]. For cw laser irradiation there is a continuous production of excited atoms with a steady state density dependent upon the effective atomic lifetime; for pulsed excitation the pulse duration has to be considered in the time dependence of the process[6].

There are many reasons for interest in studying processes (1) and (2). From a theoretical point of view we are in presence of a rare mechanism where two excitations in the atomic system are combined to give one single higher excitation. In classical physics processes leading to a more uniform distribution of the energy or towards the exchange of excitation from one atom (or molecule) to another, (see for example the sensitized fluorescence phenomenon[9]), are more common. Contrary to the multiple excitations obtained with high power lasers, the higher excitation achieved in (1) and (2) is produced internally in the system through the collisions. In this case the laser is merely a tool to create simultaneously the excited partners for the collision. A more specific theoretical interest arises because these collisions depend upon long range interactions between the two atoms. The atomic energy levels for the two atoms at infinite distance are of course well known. Also the potential curves for the two atoms at short interatomic distances, when they are bound to form the neutral molecular dimer, are reasonably well known. In the intermediate range where the asymptotic approximations fail these collisions may provide an experimental test for the calculations of potential curves and of their crossing points. Another important result is that the determination of reliable cross sections for processes (1) and (2) has indirectly given the incentive to study the intriguing phenomena of radiation diffusion and saturation in optically thick vapors excited by laser radiation[10].

From an experimental point of view the interest is even more immediate. The processes (1) and (2), followed by photoionization or collisional ionization have been proved[11] to provide, together with the multistep ionization of the dimers, the seed electrons for complete ionization of dense vapors with moderate laser powers[12,13]. Efficient breakdown and plasma formation in gases or vapors is an actual goal of applied physics; any process which may improve the ion yield without increase of laser intensity supplied from outside is of interest. Infrared laser emission has been observed[14] upon excitation of the 3P level in sodium vapor, suggesting that 3P/3P collisions may also be important in this phenomenon. Application of these collisional processes to laser isotope separation is obvious since the laser selects the excited state of the reactants and the collision yields a selected product. A(nP)/A(nP) collisions are also a promising way to populate triplet electronic excited states of the neutral molecule A_2 resulting in an excimer configuration with possible application to new tunable laser sources.

We will restrict ourselves in the following to few basic experiments and ideas, while updated results on this subject are easily found in the open literature or references /3-5/.

ENERGY POOLING COLLISIONS

The first experiment involving collisions between laser excited atoms were performed on sodium vapor, but all the alkalis have since been widely studied[3-5]. Lucatorto and McIlrath[12] observed nearly complete ionization in a 10-cm column of Na at $\simeq 10^{16} cm^{-3}$ atom density, irradiated with a pulsed laser of $\simeq 1 MW/cm^2$, tuned to the 3S-3P resonance line. Allegrini et al.[15], in a cell with a sodium density of $\simeq 10^{12} cm^{-3}$, observed fluorescence from atomic states lying higher than the 3P level, optically excited with a cw laser of less than $10 W/cm^2$. Na energy levels are shown in figure 1. As can be seen from figure 1, direct photoionization requires three yellow photons. Rigorous calculations[16,17] show that the rate of ion production by this process is negligible in both the above experiments, even if the laser power density available in the pulsed experiment is five or six orders of magnitude bigger than in the cw experiment. Also the difference between pulsed and cw excitation is not the key parameter in this case, because the pulse duration of the flash lamp pumped dye laser used by Lucatorto and McIlrath was long ($\sim 1 \mu sec$) compared to the lifetime of the 3P excited state, giving a pool of excited reactans as in the cw excitation experiment. The dominant effect in the experiment of ref./12/ was the associative ionization

$$Na(3P) + Na(3P) \longrightarrow Na_2^+ + e \qquad (3)$$

When energetically possible, two excited atoms associate during a collision to form a molecular ion plus one electron. The outcoming electron is slow because it carries an energy of few kT, namely the energy defect between the colliding 3P atoms and the state in which the molecular ion is formed. However, in presence of a high density of excited atoms, the electron, before recombination, undergoes one or more superelastic collisions.

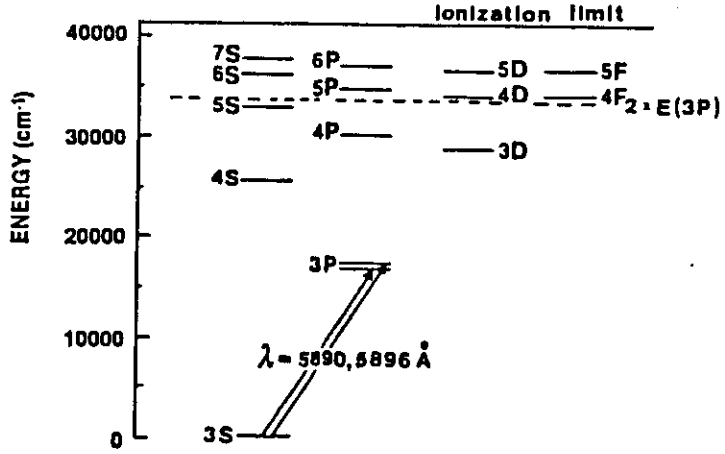

Fig. 1. Na energy levels showing the laser excitation, the ionization limit and the energy of two 3P atoms. The fine structure of the 3P level is not in scale.

$$e\ (slow) + Na(3P) \longrightarrow e\ (fast) + Na(3S) \qquad (4)$$

Fast electrons then produce, by avalanche mechanisms, the atomic ions. In the experiment of Allegrini et al.[15] the following process was observed

$$Na(3P) + Na(3P) \longrightarrow Na(nL) + Na(3S) \qquad (5)$$

where nL indicates a highly excited state with energy close to twice the 3P energy. The energy defect (positive or negative) is supplied by conversion of relative kinetic energy of the two interacting Na (3P) atoms or carried away by the final Na(nL) and Na(3S) atoms. Thus this is a peculiar process involving pooling of internal and relative kinetic energy of the atoms. The nL levels were identified simply by their characteristic radiative emission lines. A quadratic dependence of the fluorescence intensity upon the laser power and upon the atom density plus comparison with the resonance fluorescence 3P-3S versus the laser wavelength through the atomic resonance, has clearly established that two 3P excited atoms are involved in the population mechanism of the highly excited states. In process (5) there is a transfer of electronic energy as in the sensitized fluorescence phenomenon

$$A^* + B \longrightarrow A + B^* \qquad (6)$$

where during a collision between one excited atom A^* and one in the ground state B the excitation is transferred from one atom to the other. We will see later that in analogy with process (6), the rate constant K or cross section σ of process (5) has been derived by solving the rate equations at the steady state. However, the main characteristic of process (5) is the combination in the collision of two excitations to give a single higher excited product as in the associative ionization. The name "energy pooling collisions" has been used first by Leventhal[18,19] to describe both processes (3) and (5). In a few words this expression contains the physical meaning of the observed phenomena: the highly excited nL states and the molecular ions are two different products of the same collisional reaction in which the energy of the reactants peakes in one product instead of being distributed.

DETECTION METHODS

The energy pooling collisions produce atoms in excited states, which radiatively decay to the ground state, ions and electrons. Detection of photons, ions or electrons requires different techniques and apparatus and each experiment has its own particular geometry and original technical solutions that will be too long to report. We will try to give few illustrative examples of the three detection techniques.

Fluorescence

In order to look at the fluorescence spectrum of a laser excited alkali vapor the collision cell containing the metal may be an ordinary pyrex cell sealed under vacuum and heated in a temperature controlled oven. This system reaches easily a thermodynamic equilibrium, the vapor is saturated and the atom density can be determined with reasonable accuracy from the temperature, using the Nesmeyanov tables[20]. The fluorescence is collected at right angles to the laser beam, dispersed with a monochromator mounted with the proper grating and detected with a photomultiplier in the visible range or with a suitable detector for the infrared. It is common to control the laser output with a photocell for power variation checking and to attenuate with a filter the resonance fluorescence, i.e. the radiation emitted directly from the laser excited first P level, because it is orders of magnitude more intense than the fluorescence from the levels populated through process (1). The fluorescence signal coming from the nL levels is very weak and usually its detection needs amplification by techniques that differ substantially for excitation by pulsed or cw lasers. A schematic diagram of the apparatus is shown in figure 2 and two examples of such spectra are reported in figures 3 and 4. Figure 3 is taken from ref. /7/ and shows the fluorescence spectrum of sodium vapor excited to the $3P_{1/2}$ level with a broadband cw dye

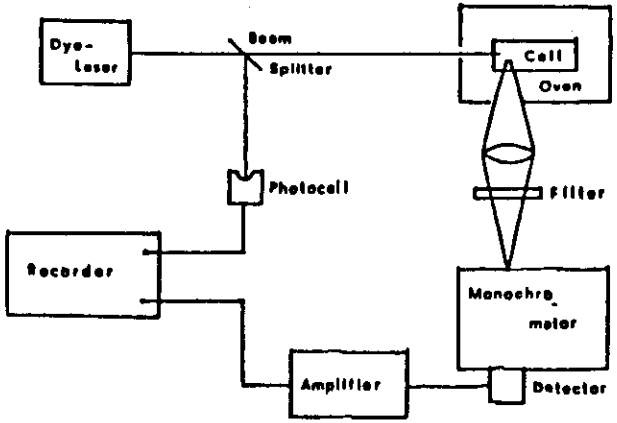

Fig. 2. General scheme for detection of the fluorescence emitted by the highly excited nL levels, populated through the energy pooling collisions.

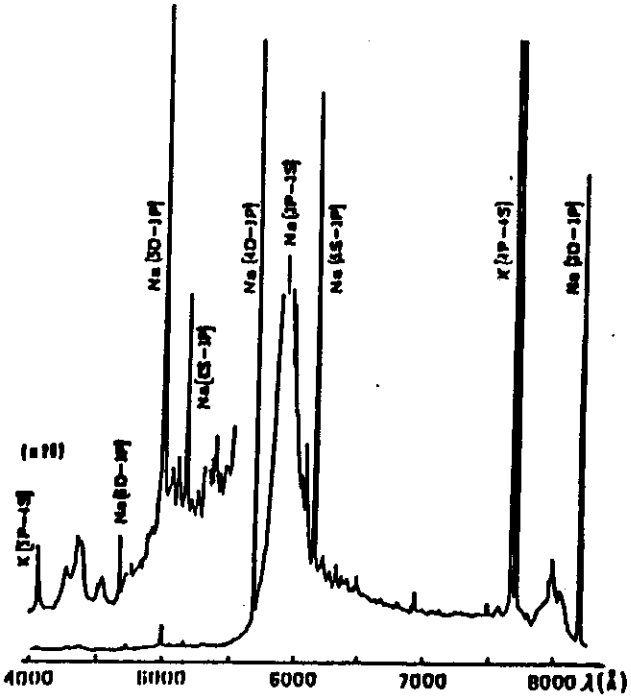

Fig. 3. Fluorescence spectrum of sodium vapor excited by a cw dye laser tuned to the $3S_{1/2} - 3P_{1/2}$ transition[7].

laser of ~40mW; since this spectrum was recorded at relatively high atom density ($N \sim 10^{15} cm^{-3}$), at which secondary collision process occur, beside the fluorescence lines emitted by the nL levels populated directly by the energy pooling collisions, it contains also lines from higher sodium levels, molecular sodium bands and potassium atomic lines, although potassium was present only as an impurity. The resonance fluorescence line, corresponding to the 3P-3S transition, was not recorded to avoid saturation and possible damage to the detection apparatus; its position is pointed out in the diagram. A similar fluorescence spectrum[21] of potassium vapor excited to the $4P_{3/2}$ level with a broadband cw dye laser of ~100mW is shown in figure 4. The resonance fluorescence, not shown in the diagram, is at ~7700Å and and it was, after correction for the spectral response of the detection apparatus, $\sim 10^4$ times more intense than the strongest line in the spectrum (6S-4P transition at 6911-6939Å).

Ions

A simple way to detect the ions formed in the laser excited vapor is to insert in the collision cell a current collecting electrode and read the total ion yield with an electrometer. A small transverse electric field may be necessary to assure complete collection. For the identification of the different species of ions mass resolved spectra are taken, for example with a quadrupole mass filter. Another common mass analysis is carried out with a time of flight drift tube which delivers current pulses whose height is proportional to the collected ion number. The collision cells used by various groups are quite different and many experiments have also been performed on ion crossing beams[3-5]. As an examole we report here the experimental set up used by Laventhal and coworkers[6,18,19] on sodium vapor. A cylindrical cell is mounted on an oven consisting of a resistance heater imbedded in a Cu block and located beneath the cell. Sodium vapor effuses into the cell through a slot in the bottom of the cell. Apertures in the cell permit the laser beam to enter and leave along the axis of the cylinder. Ions formed in the cell are collected through a side hole of ~5mm and a window on the opposite side permits also observation of photons for fluorescence spectrum recording. Because of the apertures, the cell works in non equilibrium conditions withconsequent nonuniformities in the atom density. The density can thus not be determined simply from a temperature reading as in the sealed pyrex cell of Figure 2. The ions are extracted from the cell with a set of electrostatic lenses, mass analyzed with a quadrupole mass filter and detected with a CuBe particle detector. A scheme of the apparatus is shown in figure 5. Different modes of operation are possible with this apparatus. In one mode the laser is fixed at the atomic transition wavelength and mass scans are taken; alternatively the quadrupole mass spectrometer is fixed at a specific ion mass and the laser wavelength is scanned. Figure 6 shows a spectrum of sodium vapor taken with the apparatus of figure 5 set in the

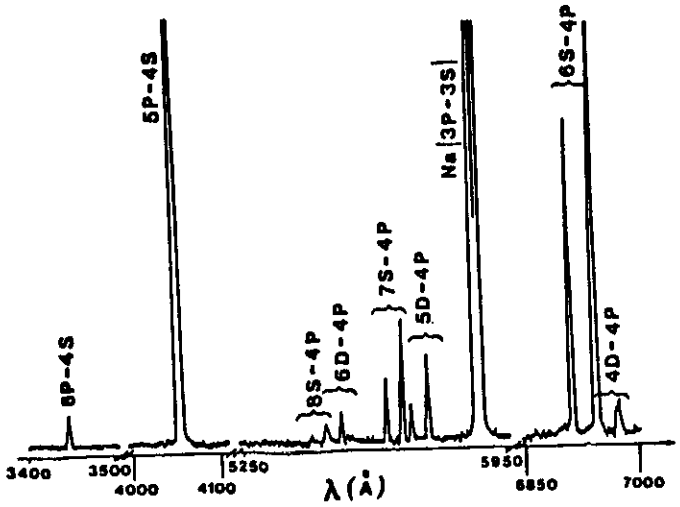

Fig. 4. Fluorescence spectrum of potassium vapor excited by a cw dye laser tuned to the $4S_{1/2} - 4P_{3/2}$ transition[21].

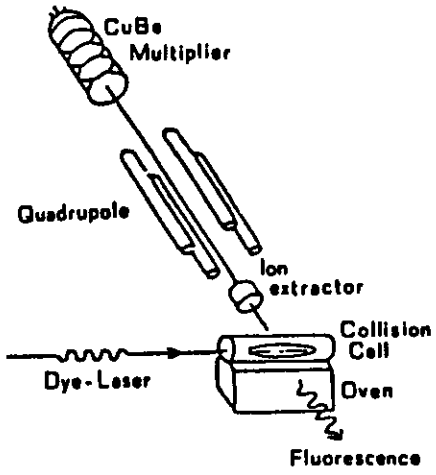

Fig. 5. Schematic diagram of the apparatus for the detection of ions formed in collisions between laser excited sodium atoms[6].

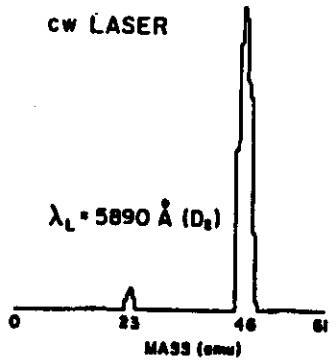

Fig. 6. Mass spectrum taken with a multimode cw laser tuned to the D_2 sodium line[6]. The spectrum is corrected for relative transmission as a function of mass. Ordinate scale is in arbitrary units.

first mode of operation. Na_2^+ ions were formed by associative ionization (process (3)) only when the laser was tuned to D_1 or D_2 sodium lines. Na_2^+ were the dominant ionic product, however a small yield of Na^+ ions, resulting from the photodissociation of nascent Na_2^+ ions, was detected[22].

Electrons

The third method to study the energy pooling collisions is the detection of the electrons created in the vapor. A simple measurement of the total current does not provide relevant information on the collisional processes and the results may be masked by the photoelectric effect. An original way to use electron detection, although it provides only indirect and qualitative information, was applied to an experiment on potassium[21]. The atom density in this experiment was between 10^{13} and $10^{14} cm^{-3}$, an intermediate value at which secondary collisional processes become important. It was our intention to distinguish the levels populated directly by the primary 4P/4P collisions, which should have a clear quadratic dependence upon the 4P density, from the levels populated through other mechanisms. The cylindrical pyrex cell was supplied from the entrance window with two internal electrodes, parallel to the cylinder axis. Optogalvanic signals, taken with a standard apparatus, as shown in figure 7, were recorded simultaneously with the fluorescence signals. Optogalvanic signals[23] arise in an electrical discharge at low pressure whenever light tuned across some characteristic transition frequency of the atoms in the cell is absorbed.

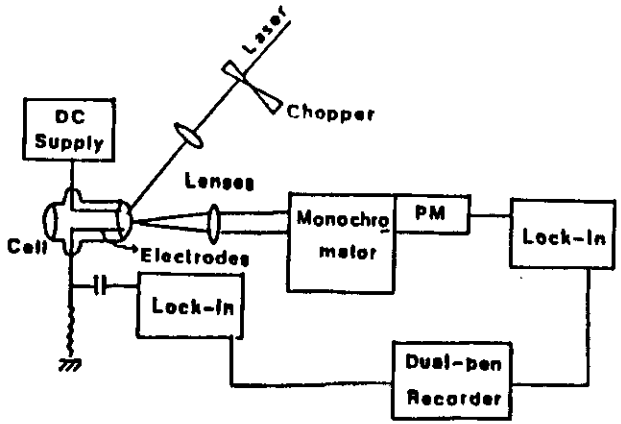

Fig. 7. Schematic diagram of the apparatus for simultaneous detection of optogalvanic and fluorescence signals.

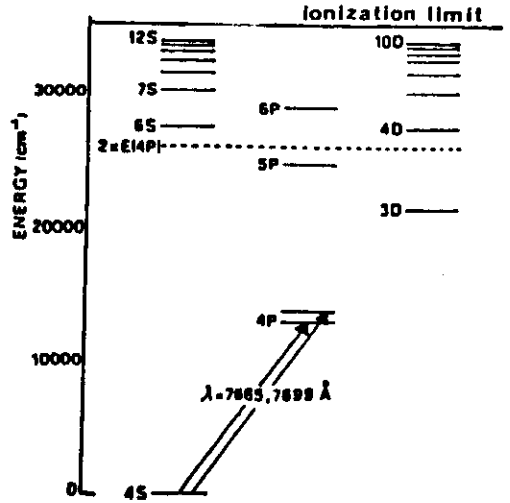

Fig. 8. Partial energy level diagram for K. The fine structure of the 4P level is not in scale.

We have compared the linewidth of the optogalvanic and fluorescence signals as a function of the laser wavelength, tuned across the resonance atomic transition 4S-4P. The ratio between the halfwidth of the resonance fluorescence signal $\Delta\nu(RF)$ and that of the optogalvanic signal $\Delta\nu(OG)$ was $\Delta\nu(RF)/\Delta\nu(OG)=\sqrt{2}$, which demonstrated that, as a consequence of the irradiation of the vapor by the laser resonant with the 4P level the electrons were produced by a process involving two 4P excited atoms, as the associative ionization

$$K(4P) + K(4P) \longrightarrow K_2^+ + e \qquad (7)$$

The direct photoionization process requires three photons (see figure 8) and was completely negligible because the laser power density was $\lesssim 10^3 W/cm^2$. The ratio between $\Delta\nu(OG)$ and the halfwidth of the fluorescence signal from one level close in energy to the 4P+4P energy (for example the 6S level) was $\Delta\nu(OG)/\Delta\nu(6S)\simeq 1$. Since the optogalvanic signal had a quadratic dependence upon the 4P atom density this demonstrated that also the population of the 6S level depends upon $N^2(4P)$, as in the process

$$K(4P) + K(4P) \longrightarrow K(6S) + K(4S) \qquad (8)$$

Finally looking at the fluorescence from a level far from the energy sum of two 4P atoms (for example the 7S level) it resulted $\Delta\nu(OG)/\Delta\nu(7S)\neq 1$, which showed that higher levels were not populated directly by the energy pooling collisions. These results[24] are shown in figure 9.

In the above experiment the detection of the variation of the electron density produced by the collisions has been indirectly used to interpret the collisional processes. A direct evidence of these processes was obtained in an important experiment[25] where an electron spectrometer was introduced for the first time to resolve the energy spectrum of the electrons created in the vapor. The experimental set up consisted in a weakly collimated effusive sodium beam excited by an orthogonal cw dye laser locked to an hyperfine component of the D_2 resonance line. The electrons emerging from the interaction zone were detected by a cylindrical mirror analyzer. The original apparatus[25] did not transmit electrons of low energy, but it has been recently modified[26] to detect also electrons of near zero energy. The absolute energy scale was accurately established and direct observationof superelastic collisions (4) was obtained. The resolved peaks in the electron energy spectrum have unambiguously proved that the primary electrons were created by purely collisional processes involving excited atoms; the first mechanism is the associative ion-

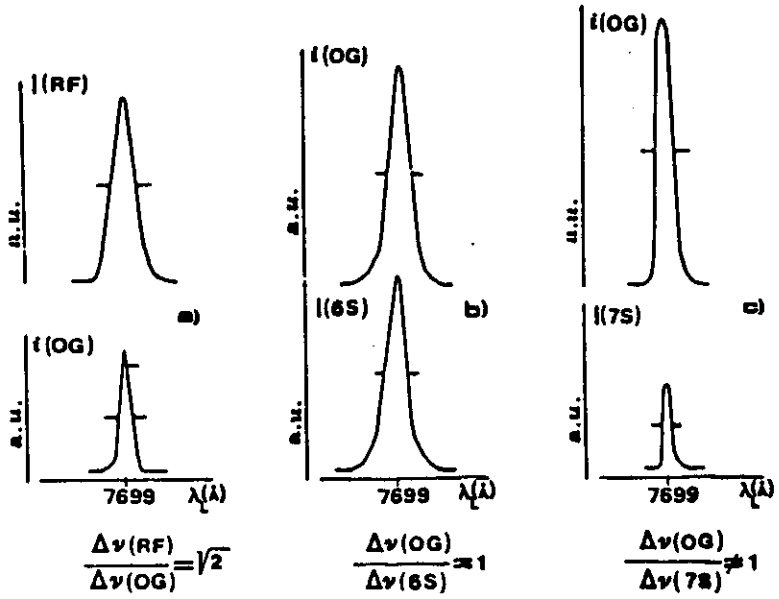

Fig. 9. Traces of the optogalvanic and resonance fluorescence ($4P_{1/2}$-$4S_{1/2}$) signals (a), of the optogalvanic and 6S-4P fluorescence signals (b) and of the optogalvanic and 7S-4P fluorescence signals (c) versus the laser wavelength, tuned across the $4S_{1/2}$-$4P_{3/2}$ atomic transition at 7699Å. The ratios between the relative widths at half maximum are also reported[24]. The shape of the signals is not uniform because the laser was scanned by hand; however this fact is insignificant for these results.

ization (3) and the second mechanism is the Penning ionization

$$Na(3P) + Na(nL) \longrightarrow Na^+ + Na(3S) + e(2.11eV - E(nL)) \qquad (9)$$

where Na(nL) are provided by the energy pooling collisions (5) and 2.11eV is the energy of a 3P atom. A typical energy spectrum of electrons ejected from the laser irradiated sodium vapor is shown in figure 10.

CROSS SECTION DETERMINATION

In the introduction we have mentioned some reasons for which it is interesting to investigate the energy pooling collisions. However, for any serious application or comparison with the theory,

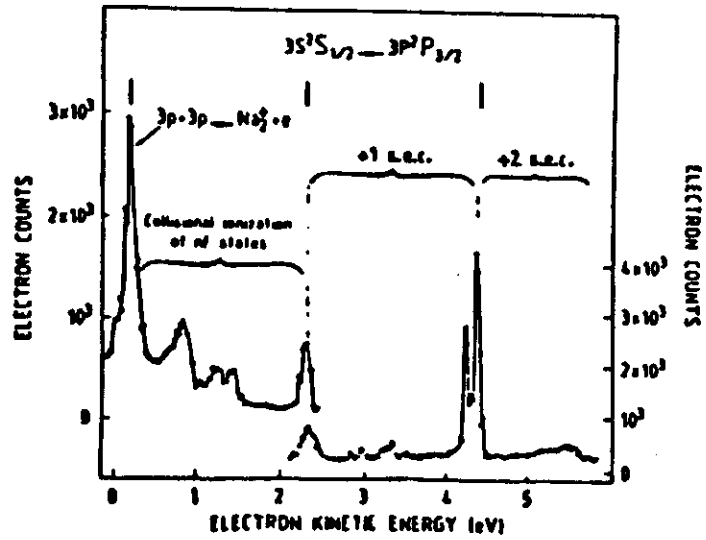

Fig. 10. Energy spectra of the electrons emitted from a cw laser excited Na vapor. Electrons from associative ionization and Penning ionization of nL states are also observed after 1 or 2 superelastic collisions with 3P state[27].

the rate coefficient K or cross section σ for the reactions (1) and (2) have to be measured with great accuracy. Since we are dealing with atoms having thermal energies we assume that K and σ are related simply by $K = \langle \sigma v \rangle = \sigma \bar{v}$, where $\bar{v} = \sqrt{8kT/\pi\mu}$ is the relative mean interatomic velocity. A common method used for the determination of the rate constants is based on the solution of the rate equations, in analogy with the familiar treatment of the sensitized fluorescence process (6)[28]. The rate equations for process (6) are

$$\dot{N}(A^*) = Z - N(A^*)/\tau(A^*) - KN(A^*)N(B) \qquad (10)$$

$$\dot{N}(B^*) = KN(B)N(A^*) - N(B^*)/\tau(B^*) \qquad (11)$$

where Z is the number of atoms excited from A to A^* per unit time and τ is the radiative lifetime of an excited level. Solution of equation (11) at the steady state gives

$$K = (1/N(B)N(A^*))(N(B^*)/\tau(B^*)) \qquad (12)$$

Usually the quantity measured in the experiments is the intensity of the fluorescence lines. Generally speaking the intensity per unit solid angle of a fluorescence line from a level i to a level j is related to the population of the level i by[29]

$$I(i,j) = \hbar\omega(i,j)A(i,j)\, N(i)\varepsilon(i,j)V/4\pi \qquad (13)$$

where $\omega(i,j)$ is the transition frequency, $A(i,j)$ is the spontaneous transition probability which is equal to $1/\tau$, $\varepsilon(i,j)$ is a factor which takes into account the instrumental response of the detecting apparatus and V is the fluorescence volume. Using relation (13) in equation (12) the rate coefficient K may be determined from the intensity ratio of the fluorescence from the excited states A^* and B^* to the ground state as

$$K = (1/N(B)\tau(A^*))(I(B^*)/I(A^*))(\omega(A^*)/\omega(B^*))(\varepsilon(A^*)/\varepsilon(B^*)) \qquad (14)$$

Therefore the measurement of K depends upon the density of ground state atoms B and the lifetime of the excited atoms A^*. While ground state atom density can be measured with great accuracy, the measurement of the lifetime of an excited state may present serious problems because of the radiation self-trapping phenomenon[30,31], which changes the natural lifetime to an effective lifetime. The error in the sensitized fluorescence cross sections is mainly due to the fact that it is difficult to measure the effective τ with great accuracy.

This same procedure can be applied to the collisions between excited atoms, however many more difficulties complicate a measurement of the rate coefficients K(nL) for process (1) and K(AI) for process (2). For sake of semplicity let us consider the experiments where all the processes other than the energy pooling can be neglected; then the following simplified rate equations can be written

$$\dot{N}(nL) = K(nL)N^2(nP) - N(nL)\sum_{n'L'} A(nL,n'L') \qquad (15)$$

$$\dot{N}(A_2^+) = K(AI)N^2(nP) \qquad (16)$$

Solution of equation (15) at the steady state gives

$$K(nL) = \sigma(nL)\bar{v} = (N(nL)/N^2(nP))\sum_{n'L'} A(nL,n'L') \qquad (17)$$

and integration of equation (16) over the time of A_2^+ production yields

$$K(AI) = N(A_2^+)/(N^2(nP)\,\Delta t) \qquad (18)$$

The population of the nL level can be determined by measuring the fluorescence intensity I(nL) and knowing the transition probabilities A(nL,n'L'), as shown in equation (13), since radiation trapping for the nL levels populated through the collisions (1) can be neglected in most of the experiments. The integrated Na_2^+ ion signal can be precisely measured in any experiment, provided the collection efficiency and the instrumental response of the overall apparatus is known. The crucial point for both K(nL) and K(AI) is the quadratic dependence upon the excited atom density N(nP), which is a quantity difficult to measure with high accuracy. Incorrect assumptions about the excited atom density and spatial distribution are the primary cause of orders of magnitude differences in the value of the cross sections measured in different experiments. In the experiments where fluorescence spectra are detected it is an advantage to take the ratio of the intensities I(nL)/I(nP) so that the absolute efficiency of the detection system and the volume do not enter directly in the calculations. However the laser-vapor interaction volume must be well definied for the determination of the excited atom density N(nP) and the fluorescence emitted from the levels nL and nP must be collected from the same volume. In a vapor the optical absorption length varies considerably with changes in the density of the absorbing atoms or in the laser intensity; as a consequence also the volume of laser-vapor interaction varies. This is one problem to be solved in the experiment. The second problem arises because of the radiation self-trapping and diffusion of the laser excited atoms. Owing to these phenomena the excited P atoms show an effective lifetime longer than the natural lifetime, as given by the transition probability, and are not confined to the laser beam cylinder. Then the radiation from the nL levels to the first P state is attenuated and the effective volume for nP/nP collisions extends outside the laser beam. A certain number of different experimental methods have been introduced to resolve all these problems and we will summarize here some of them.

In the experiments where ions can be detected a common method for the determination of the nP excited atom density relies on the measurement of the atomic ions A^+ produced by direct photoionization of the nP level with a second laser[32]. This approach has been used for example by Weiner and coworkers[32] for the determination of the absolute rate constants for process (3). Their apparatus consisted in two crossed effusive atomic sodium beams excited by a tunable flash-lamp dye laser to the $3P_{3/2}$ state from which the associative ionisation (3) takes place. A second Nd:YAG pumped dye laser provided the uv source to directly photoionize the 3P level by the process

$$Na(3P) + \hbar\omega \longrightarrow Na^+ + e \qquad (19)$$

The Na^+ ion signal was linear with the 3P atom density and the volume of production coincided with the volume swept out by the photoionizing laser. The Na_2^+ ions, before saturation, showed a quadratic dependence upon the 3P atom density and were produced in an enlarged effective volume because of the diffusion of the trapped 3P atoms outside the laser beam. The actual volume of excited atoms was determined by comparing the Na^+ signal when only the photoionizing laser was on with the Na^+ signal when both lasers were on. The correct intensity of Na_2^+ ion signal, necessary to determine the associative ionization cross section, was then given by the total Na_2^+

yield divided by this volume. The effect of radiation trapping on the lifetime of the excited atoms was determined with the same apparatus by monitoring the decrease of the Na^+ ion signal versus the time delay between the laser tuned to the $3S_{1/2}$-$3P_{3/2}$ transition and the uv laser which photoionized the 3P atoms. A similar approach, based on the direct photoionization given by a second laser, has been extensively used in the studies of Penning and associative ionizations of highly excited rubidium atoms[33] and energy pooling collisions between 5P rubidium atoms[34].

Two original methods for the excited atom density determination have been introduced by Huennekens and Gallagher[35] and by Allegrini et al.[36] during the measurement of the energy pooling cross section for the 5S and 4D states in sodium

$$Na(3P) + Na(3P) \longrightarrow Na(5S,4D) + Na(3S) \qquad (20)$$

The first approach takes advantage of radiation trapping to measure the spatial and temporal distribution of the 3P atoms, the second uses the saturation of the resonant 3P-3S fluorescence for an absolute calibration of the apparatus at low temperature, when radiation trapping is avoided. In both experiments a special collision cell was built to overcome the difficulties related to the determination of the laser-vapor interaction volume. The cell of Huennekens and Gallagher was a cross shaped 5-cm stainless steel block with vacuum sealed sapphire windows which do not react with the sodium vapor. Two sapphire rods were also placed in the opposite arms of the cross (see figure 11) to create the correct geometry for radiation trapping calculations. Pulsed excitation from a dye laser, (peak power $\simeq$ 60μJ, pulse duration $\sim$5nsec, linewidth $\sim 0.5 cm^{-1}$), tuned to the D_2 resonance line was used to produce the Na(3P) atoms. The experiment was performed in radiation trapping conditions which were well described by the Holstein theory[31]. Thus the spatial distribution of the 3P atoms was obtained by measuring the resonance fluorescence intensity and using the Holstein theory for the diffusion of the trapped atoms. The time dependence of the 3P atom density was obtained by looking at the change in the transmission of a cw laser, following the pulsed excitation. The cw laser was a single mode dye laser, highly attenuated ($\simeq$100μW) and tuned to the far wings of the D_2 resonance transition. Once the absolute value for spatial and time dependences of the 3P atom density was measured the cross sections for 5S and 4D formation by 3P/3P collisions were obtained by measuring the fluorescence ratios of 4D-3P and 5S-3P to 3P-3S and solving the rate equations (15), specifically written for process (20).

The cell of Allegrini et al.[36] was a pyrex capillary cylindrical tube of internal radius $\sim$0.9mm with two polished slices of glass rods as windows. Sodium atoms were excited to the $3P_{3/2}$ state with a broadband ($\Delta\lambda$ could be varied from 0.3Å to 0.03Å)

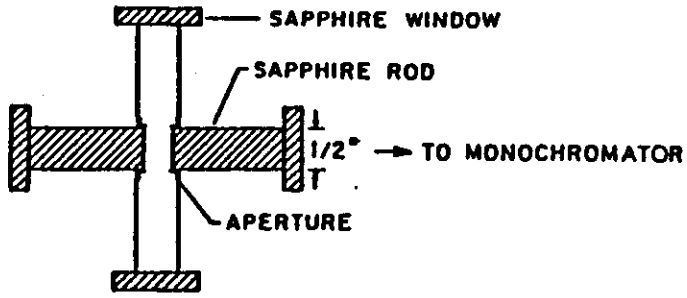

Fig. 11. Top view of the collision cell used by Huennekens and Gallagher (taken from ref. /37/).

cw dye laser of moderate power $\leq 10 W/cm^2$. The laser beam illuminated the whole cross section of the cell uniformly and the effective volume from which the fluorescence was detected was further defined by a narrow slit $\simeq$150μm placed near the entrance window. Excited atom density was determined absolutely at a low temperature T, in absence of radiation trapping, by observing the saturation of the resonance fluorescence signal. In fact at saturation the $P_{3/2}$ population density is related to the ground $S_{1/2}$ atom density simply by the level degeneracies. The 3P density at temperatures T', high enough to allow observation of fluorescence from the collision populated 5S and 4D states, was determined by comparing the intensity of the resonance fluorescence signals at T and T'. The radiation trapping present at T' was considered by correcting the natural lifetime of the 3P level with the trapped lifetime calculated from the Milne[30] theory, valid in the conditions of that experiment. Once the excited state density was known the cross sections for process (20) were obtained with the same procedure of rate equation solution and fluorescence intensity ratio measurements. The two above experiments have given results which agree within the experimental errors (see table 1), although the methods used for the excited atom density determination were very different and excitation was pulsed in one case[35] and cw in the other[36]. Previous measurements were different as much as five orders of magnitude; this fact evidences the difficulties in measuring the cross sections for energy pooling collisions, but it also proves that the solution to the many problems is not unique.

CONCLUSIONS

In these notes the background aspects of the energy pooling collisions rather than a complete review of the full work done in this field, have been presented. This presentation has been inten-

Table 1. Comparison of the Na(5S,4D) energy pooling cross sections experimentally determined in references /35/ and /36/.

Level	T(K)	σ (cm^2)	Ref.
5S	597	$(1.6 \pm 0.6)\times10^{-15}$	35
	483	$(2.0 \pm 0.7)\times10^{-15}$	36
4D	597	$(2.3 \pm 0.8)\times10^{-15}$	35
	483	$(3.2 \pm 1.1)\times10^{-15}$	36

tionally oversimplified by treating the energy pooling processes as singled out from multiphoton ionization, laser induced and other collisional processes. Seldom this is the case in the actual experiments; however the aim of these notes was to give the basic idea of the energy pooling processes and the general detection methods. While the qualitative interpretation of the phenomena involving collisions between excited atoms was immediate, many problems were met to get quantitative reliable values of the cross sections. A special emphasis has been placed here on these problems and on some approaches used for their solution. A table with updates results for the energy pooling cross sections for the alkalis can be found in ref.38.

Theoretical work has been very limited; the cross section has been calculated only for few levels populated through the collisions between excited atoms (for a complete list see ref. /38/). Although the order of magnitude of these cross sections agrees with the experimental determinations, the theoretical method used is not fully valid at the interatomic distances relevant to energy pooling collisions. Complete calculations, based on the Multi-Configuration-Self-Consisted-Field approach, are in progress[39] and they should provide a useful map of the interatomic potential energy curves for any internuclear distance.

ACKNOWLEDGMENTS

This work has been partially supported by a U.S.-Italy Cooperative Science Program, C.N.R. Grant no. 47423.

I am particularly grateful to Professor Ugo Fano for his generous contributions to this lecture. I am also indebted to Dr. Silvia Gozzini for assistance in preparing the typescript and to Dr. Mike Kelley for a critical reading of the manuscript.

REFERENCES

1. L. Jahreiss and M.C.T. Huber, Phys. Rev. A28, 3382 (1983) and references therein
2. A. Kopystynska and L. Moi, Phys. Rep. 92, 135 (1982)
3. "Photon-Assisted Collisions and Related Topics", N.K. Rahman and C. Guidotti eds., Harwood Academic, Chur (1982)
4. "Collisions and Half-Collisions with Lasers", N.K. Rahman and C. Guidotti eds., Harwood Academic, Chur (1984)
5. "Atomic and Molecular Collisions in a Laser Field", J.L. Picqué, G. Spiess and F. Wuilleumier eds., Journal de Physique, Serie des Colloques (1984)
6. M. Allegrini, W.P. Garver, V.S. Kushawaha and J.J. Leventhal, Phys. Rev. A28, 199 (1983)
7. M. Allegrini, G. Alzetta, A. Kopystynska, L. Moi and G. Orriols, Opt. Comm. 22, 329 (1977)
8. J. Keller and J. Weiner, Phys. Rev. A30, 2134 (1984)
9. A.C.G. Mitchell and M.W. Zemansky, "Resonance Radiation and Excited Atoms", Cambridge University Press (1971)
10. J. Huennekens and A. Gallagher, Phys. Rev. A28, 238 (1983)
11. R.M. Measures and P.G. Cardinal, Phys. Rev. A23, 804 (1981)
12. T.B. Lucatorto and T.J. McIlrath, Phys. Rev. Lett. 37, 428 (1976)
13. T.J. McIlrath and T.B. Lucatorto, Phys. Rev. Lett. 38, 1390 (1977)
14. W. Miller and I.V. Hertel, Appl. Phys. 24, 33 (1981)
15. M. Allegrini, G. Alzetta, A. Kopystynska, L. Moi and G. Orriols Opt. Comm. 19, 96 (1976)
16. C. Laughlin, J. Phys. B: At. Mol. Phys. 11, 1399 (1978)
17. M.H. Nayfeh, private communication
18. G.H. Bearman and J.J. Leventhal, Phys. Rev. Lett. 41, 1227 (1980)
19. V.S. Kushawaha and J.J. Leventhal, Phys. Rev. A25, 346 (1982)
20. A.N. Nesmeyanov, "Vapor Pressure of the Chemical Elements", Elsevier, New York (1963)
21. M. Allegrini, S. Gozzini, I. Longo, P. Savino and P. Bicchi, Nuovo Cimento D1, 49 (1982)
22. V.S. Kushawaha and J.J. Leventhal, J. Chem. Phys. 75, 5966 (1981)
23. R.B. Green, R.A. Keller, G.G. Luther, P.K. Schenck and J.C. Travis, Appl. Phys. Lett. 29, 727 (1976)
24. M. Allegrini and P. Bicchi, in ref. /3/ pag. 227
25. J.L. Le Gouet, J.L. Picqué, F. Wuilleumier, J.M. Bizeau, P. Dhez, P. Koch and D.L. Ederer, Phys. Rev. Lett. 48, 600 (1980)
26. J.M. Bizeau, B. Carré, P. Dhez, D.L. Ederer, P. Gerard, J.C. Keller, P.M. Koch, J.L. Le Gouet, J.L. Picqué, F. Roussel, G. Spiess and F. Wuilleumier, in ref. /5/
27. J.M. Bizeau, B. Carré, P. Dhez, D.L. Ederer, J.C. Keller, P. Koch, J.L. Le Gouet, J.L. Picqué, G. Spiess and F. Wuilleumier, Proc. XIII Int. Conf. Physics Electronic and Atomic Collisions, Berlin 1983
28. M. Elbel, in "Progress in Atomic Spectroscopy", W. Hanle and H. Kleinpoppen eds., Plenum Press, New York (1979), pag. 1299
29. W.L. Wiese, in "Progress in Atomic Spectroscopy", W. Hanle and

H. Kleinpoppen eds., Plenum Press, New York (1979), pag.1101
30. E.A. Milne, J. London Math. Soc. 1, 40 (1926)
31. T. Holstein, Phys. Rev. 72, 1212 (1947); 83, 1159 (1951)
32. R. Bonanno, J. Boulmer and J. Weiner, Phys. Rev. A28, 604 (1983)
33. M. Cheret, L. Barbier, W. Lindinger and R. Deloche, J. Phys. B: At. Mol. Phys. 15, 3463 (1982)
34. L. Barbier and M. Cheret, J. Phys. B: At. Mol. Phys. 16, 3213 (1983)
35. J. Huennekens and A. Gallagher, Phys. Rev. A27, 771 (1983)
36. M. Allegrini, P. Bicchi and L. Moi, Phys. Rev. A28, 1338 (1983)
37. J.P. Huennekens, Ph.D. thesis, University of Colorado, 1982
38. M. Allegrini, C. Gabbanini and L. Moi, in ref. /5/
39. R. Colle, private communication.

ELECTRONIC ENERGY TRANSFER INDUCED BY COLLISION BETWEEN TWO EXCITED SODIUM ATOMS

M. ALLEGRINI, G. ALZETTA, A. KOPYSTYNSKA* and L. MOI
Laboratorio di Fisica Atomica e Molecolare del C.N.R., Pisa, Italy

and

G. ORRIOLS
Departament d'Optica, Universitat de Barcelona, Barcelona, Spain

Received 5 May 1976

We have observed the sodium doublets arising from the 3^2D, 5^2S, 4^2D, 6^2S, $5^2D \rightarrow 3^2P$ and $4^2P \rightarrow 3^2S$ transitions, whenever sodium vapour is illuminated with a cw dye laser tuned to the wavelength of one of the D-lines. The phenomen is interpreted as an excitation transfer induced by collision between two excited atoms.

Fluorescence of saturated sodium vapour irradiated by a cw dye laser light tuned to the wavelength of the D_1 or D_2 resonance line has been examined in the spectral range from 3000 Å to 8300 Å. Besides the molecular sodium spectrum and the $3^2P \rightarrow 3^2S$ doublet we observed also the atomic doublets due to the transitions $3^2D \rightarrow 3^2P$, $5^2S \rightarrow 3^2P$, $4^2D \rightarrow 3^2P$, $6^2S \rightarrow 3^2P$, $5^2D \rightarrow 3^2P$ and $4^2P \rightarrow 3^2S$. The levels and transitions of interest are shown in fig. 1a. The experimental arrangement is sketched in fig. 1b.

The absorption cell containing sodium and a few torr of neon as buffer gas was made of commercial spectral lamp glass in order to avoid contamination of the walls. The temperature of the cell placed in an oven was varied in the range of 200–320°C. A cw dye laser (Rhodamine 6G pumped with an Ar^+ laser) with a beam cross-section of 0.1 cm^2, spectral width of 0.2 Å, 290 MHz mode spacing and power ranging from 10 to 200 mW was employed. Moreover, in order to increase the density of the excited atoms and to avoid self-trapping and self-absorption of the fluorescence light the beam was focused to a cross-section of about 0.02 cm^2 just behind the input window of the cell. The fluorescence arising from the small volume where

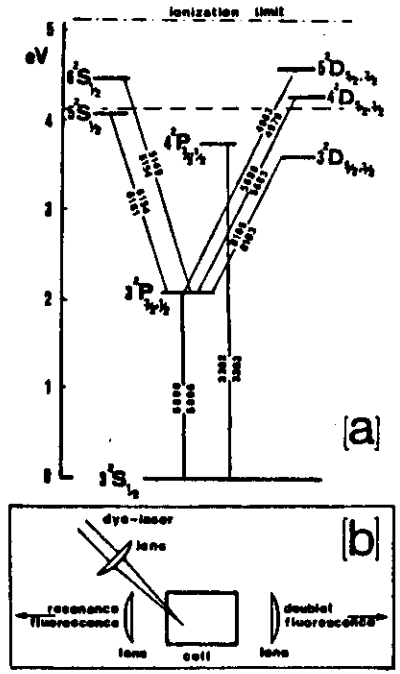

Fig. 1. a. Level diagram of Na with the observed transitions The sum of the electronic energy of two 3P excit atoms is marked by the dashed line.
b. Schematic diagram of the experimental arrangem

* On leave of absence from the Institute of Experimental Physics, University of Warsaw, Warsaw, Poland.

Table 1
Relative intensities of the observed doublets for D_1 excitation

Transition	ΔE (cm^{-1})	Relative intensities [a]			Discharge [b] lamp
		T = 250°C	T = 280°C	T = 320°C	
$3^2D \rightarrow 3^2P$	+ 4739	2.6	3.9	11.6	123
$5^2S \rightarrow 3^2P$	+ 711	1	1	1	1
$4^2D \rightarrow 3^2P$	− 637	0.4	0.7	1.0	3.0
$6^2S \rightarrow 3^2P$	− 2461	4.10^{-3}	5.10^{-3}	15.10^{-3}	80.10^{-3}
$5^2D \rightarrow 3^2P$	− 3125	5.10^{-3}	7.10^{-3}	34.10^{-3}	0.3
c) $4^2P \rightarrow 3^2S$	+ 3641	0.1	0.2	0.4	1.0

[a] For each temperature the intensities are normalized independently.
[b] Emission of 93122 E Philips spectral lamp, working at normal conditions, observed with our experimental arrangement.
[c] Values without correction for self-absorption and glass absorption.

ıe laser exciting light is almost completely absorbed
ras focalized on the slits of two monochromators in
rder to observe the resonance fluorescence and the
oublets independently, as seen in fig. 1b. The signals
erived from two photomultipliers (S-20 or S-20R)
ere amplified and simultaneously recorded. Thanks
) the geometrical disposition of the apparatus, the
sonance fluorescence did not go through the cell and
ıe effect of strong self-absorption had been avoided.
n the other side, self-absorption for the doublets (ex-
pt for the $4^2P \rightarrow 3^2S$ transition) was negligible.

The relative intensities of the doublets measured
different temperatures and with the exciting light
ined to the D_1 line are reported in table 1. It is seen
ıat the distribution of the intensities depends on the
anslational energy of the atoms, i.e. on the tempera-
ıre of the cell. The relative intensities of the doublets
)served in the light emitted by a Philips spectral lamp
orking at normal conditions are reported in the same
ble and they are quite different. Moreover, some
ansitions as $6^2D \rightarrow 3^2P$ and $7^2S \rightarrow 3^2P$ present in
e discharge emission light with intensities comparable
ith the transition $6^2S \rightarrow 3^2P$, in the fluorescence spec-
ım were not observed.

To give an order of magnitude of the ratio between
e intensity of the doublets and the intensity of the
sonance fluorescence we report a value $I(4D)/I(3P)$
10^{-5} measured at the temperature 220°C and about
)0 mW laser light power. $I(4D)$ and $I(3P)$ denote the
tensities of the respective doublet lines derived from
) and 3P levels. The intensity of each doublet in-
ıases strongly with the temperature (fig. 2) and with
the exciting laser light power (fig. 3).

The presence of both atomic D-lines in the fluores-
cence excited with the light tuned to the D_1 or D_2 line
wavelength is due to an energy transfer between fine
structure levels. This effect has been widely investigated
[1]. The presence of the doublets we have observed is
also interpreted as an electronic energy transfer induced
in a collision of two excited atoms and is to our know-
ledge reported here for the first time. The process can
be described by the following equation

$$Na(3P) + Na(3P) \rightarrow Na(3S) + Na(nX) + \Delta E, \qquad (1)$$

where $Na(nX)$ denotes the sodium atom in one of the
5S, 6S, 3D, 4D, 5D, 4P states and ΔE is the energy
defect or excess for the level nX with respect to twice
the electronic energy of the colliding Na(3P) atoms
(see table 1). ΔE is supplied from, or converted into,
translational energy of the atoms involved in the col-
lision. A third body, such as foreign gas or sodium
ground-state atom may also participate in the process
with its kinetic energy.

Let us denote by $N(3P)$ the population density of
atoms in the 3P state, and by $I(nX)$ the fluorescence
intensity arising from the nX level. The number of
processes per unit time, Z_{nX}, described by eq. (1),
and therefore the intensity $I(nX)$, depends on $N^2(3P)$.

$$I(nX) \sim Z_{nX} = \sigma_{nX} \bar{v} N^2(3P), \qquad (2)$$

where $\bar{v}$ is the mean relative velocity of the colliding
partners and σ_{nX} the cross-section of the process. The
$N(3P)$ density is related to the n_{Na} atomic density, to

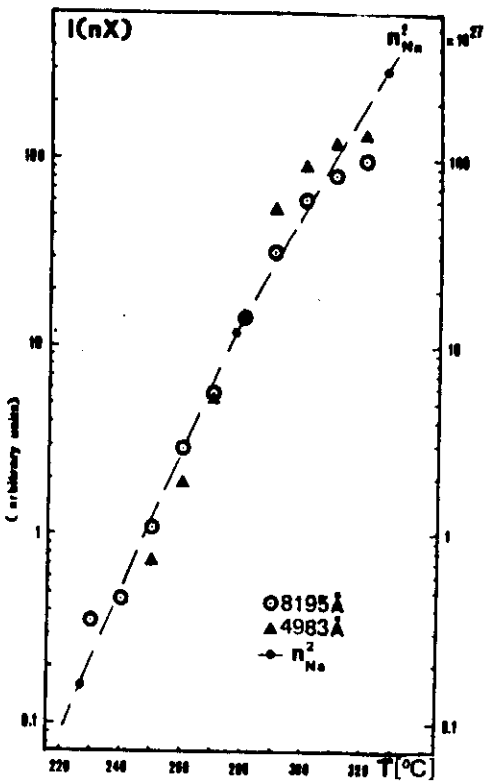

Fig. 2. Intensity of the doublets as a function of the temperature. The intensity values are normalized independently. The dashed line indicates the calculated square density of Na following Nesmeyanov's data [5].

the mean lifetime of the 3P state and to the intensity of the exciting light. Therefore, according to eq. (2) we could expect that the doublet intensities follow qualitatively the dependence of n^2_{Na} on the temperature and a square dependence on the power of the exciting light, as is confirmed by the experimental data reported in fig. 2 and fig. 3. The effect of self-trapping of the resonance fluorescence has been considered and in a qualitative analysis it can be neglected. Indeed, consistent results were obtained when the density of the excited atoms $N(3P)$ was changing at constant temperature and constant light intensity by sweeping the laser light wavelength λ_L over the broadened absorption profile of the D_1 or D_2 line. Simultaneous recording of $I(nX)$ and $I(3P)$ as a function of λ_L gave the dependence of $N(nX)$ on $N(3P)$. An example for the 5688 Å and 5153 Å lines is presented in fig. 4 and shows that the influence of the self-trapping is negligible. The plot in logarithmic coordinates of $I(nX)$ versus $I(3P)$ exhibits a slope equal to two.

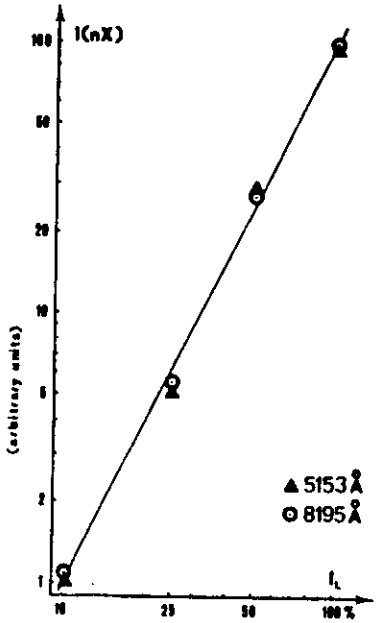

Fig. 3. Intensity of the doublets as a function of the intensity of the excitation light tuned to the D_1 line.

To test the effect of a foreign gas pressure we used another cell connected with a vacuum line and a reservoir of neon gas. In the residual presence of the gas ($< 10^{-3}$ torr) all the doublets previously reported in table 1 were observed only when the temperature of the cell was high enough (> 300°C). At lower temperature the $5^2D \rightarrow 3^2P$ and $6^2S \rightarrow 3^2P$ transitions could be observed only at higher neon pressure (~ 10 torr at 280°C). The relative intensities of the doublets show significant variations for pressure change from 10^{-3} torr up to about 10 torr, the transitions involving large values of ΔE being the most affected by the presence of a foreign gas.

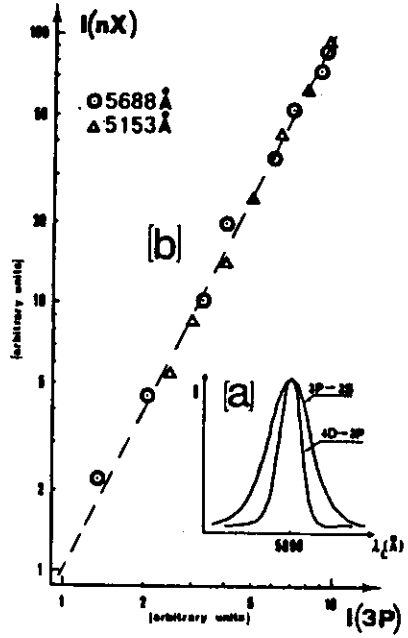

Fig. 4. a. A recording of the 3P → 3S and 4D → 3P fluorescence as a function of the exciting dye laser wavelength λ_L. The intensities have been normalized to the maximum of resonance fluorescence.
b. Intensity of the doublets 4D → 3P and 6S → 3P versus the intensity of the resonance fluorescence.

When the excitation with the D_1 line was substituted by the D_2 line similar results have been obtained but the relative intensities of the doublets were different. This can be related to the variation of ΔE values and to a different collisional behaviour of $3^2P_{1/2}$ or $3^2P_{3/2}$ excited atoms. As an example table 2 reports for both excitations the intensities of the doublets originated from the levels 4^2D, 5^2S and 3^2D.

The observed ratios $I(nX)/I(3P)$ indicate that the cross sections σ_{nX} ought to be relatively large and do not only depend on the energy defect, ΔE [2,3]. Precise measurements of the σ_{nX} values have not been carried out due to the lack of exact knowledge of the vapour density and of the effect of the radiation self-trapping. A rough evaluation supports the idea that the interaction between two excited atoms is of longer range and stronger than the interaction between one excited and one unexcited atom.

The study of such a type of interactions would be very important from the point of view of excited-atom collision spectroscopy [4] which certainly is involved in stellar processes, excited state chemistry, chemical reaction under laser radiation, etc.

Acknowledgement

Two of us (A.K. and G.O.) wish to express sincere thanks to Professors G. Alzetta and A. Gozzini for the kind invitation and the warm hospitality at LAFAM, Pisa.

References

[1] L. Krause, Physics of Electronic and Atomic Collisions, VII ICPEAC, 1971 (Amsterdam, 1972) p.65, and previous references cited therein.
[2] J. Pascale and J. Vandeplanque, J. Chem. Phys. 60 (1974) 2278.
[3] J. Cuvellier, P.R. Fournier, F. Gounand, J. Pascale and J. Berlande, Phys. Rev. A11 (1975) 846.
[4] C. Manus, Physics 82C (1976) 165.
[5] A.N. Nesmeyanov, Vapour Pressure of the Elements (New York, N.Y., 1963).

Table 2. Relative intensities of some observed doublets for D_1 and D_2 excitation at the temperature 280°C

Transition	ΔE(cm^{-1})		Relative intensities a)			
	D_1 exc.	D_2 exc.	b) D_1 exc.	D_2 exc.	c) D_1 exc.	D_2 exc.
$4^2D \rightarrow 3^2P$	− 637	− 603	0.7	1.3	0.8	0.9
$5^2S \rightarrow 3^2P$	+ 711	+ 745	1	1	1	1
$3^2D \rightarrow 3^2P$	+ 4739	+ 4773	2.0	1.7	3.9	3.7

a) For each row the intensities are normalized independently.
b) Measured at residual pressure of neon gas.
c) Measured at ~ 5 torr of neon gas.

MOLECULE FORMATION AND ENERGY TRANSFER PROCESSES IN A VAPOR WITH HIGH DENSITY OF 3P-EXCITED SODIUM ATOMS

M. ALLEGRINI[1], G. ALZETTA, A. KOPYSTYNSKA[2], L. MOI and G. ORRIOLS[3]
Laboratorio di Fisica Atomica e Molecolare del CNR, Pisa, Italy

Received 8 June 1977

A rich fluorescence spectrum extending between 4000 and 8200 Å has been observed whenever sodium vapor is excite by dye laser light tuned to the $3^2S \rightarrow 3^2P$ transition. Molecule formation due to collisions between excited and unexcite atoms is manifested by the presence of an emission band of sodium in the spectral range 4160–4570 Å.

In a dense sodium vapor (10^{13}–10^{15} atom cm^{-3}) irradiated by dye laser light tuned to the $3^2S_{1/2} \rightarrow 3^2P_{1/2}$ or $3^2P_{3/2}$ transition, a high density of excited atoms can be created. Collisions involving these excited atoms lead to several processes of excitation energy transfer and molecule formation which cause a spectacular enrichment of the fluorescence spectrum.

The spectral analysis of the fluorescence light has been performed in an experimental arrangement similar to that previously described [1]. The cell, containing distilled sodium with residual potassium impurities and a few torr of neon, was maintained at constant temperature in the range of 250–400°C. A cw dye laser beam (maximum power ≃ 100 mW, spectral width ≈ 0.4 Å) was slightly focused just behind the input window and the fluorescence light was observed from the same side of the cell. Different filters were placed in front of monochromator in order to avoid the scattered laser light. A nitrogen pumped dye laser with the dyes Rhodamine 6G, Coumarin, POPOP and Delft Weiss BSW [2] has been also used. The maximum peak power of the nitrogen laser is 400 kW at 3371 Å.

In fig. 1 are shown the fluorescence spectra record-

[1] Present address: National Research Council, Herzberg Institut of Astrophysics, Ottawa, Canada.
[2] On leave of absence from the Institute of Experimental Physics, University of Warsaw, Poland.
[3] On leave of absence from the Department of Optics, University of Barcelona, Barcelona, Spain.

ed at the cell temperature of 380°C when the cw dy laser light frequency was in resonance with the 3^2S 3^2P transition (fig. 1a), and for comparison, when it

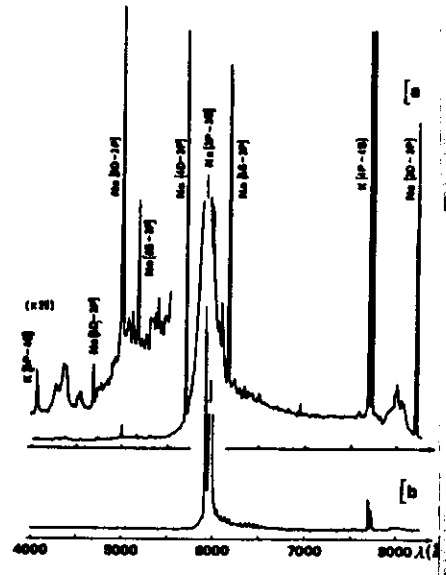

Fig. 1. Fluorescence spectra excited by cw dye laser. a) Lase tuned to the $3^2S_{1/2} \rightarrow 3^2P_{1/2}$ transition, b) laser out of the sodium resonance lines (5940 Å). Temperature – 380°C, lig power – 40 mW.

was out of the resonance (fig. 1b). In the latter case the laser light with wavelength 5940 Å excites the $B\,^1\Sigma^+$ and $C\,^1\Pi$ states of NaK molecules [3,4] present in the cell as a consequence of potassium impurities, and with much less probability the $A\,^1\Sigma_u^+$ state of Na_2 molecules [5,6], giving rise to emission of the overlapping bands as well as to the atomic fluorescence originating from the dissociation products of the respective molecular states [7]. Electronic energy transfer from excited molecules to sodium and potassium atoms can also contribute to the population of the atomic levels [8].

Whenever the cw dye laser light is tuned to the $3\,^2S_{1/2} \rightarrow 3\,^2P_{1/2}$ or $3\,^2P_{3/2}$ transition, the fluorescence spectrum is enriched by the occurrence of several sodium and potassium atomic doublets, the well known Na_2 and NaK molecular bands (the number of K_2 molecules is negligible) and a diffuse band extending from 4160 to 4570 Å which does not correspond to any reported alkali diatomic molecular band. The general features of the spectrum do not show appreciable dissimilarities when instead of the cw dye laser the pulsed dye laser is used.

The spectrum is almost completely due to the collision processes involving sodium excited atoms, schematically presented in fig. 2. Moreover, some secondary processes can contribute to the spectrum, and their share increases with the temperature. A more detailed description of the several fluorescence components with a brief analysis of their origin will be given below. The intensities reported here (measurement performed at the cell temperature of 380°C and the laser power of 40 mW) are corrected for monochromator and photomultiplier spectral responses and then normalized to the resonance fluorescence line intensity. The values obtained in this way give an idea of the weights of the discussed processes. Owing to the strong selftrapping of the sodium resonance radiation, the normalized intensities cannot be directly related to the probabilities of the respective processes.

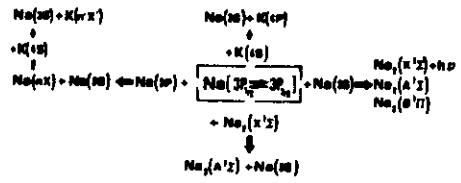

Fig. 2. Processes occurring in a vapor with high density of Na(3P) atoms.

Atomic doublets. The line corresponding to the transitions: $3\,^2P \rightarrow 3\,^2S$ for sodium and $4\,^2P \rightarrow 4\,^2S$ for potassium, are the most intense in the spectrum. The appearance in the fluorescence of both the D sodium lines when the exciting light is tuned either to the $3\,^2S_{1/2} \rightarrow 3\,^2P_{1/2}$ or the $3\,^2S_{1/2} \rightarrow 3\,^2P_{3/2}$ transition is due to the energy transfer between fine structure levels. The potassium fundamental doublet is due to an electronic energy transfer induced by collisions between Na(3P) and K(4S) atoms [9]. Relative intensity of the doublet is 5×10^{-2}, whereas about 2% is due to the fluorescence from NaK dissociation and molecule–atom energy transfer.

The occurrence in the spectrum of the fluorescence lines originating from higher sodium levels has been recently reported [1] and interpreted as due to the collisions between two excited atoms leading to the energy transfer process:

$$\mathrm{Na(3P) + Na(3P) \rightarrow Na(3S) + Na}(n\mathrm{X}) + \Delta E, \qquad (1)$$

where Na(nX) denotes a sodium atom in one of the high excited states and ΔE denotes an energy defect or excess for the level nX with respect to twice the energy of 3P level. The normalized intensity of each of the strongest doublets (5686, 6159 and 8191 Å) is about 10^{-3}. The present experiment has been performed for higher temperatures of the vapor than previously, thus, besides those already reported, the doublets corresponding to the transitions: $7\,^2D \rightarrow 3\,^2P$ (4497 Å), $6\,^2D \rightarrow 3\,^2P$ (4667 Å) and $7\,^2S \rightarrow 3\,^2P$ (4751 Å) are also observed. The normalized intensity of the 4667 Å line is about 2×10^{-5}. All the doublets follow rather well a quadratic dependence on the laser light intensity up to the highest power obtained by means of the pulsed dye laser. Since, however, the energy defect ΔE in eq. (1) becomes large, we do not exclude the contribution of secondary collisional processes transferring population from a nX level to a higher one. A process of one-photon ionization of a nX level [10] is energetically possible and after electron recombination it may produce a population of higher levels. Nevertheless, the quadratic dependence on the light intensity is in favour of collisional character of the effective process.

Population of high excited potassium levels is evidenced by the presence of some potassium doublets

in the spectrum. These populations can be attributed to the secondary collisional processes as

$$\mathrm{Na(3P) + K(4P)} \quad \text{or}$$

$$\mathrm{Na}(n\mathrm{X}) + \mathrm{K(4S) \rightarrow Na(3S) + K}(n'\mathrm{X}') \qquad (2)$$

The most intense doublet corresponds to the transition $5\,^2P \rightarrow 4\,^2S$ (4045 Å) with normalized intensity about 6×10^{-5}.

Molecular bands. The Na_2 red ($A\,^1\Sigma_u^+ \rightarrow X\,^1\Sigma_g^+$) and NaK orange ($B\,^1\Sigma^+$, $C\,^1\Pi \rightarrow X\,^1\Sigma^+$) overlapping bands extending between 5600 and 8000 Å with the total intensity of $\sim 4 \times 10^{-2}$, and the Na_2 green ($B\,^1\Pi_u \rightarrow X\,^1\Sigma_g^+$) band [11] extending from 4600 to 5600 Å with the intensity of $\sim 7 \times 10^{-4}$ are seen in the spectrum. The presence of these bands is attributed either to an excitation energy transfer between 3P-excited atom and ground state molecule or to a molecule formation resulting from a recombination in collision between one excited and one unexcited atom [12]. The contribution of the two processes cannot be distinguished by a simple analysis of the fluorescence spectrum, but the former is almost resonant for the $A\,^1\Sigma_u^+$ state population and exhibits an energy defect of 3000–5000 cm^{-1} for the $B\,^1\Pi_u$ state population. Thus, in the green band case a participation of the molecule formation process seems to be dominating.

Diffuse emission band. This band, with the total intensity of 2×10^{-4}, extends between 4160 and 4570 Å and exhibits three well distinguished maxima at about 4260, 4340 and 4525 Å with a deep minimum at about 4470 Å (see fig. 3). Improving the resolution of the monochromator up to 1 Å, we have not observed a more detailed structure. The intensity of the band increases linearly with the exciting laser light intensity and, moreover, approximatively follows a square dependence of the sodium atomic density on temperature. The diffuse band has been also observed using a cell without foreign gas ($< 10^{-3}$ torr). An analogous band has been reported [13] for a cesium vapor.

Taking into account the above observations, the band is interpreted as due to molecule formation in a two-body collision with emission of radiation:

$$\mathrm{Na(3P) + Na(3S) \rightarrow Na_2}(X\,^1\Sigma_g^+) + h\nu. \qquad (3)$$

In order to test this interpretation the cell has been irradiated by the pulsed dye laser swept from 4170 to

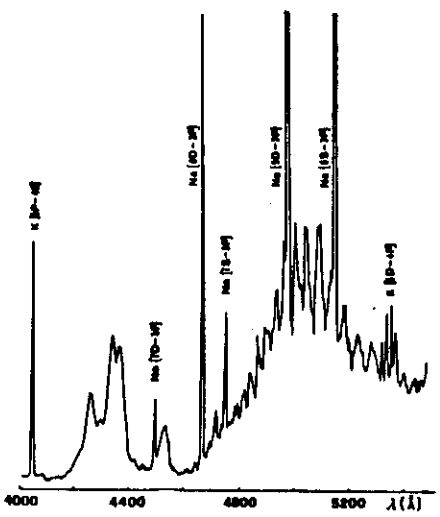

Fig. 3. Diffused band and green sodium band recorded at the cell temperature of 400°C and laser power of 80 mW.

4600 Å. In the spectral range of the diffuse band no fluorescence has been observed. Thus, the band does not originate from a bound state. Moreover, it is evident that the band cannot be due to a residual presence of potassium in the cell. In fact, a cell with potassium irradiated in the same way gives a molecular fluorescence extending between 4100 and 4800 Å due to the $C\,^1\Sigma_u^+ \rightarrow X\,^1\Sigma_g^+$ transition [14]. The shape of this band is quite different from the shape of the diffuse band.

The molecule formation observed in this experiment can be explained as follows. In a sufficiently dense vapor the atoms are relatively often in the state of collision, moreover, for high enough concentration of excited atoms, a great deal of these collisions occur between excited and unexcited atoms. For a central collision [15] we can define the turning point of the motion as the point of intersection of the horizontal line AC (see fig. 4) corresponding to the total energy of the system with the potential curve. The atoms spend most of the collision time near to the turning point. According to the Franck–Condon principle the radiative transition from this point goes vertically downward. If the transition A → B, shown in

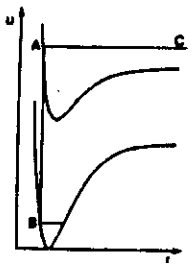

Fig. 4. Potential curves explaining molecule formation in two-body collision with emission of radiation.

fig. 4, leads to a bound vibrational level of the ground state, we have an example of the molecule formation. Since, however, in different individual collisions are involved different amounts of kinetic energy (different heights of the point A), we obtain a diffuse emission spectrum. The shape of this spectrum depends on the vicinity to the point A of other potential curves. For instance, the deep minimum seen in the diffused sodium band can be interpreted as due to a crossing with a potential curve of a state with forbidden radiative transition to the ground state.

In the case of noncentral collision [16] the atoms do not approach each other and at no point is their relative velocity zero. The colliding atoms with determinate impact parameters (angular momenta) interact in such a way, that they make a number of turns around one another and after fly off. Thus, the atoms are in interaction for a definite time. During this time the radiative transition to the molecular ground state can take place resulting in a diffuse emission band. The diffuse band ought to have a rotational structure. Nevertheless, due to the low resolution of our monochromator we could not observe such a structure.

The position of the diffused sodium band in the fluorescence spectrum has been calculated on the basis of the above explanation. Using the data after Demtröder and Stock [11] for $B\,^1\Pi_u$ and $X\,^1\Sigma_g^+$ sodium states, and according to the Franck–Condon principle it has been found, that the band originates just above the last bound level ($v' = 29$) of the $B\,^1\Pi_u$ state. The transition $v' = 29 \rightarrow v'' = 8$ corresponds to the wavelength of 4573 Å. Indeed, the band extends between 4160 and 4570 Å with the highest maximum at about 4340 Å. Supposing that the maximum corresponds to a transition to the vibrational level $v' = 10$ or 9, the kinetic energy of colliding atoms is 3.5–3.8 kT for $T = 653$ K.

In conclusion, we want to emphasize that laser excitation of sodium in a dense vapor leads to a great variety of collision processes which are manifested by sensitized fluorescence. It is also possible to observe rather rare process of molecule formation in two-body collision with emission of radiation. Finally the processes of excitation transfer from sodium atoms to potassium atoms and to sodium molecules are dominant and their large energy excess is converted to kinetic energy of colliding partners. This fact may be considered in order to explain other processes occurring in the vapor.

Two of us (A.K. and G.O.) wish to express sincere thanks to Professor Adriano Gozzini and to the colleagues from LAFAM for the kind invitation and the warm hospitality in Pisa.

References

[1] M. Allegrini, G. Alzetta, A. Kopystynska, L. Moi and G. Orriols, Opt. Commun. 19 (1976) 96.
[2] W. Majewski and J. Krasinski, Opt. Commun. 18 (1976) 255.
[3] F.W. Loomis and M.J. Arvin, Phys. Rev. 46 (1934) 286.
[4] M. Allegrini, L. Moi and E. Arimondo, Chem. Phys. Letters 45 (1977) 245.
[5] F.W. Loomis and S.W. Nile, Phys. Rev. 32 (1928) 873.
[6] S.E. Johnson, Katsumi Sakurai and H.P. Broida, J. Chem. Phys. 52 (1970) 6441.
[7] G. Alzetta, A. Kopystynska and L. Moi, Nuovo Cimento Lett. 6 (1973) 677.
[8] E.K. Kraulinya, E.K. Kopeikina and M.L. Janson, Chem. Phys. Letters 39 (1976) 565.
[9] M. Allegrini, G. Alzetta, L. Moi and D. Giulietti, Nuovo Cimento 28B (1975) 69.
[10] T.B. Lucatorto and T.J. McIlrath, Phys. Rev. Letters 37 (1976) 428.
[11] W. Demtröder and M. Stock, J. Mol. Spectr. 55 (1975) 476.
[12] G. York and A. Gallagher, JILA Report N.114, University of Colorado, Boulder, 1974.
[13] A.M. Bonch-Bruevich, S.G. Przhibelskii, V.A. Khodovoĭ and U.V. Khromov, Kvant. Elektron (Moscow) 3 (1976) 763.
[14] S.P. Sinha, Proc. Phys. Soc. 40 (1947) 436.
[15] G. Herzberg, Spectra of Diatomic Molecules (Van Nostrand, Princeton, 1950) p. 400.
[16] I. Lukach and Y.A. Smorodinskii, Zh. Eksp. Teor. Fiz. 55 (1968) 1296.

LETTERE AL NUOVO CIMENTO VOL. 31, N. 3 16 Maggio 1981

On the Process of Energy Transfer Induced by Collisions Between Two Excited Atoms.

M. ALLEGRINI, G. ALZETTA, A. KOPYSTYŃSKA (*), L. MOI and G. ORRIOLS (**)
Istituto di Fisica Atomica e Molecolare del C.N.R. - Via del Giardino 3, 56100 Pisa, Italia

(ricevuto il 16 Marzo 1981)

We come back to an experiment [1-5] dealing with energy-pooling collisions recently discussed by KRASIŃSKI *et al.* [3]. The experimental arrangement is described in ref. [1-4]. A cell containing sodium at atomic densities in the range $(10^{15} \div 10^{16})$ cm^{-3} and a few Torr of neon was irradiated by a c.w. dye-laser tuned to one of the resonance D-lines. The laser line width was about 30 GHz and the power could be ranged from 10 to 200 mW. The laser beam was focused inside the cell by a lens with focal length of 50 cm, but the phenomena reported were observed also without focalization. In the laser-induced fluorescence we observed several lines originating from levels lying higher than the $3P$-levels. For these lines we checked intensity dependences on the temperature of the cell, on the laser light intensity and on the laser line wave-length swept around the D_1 or D_2 lines. All dependences showed a quadratic behaviour and this allowed us to suppose that in the process of population of the nX high-lying levels two Na($3P$) atoms are involved. We wrote down this process in the form

$$\text{Na}(3P) + \text{Na}(3P) \rightarrow \text{Na}(3S) + \text{Na}(nX) + \Delta E, \tag{1}$$

where ΔE is the energy defect or excess for each nX level with respect to twice the energy of the $3P$-level.

The cross-section σ for this process has not been measured, however a theoretical estimation for the $4D$-level has been given by KOWALCZYK [6]. For example, at large interatomic distances (> 10 Å) and at a temperature of 277 °C σ results $2.3 \cdot 10^{-16}$ cm^2.

(*) Present address: Institute of Experimental Physics, University of Warsaw, ul. Hoża 69, 00-681 Warsaw, Poland.
(**) Present address: Department de Fisica Fondamental, Universitat Autónoma de Barcelona, Bellaterra (Barcelona), Spain.
(1) M. ALLEGRINI, G. ALZETTA, A. KOPYSTYŃSKA, L. MOI and G. ORRIOLS: *Opt. Commun.*, 19, 96 (1976).
(2) M. ALLEGRINI, G. ALZETTA, A. KOPYSTYŃSKA, L. MOI and G. ORRIOLS: *Opt. Commun.*, 22, 338 (1977).
(3) J. KRASIŃSKI, T. STACEWICZ and C. R. STROUD Jr.: *Opt. Commun.*, 33, 153 (1980).
(4) P. KOWALCZYK: *Chem. Phys. Lett.*, 68, 203 (1979).

By using the relative intensity of the $4D$-$3P$ transition with respect to the resonance fluorescence measured in our experiment (table I of ref. [1]), we may also estimate the experimental cross-section. In the steady-state regime the rate k_n of the nX-level population produced by mechanism (1) including cascade transitions is given by

$$k_n = \sigma_n \bar{v} = \frac{1}{N_{3P}^2}\left(\sum_j A_{nj} N_n - \sum_i A_{in} N_i\right), \tag{2}$$

where σ_n is the average cross-section of process (1), $\bar{v}$ is the mean relative velocity of the colliding partners, N_j denotes the population density of the j-level and A_{ij} is the radiative decay rate for the transition from level i to level j. The intensity of the fluorescence line emitted from the volume V per unit solid angle, due to the i-j transition, can be expressed by

$$I_{ij} = \frac{V}{4\pi} \hbar \omega_{ij} A_{ij} S_{ij} N_i , \tag{3}$$

where ω_{ij} is the transition frequency and S_{ij} is a number < 1 which describes in a qualitative way the influence of self-trapping.

For the $4D$-level the contribution of cascade transitions can be neglected and then eq. (2) takes the form

$$k_{4D} = \frac{A_{3P,3S}}{N_{3P}} \frac{\omega_{3P,3S}}{\omega_{4D,3P}} \frac{S_{3P,3S}}{S_{4D,3P}} \frac{I_{4D,3P}}{I_{3P,3S}}, \tag{4}$$

where expression (3) has been employed two times. Substituting into the above equation the ratio $I_{4D,3P}/I_{3P,3S} \approx 10^{-4}$ measured at 220 °C [1] and taking as reasonable values $A_{3P,3S} \approx 10^8\ \mathrm{s}^{-1}$, $N_{3P} < 5 \cdot 10^{13}\ \mathrm{cm}^{-3}$, $\bar{v} \approx 10^5\ \mathrm{cm\ s}^{-1}$ and $S_{3P,3S}/S_{4D,3P} \approx 10^{-1}$, we obtain $\sigma_{4D} > 10^{-16}\ \mathrm{cm}^2$. Very recently Lucatorto and McIlrath [5] have evaluated the cross-section of process (1) for all the levels observed in ref. [1]. The values vary from 10^{-15} to $10^{-17}\ \mathrm{cm}^2$, showing that mechanism (1) is not negligible as claimed by Krasiński *et al.* [3].

In the case of the lower-lying $3D$ and $4P$ levels an additional population by cascade transitions from higher levels populated directly by mechanism (1) may be remarkable. However, these cascade transitions lie in the infra-red region of the spectrum that was not analysed and, therefore, the corresponding cross-sections cannot be estimated. On the other hand, for the $5D$ and $6S$ levels, whose energy defect ΔE reaches values of about $8\ kT$, processes other than (1) may contribute to the population [3].

During the last few years a large number of experiments [6-16] dealing with phenomena occuring in dense metal vapours illuminated with resonant laser radiation have been performed. Almost complete ionization was observed in several metallic vapours [6,7] at atomic densities larger than $10^{14}\ \mathrm{cm}^{-3}$ and with laser power densities $> 1\ \mathrm{MW\ cm}^{-2}$. Some plasma features were observed in very dense ($\sim 10^{17}\ \mathrm{cm}^{-3}$) Cs [8] and Na [9] vapours irradiated by low-power c.w. lasers tuned to a transition starting from the first-excited level. In the experiment of ref. [10] performed in conditions similar to ours [1], it was found that besides the energy-pooling collisions leading to the population of high-lying levels also both Na_2^+ and Na^+ ions were formed in the ratio 10:1. The degree of ionization was low, because an estimated fractional ionization for Na^+ was 10^{-5}. Both the ions signals showed a quadratic dependence on the $3P$-level population. Recently Krasiński *et al.* [3] presented some arguments and also experimental results to prove that the fluorescence arising from high-lying levels which we observed cannot be produced by mechanism (1). They proposed another explanation, namely the direct excitation from $3S$- or $3P$-level by collisions of sodium atoms with superheated electrons. Such electrons would be produced by some ionization processes followed by superelastic collisions with the laser-excited atoms. Moreover, Krasiński *et al.* claim that in our experimental conditions [1,3] the laser-irradiated vapour is close to the total ionization. Hot electrons have been previously invoked to explain the full ionization observed in other experiments [6,7].

First of all it is necessary to clarify the assertion by Krasiński *et al.* [3] that in our experiment the fluorescence produced by mechanism (1) should show no dependence on the laser intensity, because the laser beam reaches intensities which are many times that required to saturate the $3S$-$3P$ transition and so the number of $3P$ excited atoms should remain unchanged. Nevertheless, in our experimental conditions the yellow fluorescence from the $3P$-levels increases with the laser power or when the resonant light intensity is increased by changing the tuning of the laser line over the narrower absorption line [1], showing that the number of $3P$ atoms in the volume observed by the photomultiplier increases too. With respect to this, we would like to mention some effects which must be taken into account when the optical saturation of a vapour by a c.w. laser beam is analysed: i) The discrete spectrum of the multimode laser implies that only a small fraction of atoms is coupled to the optical waves. Such a fraction increases with laser intensity as a consequence of the power broadening of the homogeneous absorption line. This effect is theoretically well known [16] and is responsible for the fact that in the saturation the absorbed power increases with the square root of intensity until the homogeneous width approaches the laser mode spacing. ii) The laser beam intensity shows a nonuniform spatial distribution due to the nonuniform intensity distribution across the beam and the eventual focalization. Moreover, when the vapour is dense enough, the laser beam is strongly attenuated along its way inside the cell. Such nonuniformities imply an expansion of the saturated volume with increasing laser power. Finally, let us remark that «anomalous» behaviours in the saturation of sodium and other metallic vapours have been actually observed in experiments with high-power pulsed lasers [11,17].

The first experiment by Krasiński *et al.*, performed in conditions similar to ours [1], consisted in the measurement of the width of the $3D$-$3P$ lines. If mechanism (1) is directly responsible for the $3D$ population, then the line width must be influenced by the energy excess ($\Delta E \approx 10\ \mathrm{kT}$). If the $3D$-excited atoms radiate before anything else happens, then the emitted line should show a flat-topped profile with a width of

(5) T. B. Lucatorto and T. J. McIlrath: *Appl. Opt.*, **19**, 3948 (1980).
(6) T. B. Lucatorto and T. J. McIlrath: *Phys. Rev. Lett.*, **37**, 428 (1976); **38**, 1390 (1977).
(7) C. H. Skinner: *J. Phys. B*, **13**, 55 (1980).
(8) A. C. Tam and W. Happer: *Opt. Commun.*, **21**, 403 (1977).
(9) M. E. Koch, K. K. Verma and W. C. Stwalley: *J. Opt. Soc. Am.*, **70**, 627 (1980).
(10) G. H. Bearman and J. J. Leventhal: *Phys. Rev. Lett.*, **41**, 1727 (1978).
(11) H. A. Bachor and M. Kock: *J. Phys. B*, **13**, L369 (1980).
(12) S. G. Leslie, J. T. Verdeyen and W. S. Millar: *J. Appl. Phys.*, **48**, 4444 (1977).
(13) T. Yabuzaki, A. C. Tam, M. Hou, W. Happer and S. M. Curry: *Opt. Commun.*, **24**, 305 (1978).
(14) A. Kopystyńska and P. Kowalczyk: *Opt. Commun.*, **25**, 351 (1978).
(15) V. S. Letokhov and V. P. Chebotayev: *Nonlinear Laser Spectroscopy* (Berlin, 1977), p. 50.
(16) D. D. Burgess and M. J. Eckart: *J. Phys. B*, **9**, L519 (1976); R. D. Driver and J. L. Snider:

about 3 times the thermal Doppler width. If only elastic collisions with a gas kinetic cross-section are considered, the time between collisions is longer than the $3D$-level decay time. However, this assumption is not so obvious because other perturbing processes cannot be excluded. For instance, in the presence of high density of $3P$ excited atoms, the long-range resonant excitation transfers between superthermal and thermal atoms may occur before the radiation from the $3D$-level takes place. Thus the observed lines should consist of two components resulting from the superthermal and thermal contributions. The thermal component becomes more important at higher atomic densities and should be affected by resonance broadening. Such effects cannot be omitted when the line shapes are analysed and their widths are determined. They are well known from the analysis of lines emitted after the dissociative recombination in the plasma afterglows ([18]).

On the other hand, population of the $3D$-level can be mainly due to cascade transition from the $4F$-level, for which $\Delta E \approx -1.5\,\mathrm{kT}$, and thus process (1) leading to the $4F$ population is expected to be much more probable. In such a case the superthermal effects would be negligible.

The pronounced increase of the line width with the temperature shown in fig. 4 of ref. ([2]) was not explained by the authors. Between the several possible explanations, Stark broadening can be invoked owing to the presence of ions inside the vapour.

However, a simple estimation based on the data taken after GRIEM ([19]) shows that the electron impact width for the $3D$-$3P$ line would not be sufficient to justify the reported widths, even if complete ionization is assumed, *i.e.* with an electron density equal to the atomic density the calculated values are 0.1 and 0.5 GHz for 277 °C and 327 °C, respectively. Since the density of $3P$ atoms is high, the resonance broadening may be also considered; unfortunately, to our knowledge, no theoretical or experimental data are available for the self-broadening of the $3D$-$3P$ lines. As a matter of fact, we found that the reported experimental points follow very closely a linear dependence on $\sqrt{N(T)}$ in the form $\Delta\nu = \Delta\nu_D + B\sqrt{N(T)}$, where $\Delta\nu_D$ is the Doppler width, B is a constant and N denotes sodium atomic densities drawn from Nesmeyanov's table ([20]).

KRASIŃSKI *et al.* ([2]) have performed a second experiment with the aim of discriminating the contribution of process (1) in the high-lying level population with respect to other processes. The vapour was irradiated by two pulsed dye-lasers with a power density of about $10^6\,\mathrm{W\,cm^{-2}}$, one of them tuned to $3S$-$3P$ resonance and the second detuned somewhat from resonance. The fluorescence from the high-lying levels and the electric current obtained with two electrodes inside the cell were the measured signals. The experiment consisted in comparing the signals obtained when the vapour was irradiated by only the resonant laser and when the two lasers acted simultaneously. In analysing the experiment, the most significant levels are expected to be the $5S$ and $4D$ ones which have the lowest ΔE values involved in (1) ($\sim 1\,\mathrm{kT}$). Instead the reported results concern the $5D$ and $6S$ levels, whose ΔE values are about $-8\,\mathrm{kT}$ and, therefore, process (1) is expected to be less probable. In such a case other mechanisms involving nonlinear radiative processes could be predominant owing to the high power densities employed in the experiment, namely 10^6 or 10^7 times higher than that used in our experiment ([1]). Moreover, the meaning of the experiment is not straightforward since some important details have not been specified, such as the detuning of laser 2,

([18]) M. A. BIONDI: *Principles of Laser Plasmas*, edited by G. BEKEFI (New York, N. Y., 1976), p. 131.
([19]) H. R. GRIEM: *Spectral Line Broadening by Plasmas* (New York, N. Y., 1974).
([20]) A. N. NESMEYANOV: *Vapour Pressure of the Elements* (New York, N. Y., 1963).

the dependence of the fluorescence and electric-current signal upon the detuning, wh signal is produced by laser 2 alone in the absence of laser 1.

Finally, KRASIŃSKI *et al.* ([2]) have published some misrepresented facts which mu be clarified: 1) BEARMAN and LEVENTHAL ([16]) observed the processes denoted in ref. (as (1) and (4) and they excluded a participation of hot electrons in the excitation $n\mathcal{L}$ levels. Actually the experiment has been repeated with great care ([21]) and su ports the idea that the energy-pooling collisions produce the population of high-lyi levels. 2) UZER and DALGARNO ([22]) calculated the effective cross-section for the phot dissociation of Na_2^+ ions in vibrational levels populated by absorption from the $B^1\Pi$ state of Na_2, and this is not relevant to the discussed experiments.

In conclusion, we retain that the work of Krasinski *et al.* ([2]) does not invalidate o results about the energy-pooling collisions in sodium vapour ([1,2]).

([21]) V. S. KUSHAWAHA and J. J. LEVENTHAL: *Phys. Rev. A*, **22**, 2468 (1980).
([22]) T. UZER and A. DALGARNO: *Chem. Phys. Lett.*, **61**, 213 (1979).

IL NUOVO CIMENTO Vol. 1 D, N. 1 Gennaio-Febbraio 1982

Resonant Laser Excitation of Potassium Vapour: Experimental Investigation of Energy-Pooling Collisions and Plasma Production.

M. ALLEGRINI, S. GOZZINI, I. LONGO and P. SAVINO

Istituto di Fisica Atomica e Molecolare del C.N.R. - Via del Giardino 3, 56100 *Pisa, Italia*

P. BICCHI

Istituto di Fisica Atomica e Molecolare del C.N.R. - Via del Giardino 3, 56100 *Pisa, Italia*
Istituto di Fisica dell'Università - Via Banchi di Sotto 57, 53100 *Siena, Italia*

(ricevuto il 29 Giugno 1981)

Summary. — The illumination of potassium vapour by means of a c.w. dye-laser resonant with the fundamental $4S \rightarrow 4P$ transitions results in the excitation of high-lying atomic and molecular states. In the present paper we report a spectroscopic study of this phenomenon and experimental evidence that the mechanisms responsible for the population of some of the levels not directly excited by the laser involve the creation of a plasma in the vapour.

1. – Introduction.

Multiphoton and collisional processes in alkali vapours irradiated by a laser tuned to a resonance transition have been recently considered in several experimental and theoretical papers (1).

The emission from highly excited atomic states following absorption of a c.w. dye-laser beam, tuned to the D_1 or D_2 line, was firstly detected in sodium

(1) For a review see T. B. LUCATORTO and T. J. MCILRATH: *Appl. Opt.*, 19, 3948 (1980).

vapour (2) and the effective lifetimes of some of these atomic states were measured (3). More recently the line width of one of the emitted lines was measured (4) in the effort to clarify the mechanism responsible for the fluorescence from the highly excited levels. Similar experiments on Cs vapour have been performed by TAM and HAPPER (5) with a c.w. dye-laser resonant with the $6P_{\frac{1}{2}} \rightarrow 8D_{\frac{1}{2}}$ transition and by LESLIE *et al.* (6) through pulsed-laser excitation tuned to the second resonance line. We have recently observed fluorescence from highly excited potassium atoms produced in collisions between sodium and potassium atoms (7).

In an experiment, simultaneous to the first report (8) on the excitation of the high-lying atomic states, almost complete ionization was observed in a 10 cm column of sodium, at atomic density $\simeq 10^{14}$ cm^{-3}, irradiated by a 1 MW pulsed-laser resonant with the $3S \rightarrow 3P$ transitions (9). Similar results were obtained soon after in Li (9,10) and again in Na (4,11-13).

The observations of fluorescence from atomic levels with energy higher than the level excited by the laser and of laser-driven ionization are two different approaches to the complicated problem of laser-vapour interaction. The link between the two experimental observations and the processes suggested for their explanation is evident in more complete works (9,14) where both the spectroscopic study and the analysis of the ionization products are made.

From the theoretical point of view, MEASURES, back in 1970 (17), suggested that laser excitation of an alkali vapour could result in an efficient ionization and, as a consequence of the experimental activity in this field, also the theo-

(2) M. ALLEGRINI, G. ALZETTA, A. KOPYSTYNSKA, L. MOI and G. ORRIOLS: *Opt. Commun.*, 19, 96 (1976); 22, 329 (1977).
(3) A. KOPYSTYNSKA and P. KOWALCZYK: *Opt. Commun.*, 25, 351 (1978).
(4) J. KRASINSKI, T. STACEWICZ and C. R. STROUD jr.: *Opt. Commun.*, 33, 158 (1980).
(5) A. C. TAM and W. HAPPER: *Opt. Commun.*, 21, 403 (1977).
(6) S. G. LESLIE, J. T. VERDEYEN and W. S. MILLAR: *J. Appl. Phys.*, 48, 4444 (1977).
(7) M. ALLEGRINI, P. BICCHI, S. GOZZINI and P. SAVINO: *Opt. Commun.*, 36, 449 (1981).
(8) T. B. LUCATORTO and T. J. MCILRATH: *Phys. Rev. Lett.*, 37, 426 (1976).
(9) T. J. MCILRATH and T. B. LUCATORTO: *Phys. Rev. Lett.*, 38, 1390 (1977).
(10) A. V. HELLFELD, J. CADDICK and J. WEINER: *Phys. Rev. Lett.*, 40, 1369 (1978).
(11) A. DE JONG and F. VAN DER VALK: *J. Phys. B.* 12, L561 (1979).
(12) P. POLAK-DINGELS, J. F. DELPECH and J. WEINER: *Phys. Rev. Lett.*, 44, 1663 (1980); J. WEINER and P. POLAK-DINGELS: *J. Chem. Phys.*, 74, 508 (1981).
(13) M. E. KOCH, K. K. VERNIA and W. C. STWALLEY: *Proceedings of the IQEC* (Boston, Mass., 1980), p. 627; *Proceedings of the IEEE Conference on Plasma Science* (Madison, Wis., 1980), p. 64.
(14) T. STACEWICZ: *Opt. Commun.*, 35, 239 (1980).
(15) F. ROUSSEL, P. BREGER, G. SPIESS, C. MANUS and S. GELTMAN: *J. Phys. B*, 13, L631 (1980).
(16) G. H. BEARMAN and J. J. LEVENTHAL: *Phys. Rev. Lett.*, 41, 1227 (1978); V. S.

retical interest has rapidly increased. A large number of processes has been considered and the relative cross-sections have been calculated [16-20].

In this paper we report the first experimental results concerning potassium. The phenomenon, as in the case of Cs vapour [5], is very spectacular to observe: by irradiating the vapour with the laser tuned to a resonant line, a bright white spot (fig. 1) appears at the entrance window of the cell containing potassium or in the focus of the lens if the laser beam is focused. The spectroscopic analysis of this white glow shows several lines, due to transitions from highly excited atomic states, and some molecular bands.

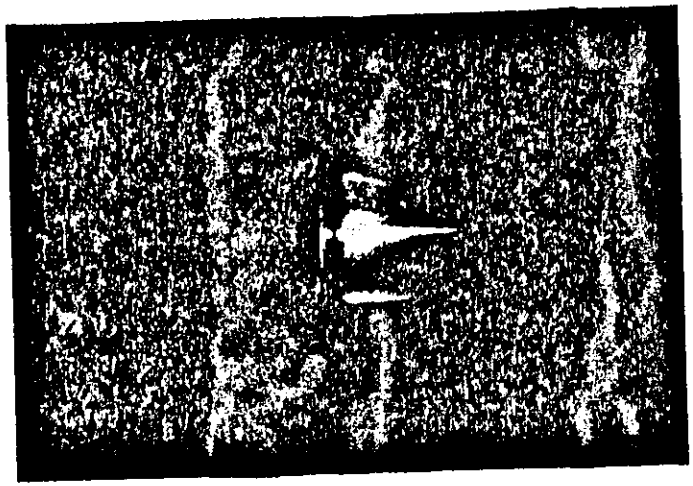

Fig. 1. – Photograph showing the white fluorescence inside the cell, produced by the resonant laser beam along its path.

2. – Description of the fluorescence spectrum.

The experimental apparatus is sketched in fig. 2. A pyrex cell containing potassium is irradiated with a c.w. dye-laser (Oxazine 1 Perchlorate), pumped by the two red lines of a Kr^+ laser, tuned to either D_2 (7665 Å) or D_1 (7699 Å) resonant lines. The dye-laser is broad band ($\Delta\lambda \simeq 0.5$ Å), multimode (mode spacing $\simeq$ 400 MHz) and of low power ($\sim(10 \div 100)$ mW); a beam splitter directs

[16] R. M. MEASURES: *J. Appl. Phys.* **48**, 7 (1977); R. M. MEASURES, P. L. WIZINOWICH and P. G. CARDINAL: *J. Appl. Phys.*, **51**, 3622 (1980); R. M. MEASURES and P. G. CARDINAL: *Phys. Rev. A*, **23**, 804 (1981).
[19] S. GELTMAN: *J. Phys. B*, **10**, 3057 (1977); **13**, 115 (1980).
[20] P. KOWALCZYK: *Chem. Phys. Lett.*, **68**, 203 (1979); **74**, 80 (1980).

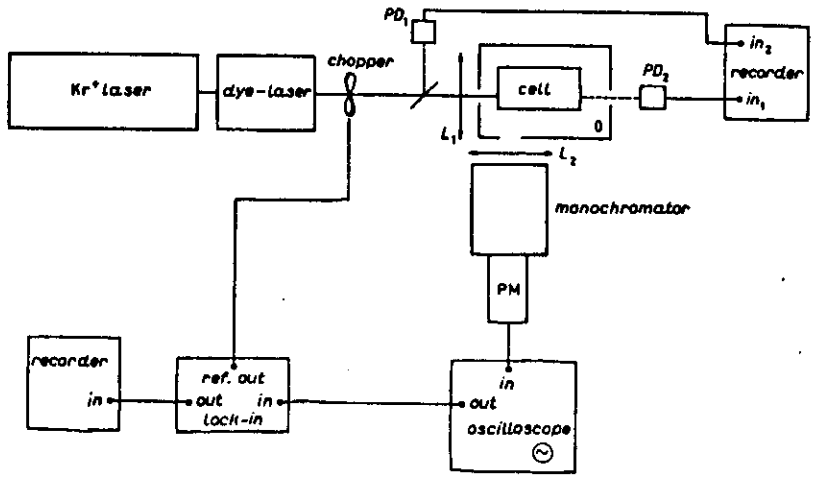

Fig. 2. – Experimental set-up.

a small fraction of the laser beam into a photocell and a second photocell monitors the light transmitted through the cell in order to control the variations of the laser power. The laser intensity is varied with calibrated neutral filters and in a continuous way with an interference filter or a polarization prism. The temperature of the cell is varied between 150 and 230 °C, corresponding to a potassium atomic density of $\sim(10^{13} \div 10^{14})$ atoms/cm^3 [21] and a Doppler width of $\sim$1 GHz, so that only two or three laser modes fall inside the inhomogeneously broadened atomic line. A buffer gas may be added into the cell at different pressures. To get a better signal-to-noise ratio, the beam is modulated by a mechanical chopper driven by the lock-in amplifier used for the phase-sensitive detection. The fluorescence is collected at right angles to the pump beam, dispersed by a $\frac{1}{2}$ m monochromator and detected by a photomultiplier sensitive in the spectral region (3400÷8200) Å. Self-absorption effects of the fluorescence light are avoided to some extent by focusing the input beam very near the exit window of the cell. Although the phenomenon is observable without any focusing, during the measurements we have focused the laser beam by a lens with 15 cm focal length; the laser beam waist is not changed appreciably by the lens and the maximum laser power density in this geometrical configuration results $\sim 10^3$ W/cm^2. The geometry of excitation and detection has to be carefully controlled because the volume of the vapour ex-

[21] A. N. NESMEYANOV: *Vapour Pressure of the Chemical Elements*, edited by R. GARY (Amsterdam, London, and New York, N. Y., 1963).

cited by the laser and then the density of excited atoms change with the temperature and the laser power. Although it is possible to take into account theoretically ([11]) the volume effects, we have experimentally overcome this problem by using a diaphragm in front of the monochromator slits.

The fluorescence spectrum contains lines due to transitions from many of the highly excited atomic states, up to the $12S$ level; of particular interest is the $3D \rightarrow 4S$ transition which is only quadrupole allowed. The levels involved in the transitions are reported in fig. 3 and a portion of the uncorrected

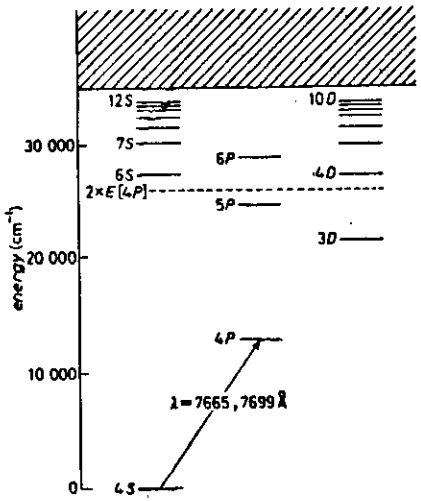

Fig. 3. – Sketch of the atomic levels of potassium from which fluorescence is monitored with our detection apparatus sensible in the spectral range (3400 ÷ 8200) Å.

spectrum showing the strongest lines is reported in fig. 4. The relative intensity of the transitions from the higher levels compared to the resonance fluorescence varies from $\sim 10^{-4}$ for the strongest lines to $\sim 10^{-9}$ for the weakest lines. Table I resumes the transitions observed in a cell containing potassium and 5 Torr of Ar at $T = 200$ °C; the energy difference ΔE between the upper level involved in the transition and the sum energy of two atoms in the $4P$-state is an important parameter and it is reported in the table in units of kT.

The density of potassium molecules at the temperatures of our experiment is only a few % of the atomic density and the laser frequency is not resonant with any molecular transition. Nevertheless we have observed in the spectrum three molecular bands: the $B^1\Pi_u \rightarrow X^1\Sigma_g^+$, which is very weak but well

([11]) S. GOZZINI: Thesis, Università di Pisa (1981).

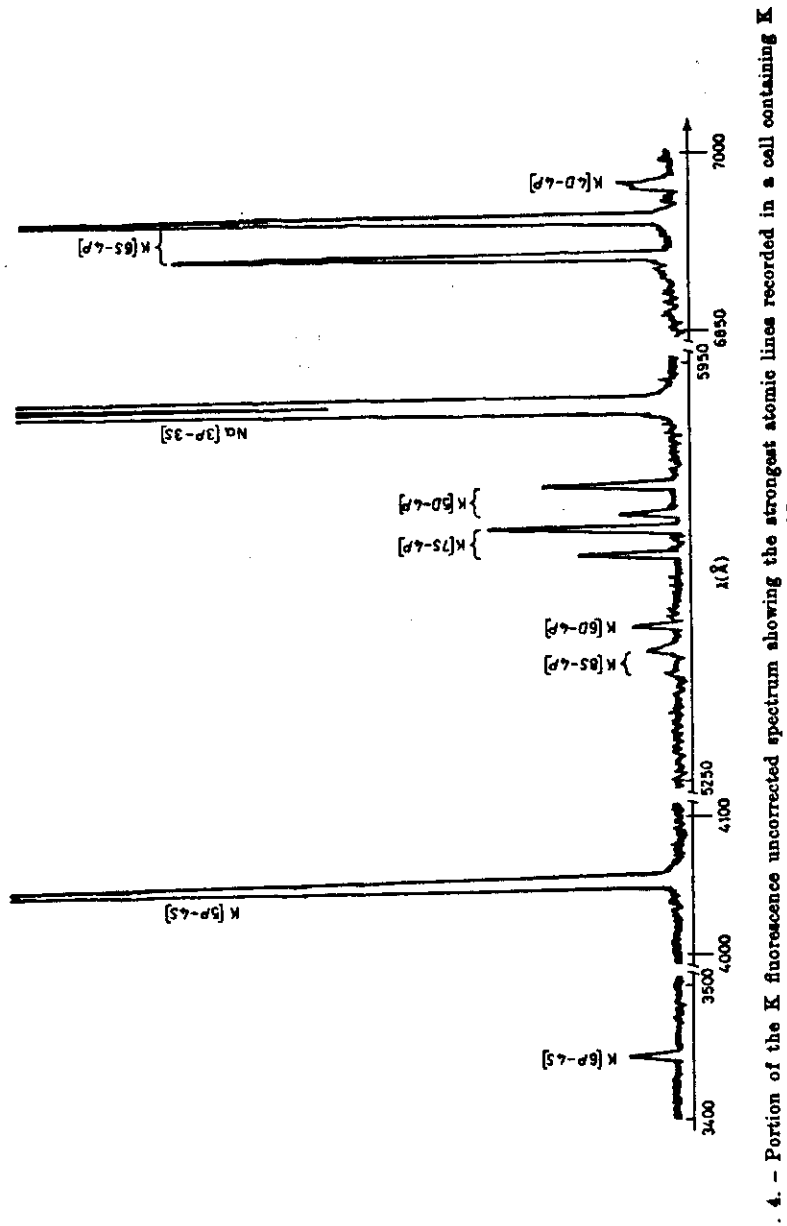

4. – Portion of the K fluorescence uncorrected spectrum showing the strongest atomic lines recorded in a cell containing K
5 Torr of Ar. The laser power is ~ 100 mW and the temperature 170 °C.

TABLE I. – *Atomic transitions of potassium observed in the spectral region* (3400 ÷ 8200) Å *in a cell containing* K *and* 5 Torr *of* Ar, *under excitation of the* D_2*-resonance line.* $T = 200$ °C, $kT = 329$ cm^{-1}, $P_L \simeq 100$ mW.

Transition	Wave-length (Å)	Relative intensity (a)	ΔE (b)
$4P \rightarrow 4S$	7665 ÷ 7699	1	
$5P \rightarrow 4S$	4044 ÷ 4047	10^{-4}	+ 4
$6P \rightarrow 4S$	3446 ÷ 3447	10^{-6}	— 9
$6S \rightarrow 4P$	6911 ÷ 6939	$5 \cdot 10^{-4}$	— 4
$7S \rightarrow 4P$	5782 ÷ 5802	10^{-5}	— 13
$8S \rightarrow 4P$	5323 ÷ 5340	$2 \cdot 10^{-6}$	— 17
$9S \rightarrow 4P$	5084 ÷ 5099	10^{-6}	— 20
$10S \rightarrow 4P$	4942 ÷ 4956	10^{-7}	— 22
$11S \rightarrow 4P$	4850 ÷ 4864	$3 \cdot 10^{-8}$	— 23
$12S \rightarrow 4P$	4787 ÷ 4800	10^{-8}	— 24
$4D \rightarrow 4P$	6936 ÷ 6965	$6 \cdot 10^{-5}$	— 4
$5D \rightarrow 4P$	5812 ÷ 5832	$6 \cdot 10^{-6}$	— 12
$6D \rightarrow 4P$	5343 ÷ 5360	10^{-6}	— 17
$7D \rightarrow 4P$	5097 ÷ 5112	$8 \cdot 10^{-7}$	— 20
$8D \rightarrow 4P$	4951 ÷ 4965	$2 \cdot 10^{-7}$	— 22
$9D \rightarrow 4P$	4856 ÷ 4870	$6 \cdot 10^{-8}$	— 23
$10D \rightarrow 4P$	4791 ÷ 4804	10^{-8}	— 24
$3D \rightarrow 4S$ (c)	4642	10^{-6}	

(a) The intensities are corrected according to the response of the elements of the detection apparatus. The relative intensities depend strongly upon the laser power, the temperature of the cell and the pressure and kind of buffer gas added in the cell. Thus the values here reported have to be considered approximate.
(b) ΔE is the difference between twice the energy of the $4P$-level excited directly by the laser and the upper level involved in the transition, expressed in unit of kT.
(c) Quadrupole-allowed transition.

identified by the vibrational constant ω_e of K_2; a very strong band in the red ($\sim$ (7200 ÷ 8000) Å), where the $A^1\Sigma_u^+ \rightarrow X^1\Sigma_g^+$ band is expected, and a diffuse band peaking at $\sim$ 5725 Å. The intensity of this band relative to the atomic transitions in the same spectral region can be inferred from fig. 5. The diffuse band shows a behaviour different from that of all the other atomic and molecular lines in the spectrum, first because it is present also when the laser is detuned from the atomic transition $4S \rightarrow 4P$ and secondly because it extends all along the laser path in the cell outside the white glow. Similar bands have been observed in low-power potassium discharges ([24]) and in our case can be

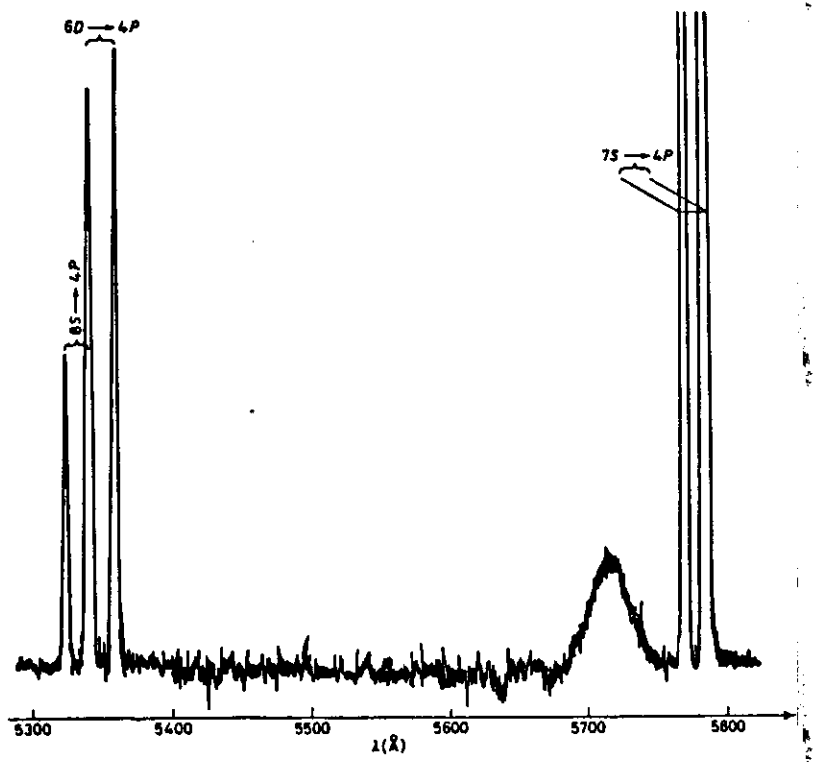

Fig. 5. – Diffuse molecular band peaking at 5725 Å and K atomic transitions in the same region of the spectrum.

due to two-photon transitions in the molecule; however, further work is needed to understand the mechanism of population of the molecular levels and their identification.

Another strong line present in the spectrum is due to the resonance transition $3P \rightarrow 3S$ of sodium which is present in the cell only as an impurity. The usual process of sensitive fluorescence, namely $K^*(4P) + Na(3S) \rightarrow K(4S) + Na^*(3P)$, has a small probability because the reaction is too endothermic and requires a conversion of ~ 0.5 eV of kinetic energy to internal energy. The presence of $3P$-excited sodium atoms is instead a consequence of electron impact excitation of the type $e^- + Na(3S) \rightarrow e^-(slow) + Na^*(3P)$, once the electrons have been created in the cell because of the processes induced by the laser on the potassium vapour. Indeed the cross-sections for the sensitive fluorescence process and the electron impact excitation have been calculated ([25])

We have analysed the fluorescence signal from each atomic level as a function of the laser intensity, the temperature of the cell and the pressure of the buffer gas and we were expecting the same dependences as already found in sodium (3). On the contrary, it is evident that the transitions arising from levels whose energy is within a few kT, the sum energy of two atoms in the $4P$-state, directly excited by the laser, have a different behaviour from the transitions coming from levels lying far away from $2 \times E(4P)$. A quantitative example is shown in fig. 6, where the intensities, measured in a cell containing

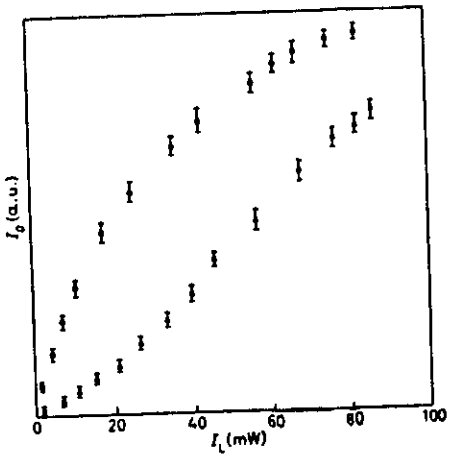

Fig. 6. – Fluorescence intensities (I_f) of the transitions $6S_{\frac{1}{2}} \rightarrow 4P_{\frac{1}{2}}$ (•) and $7S_{\frac{1}{2}} \rightarrow 4P_{\frac{1}{2}}$ (▲) *vs.* the laser intensity (I_L). The relative intensities are not comparable with each other.

K+5 Torr Ar, of the $6S_{\frac{1}{2}} \rightarrow 4P_{\frac{1}{2}}$ ($\Delta E \sim -4kT$) and $7S_{\frac{1}{2}} \rightarrow 4P_{\frac{1}{2}}$ ($\Delta E \sim -13kT$) transitions, are reported *vs.* the laser intensity at fixed temperature $T = 210$ °C. The same difference has also been found as a function of temperature at fixed laser intensity. The measurements as a function of the buffer gas have been made in a special cell with the possibility of changing the type and the pressure of the gas. As buffer gases we have used He, Ne and Ar. Unfortunately the results are not easily quantized. We can only assert that the intensity of the fluorescence from the highly excited atomic levels as a function of the buffer gas pressure becomes appreciable above a threshold, increases continuously till a maximum value to decrease drastically afterwards. The buffer gas pressure value, corresponding to the maximum fluorescence intensity, increases with the decrease of the atomic weight of the noble gas. For the three gases considered, the fluorescence is no longer observable for $P < 10^{-4}$ Torr and $P > 200$ Torr.

3. – On the mechanisms of production of the highly excited atomic states.

Several mechanisms are present in the literature leading to an appreciable population of the high-lying atomic states. A brief discussion on them, related to our experimental observations, will follow.

The energy excitation transfer,

$$K^* + K^* \rightarrow K^{**} + K \pm \Delta E, \tag{1}$$

where the star and the double star indicate the first P-excited level and a highly excited level, respectively, may be responsible for the population of the $6S_{\frac{1}{2}}$ and $4D$ levels of potassium, whose energy defect is $\Delta E \simeq 4kT$, at $T = 200$ °C, but it cannot explain by itself alone the population of levels such as the $12S$ whose $\Delta E \simeq 24\ kT$. In this process the energy difference is supplied or carried away by the translational motion of the colliding K atoms and/or buffer gas atoms, so that, if the energy defect ΔE increases, the number of atoms with the necessary kinetic energy decreases. The observed fluorescence dependence on the presence of the buffer gas and on its pressure would also be confirmed. For very low buffer gas pressures there are few atoms carrying the necessary kinetic energy, whereas at high pressures the collisions of K* atoms would be inhibited.

The expected dependence of the fluorescence on the laser intensity would be $I_f \propto I_L^2$ (I_f = fluorescence intensity, I_L = laser beam intensity) and that on the vapour density would be $I_f \propto [K^*]^2$. Indeed these dependences were observed in sodium (3) at low power density, but in this case with an increased laser power density the influence of other processes must be considered, as will be pointed out in the following. An exact dependence of the cross-section of the energy excitation transfer on the energy defect is unknown, but it is reasonable to suppose that, when a large energy amount has to be supplied by the translational motion, the cross-section becomes small. In sodium, for levels with an energy defect of $\Delta E \simeq kT$, the cross-section has been estimated to be $\simeq 10^{-15}$ cm^2 (30) and it decreases by an order of magnitude for levels with an energy defect up to $\sim 7\ kT$ (1).

As will be extensively dealt with in the next section, the observed phenomena can be explained by the presence of electrons, whose successive recombination with ions can populate the high-lying levels. In our experimental conditions we can exclude the influence of the two-photon ionization:

$$K^* + 2h\nu \rightarrow K^+ + e^-, \tag{2}$$

and the laser-induced ionization:

because of the low cross-section of these processes at our power density. The cross-section for the laser-induced ionization has been extimated by GELTMAN [25] and it is proportional to the laser intensity. At 10^3 W/cm^2 laser power density, the cross-section for potassium atoms is very small, $\sim 5 \cdot 10^{-25}$ cm^2.

The associative ionization

$$K^* + K^* \rightarrow K_2^+ + e^- \pm \Delta E \tag{4}$$

followed by the dissociative recombination process

$$K_2^+ + e^- \rightarrow K^{**} + K \pm \Delta E \tag{5}$$

has a cross-section $\sim 10^{-17}$ cm^2 [24] and may be responsible for the fluorescence observed only for rather high temperatures, the atomic states reached through process (5) depending on the electron energy in the recombination step. For thermal electrons only the K states almost resonant with twice the energy of K* can be produced, as in the energy excitation transfer. However, if the electrons undergo superelastic collisions with K* atoms, the dissociative recombination may populate the high-lying energy levels. An estimation of the feasibility of superelastic collisions can be given by using the available formula and data [25]. In potassium vapour at $T = 152$ °C and atomic density $\simeq 1.25 \cdot 10^{13}$ atoms/cm^3 the mean free path of the electrons is large compared to the dimensions of our cell and superelastic collisions have a negligible influence, as already pointed out in sodium [5]. At $T = 202$ °C and atomic density $\simeq 1.4 \cdot 10^{14}$ atoms/cm^3, the diffusion of the superelastic electrons is inhibited by the elastic collisions with the buffer gas, usually present in the cell, and, therefore, the superelastic collisions may be an important process in creating K** atoms. The number of K_2^+ ions depends on $[K^*]^2$ and has the same functional dependence on the laser intensity as in process (1). The processes so far considered do not explain completely our experimental results, thus we suggest two other possible mechanisms: the atomic ionization in energy pooling of three excited atoms:

$$\begin{array}{l} K^* + K^* \rightarrow K^{**} + K \\ \qquad\quad \hookrightarrow + K^* \rightarrow K^+ + K + e^-, \end{array} \tag{6}$$

or the absorption of a photon and the photoionization from a high-lying state:

$$\begin{array}{l} K^* + K^* \rightarrow K^{**} + K \\ \qquad\quad \hookrightarrow + h\nu \rightarrow K^+ + e^-, \end{array} \tag{7}$$

[24] A. KLUCHAREV, V. SEPMAN and V. VUJNOVIC: *J. Phys. B*, **10**, 715 (1977).
[25] H. S. W. MASSEY and E. H. S. BURHOP: *Electronic and Ionic Impact Phenomena*, Vol. 1, *Collision of Electrons with Atoms* (Oxford, 1969).

where K** indicates now a potassium atom in the $6S$ or $4D$ level. In fig. 7 there are reported the fluorescence intensities of the $6S_{\frac{1}{2}} \rightarrow 4P_{\frac{1}{2}}(a)$ and the $7S_{\frac{1}{2}} \rightarrow 4P_{\frac{1}{2}}(b)$ transitions *vs.* the laser intensity in a bilogarithmic scale. As can be seen, the slope of curve *a*) decreases, while the laser intensity increases; correspondingly there is an increase in the slope of curve *b*). This is due to

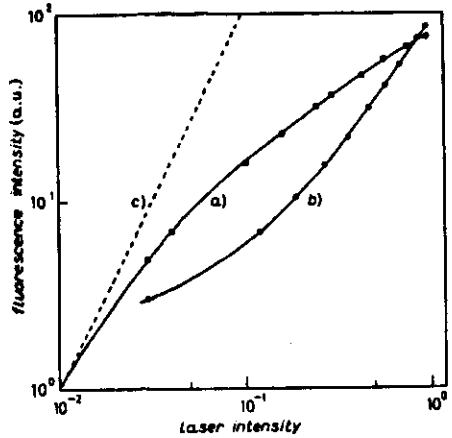

Fig. 7. – Fluorescence intensity of the $6S_{\frac{1}{2}} \rightarrow 4P_{\frac{1}{2}}$ (*a*)) and the $7S_{\frac{1}{2}} \rightarrow 4P_{\frac{1}{2}}$ (*b*)) transitions *vs.* the laser intensity in a bilogarithmic scale. The dashed curve (*c*)) has a slope = 2 and is used as a reference.

the fact that, by increasing the laser power, processes (6) and (7) become even more important and thus the level $6S$ is depopulated in favour of the higher ones and its fluorescence does not show the quadratic dependence that could be expected (dashed line *c*)). The intermediate step of processes (6) and (7) may also be an excited molecular state giving rise to processes similar to the preceding ones:

$$\begin{array}{l} K^* + K^* + B \rightarrow K_2^{**} + B \\ \qquad\quad \hookrightarrow + K^* \rightarrow K_2^+ + K + e^- \\ \qquad\qquad\quad \hookrightarrow K^+ + K, \end{array} \tag{6 bis}$$

or

$$\begin{array}{l} K^* + K^* + B \rightarrow K_2^{**} + B \\ \qquad\quad \hookrightarrow + h\nu \rightarrow K_2^+ + e^- \\ \qquad\qquad\quad \hookrightarrow K^+ + K. \end{array} \tag{7 bis}$$

In the balance of these expressions, the presence of a third atom B, which may be a buffer gas atom or an alkali ground-state one, is necessary, for the formation of the molecule. The excited molecule, for energy reasons, is probably in a triplet state ([26]) which dissociates with formation of an atomic ion.

4. – Evidence for plasma production.

To evidence the ionization of the atoms whose recombination would lead to the population of the very highly excited levels, we checked if the strong white glow, localized around the laser-focused beam, could be ascribed to the presence of a potassium plasma.

Such a check has been done either by microwave diagnosis or by optogalvanic detection. For the microwave diagnosis two special cells were used, in which the interaction of microwave power at 24 GHz with the laser-excited vapours was observed.

We describe with some details the construction and the characteristics of the cells, their design being original. The experimental apparatus and the relevant results will also be given.

Reflection cell (fig. 8*a*)). In this cell the microwave power is guided by a 10 mm fused quartz rod inside a pyrex tubing. The quartz rod is soldered to the coaxial tubing by means of a graded joint. The dielectric wave guide is tapered to become a dielectric aerial ([27]) inside the cell; it is tapered also at the other end, to fill the open end of a circular metallic wave guide ([28]).

The dielectric aerial faces a pyrex window, soldered with its plane perpendicular to the wave guide axis to the pyrex cell. The distance between the dielectric aerial and the pyrex window is 2 cm. The outer face of the window is covered with a vacuum-made deposit of alluminium, in order to reflect the wave irradiated by the aerial. A small hole in the deposit enables the laser beam to enter the cell along the axis to reach the aerial. The total insertion losses of the reflection cell are 6 db and the reflection coefficient (when the reflection of the coated window is not accounted for) is 2 db.

Transmission cell (fig. 8*b*)). The microwave is guided by a 10 mm fused quartz rod. In this case the wave guide crosses the pyrex cell perpendicularly to the axis and is tapered at both the ends. At the centre of the quartz rod, a 4 mm hole has been drilled. Two pyrex windows, parallel to each other, are soldered to the cell through re-entrant wells. The input window is about 5 mm apart from the quartz rod. The total insertion losses of the transmission cell are 4 db and the reflection coefficient is 1.2 db.

([26]) A. VALANCE: *J. Chem. Phys.*, **69**, 335 (1978).
([27]) D. G. KIELY: *Dielectric Aerials* (London, 1953).

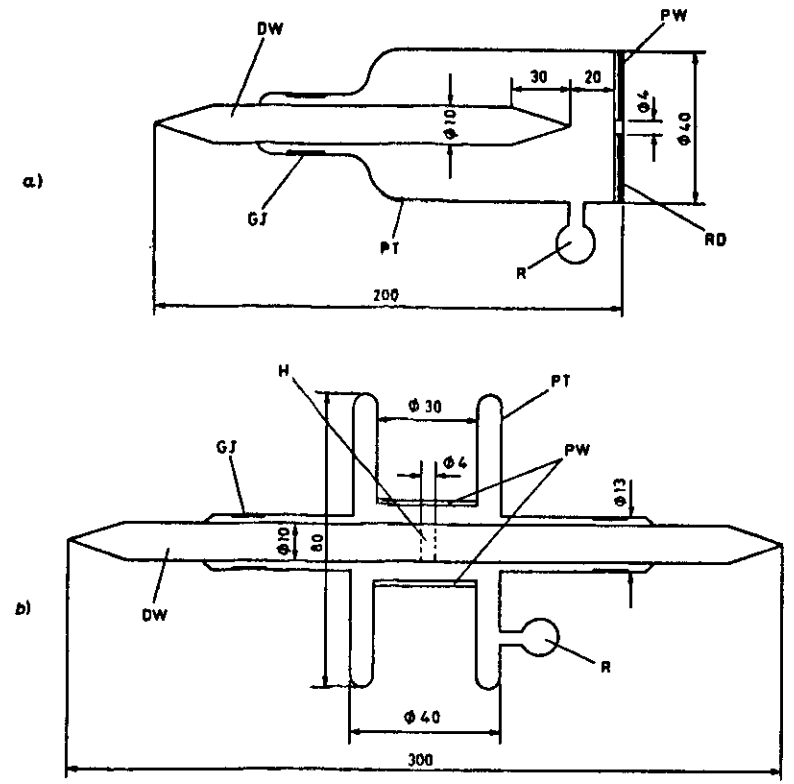

Fig. 8. – *a*) Reflection cell, longitudinal section: DW dielectric wave guide, GJ graded joint, PW pyrex window, RD reflective deposit, R reservoir, PT pyrex tubing. The size dimensions are in millimeters. *b*) Transmission cell, longitudinal section, top view. H 4 mm hole, DW dielectric wave guide, PT pyrex tubing, PW pyrex window, R reservoir, GJ graded joint. The size dimensions are in millimeters.

Both the cells lasted more than 20 hours at 200 °C without deterioration. The two cells are wide-band devices and during the experiment the klystron oscillator (Varian V 98) could be used without any frequency-stabilizing circuit.

Experimental set-up and results. The microwave and the electronic apparatus we used with the reflection cell are illustrated in fig. 9. The dielectric wave guide is fed through a rectangular to circular wave guide mode launcher; it is irradiated by the aerial, is reflected back by the metallized window, leaves the cell and, through the 2 and 3 ports of the circulator, reaches the crystal detector (1N 26). The chopped laser beam impinges upon the potassium vapour inside the cell. The resulting signals detected by the micro-

wave diode are phase amplified and drive a chart recorder. The volume occupied by the excited potassium vapour, in a typical experimental situation, is 10^3 times smaller than the volume occupied by the relevant part of the microwave power, in the region between the aerial and the reflective window. As an order of magnitude of the signals, we report the alternate voltage signal

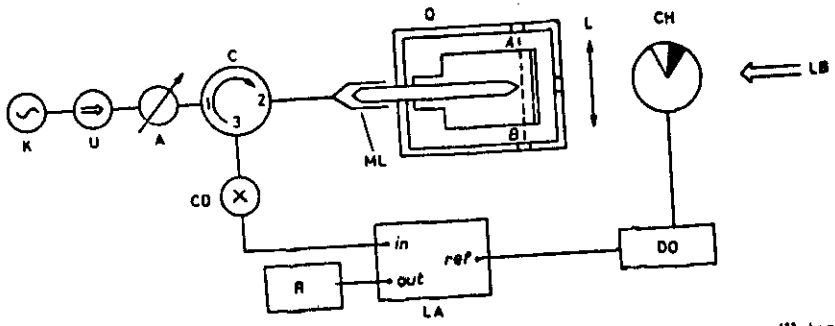

Fig. 9. – Reflection cell: microwave and electronic set-up. K klystron oscillator, U uniline, A variable attenuator, C 3-port circulator, CD crystal detector, O oven, L lens, CH chopper, LB laser beam, R recorder, LA lock-in amplifier, DO driver oscillator, ML mode launcher.

at the chopper frequency given by the resulting power variation when the laser and the klystron powers, the lens focusing and the vapour pressure are optimized. We have

$$\Delta S = 0.5 \text{ mV} \qquad \text{(peak to peak)},$$

the crystal detector being directly connected to a wide-band oscilloscope vertical amplifier. When the laser is turned off, or is off resonance, the detected microwave d.c. level is

$$S_0 = 800 \text{ mV}.$$

The signal-to-noise ratio is $\Delta S/N = 5$.

In another experiment the laser beam has been directed inside the cell through the path AB (see fig. 9) perpendicularly to the cell axis and between the aerial and the window. Displacing the laser beam along the axis of the cell, one obtains an amplitude-modulated signal, the spatial periodicity being $\lambda/2$ (λ = microwave wave-length). This is due to the presence of standing waves produced by the reflection of the microwaves by the plasma.

These effects are observed only if the laser beam is tuned to the D_1 or D_2

lines and if its intensity is sufficient to produce the white fluorescence, or if, once fixed the laser intensity, the vapour pressure is sufficient to give rise to the white glow.

Since we observed that the microwave reflected power was dependent upon the laser intensity, it is reasonable to state that

$$\omega_p < \omega,$$

ω_p and ω being the plasma and the microwave frequency, respectively. We have [25]

$$\omega_p = \sqrt{\frac{4\pi N_e e^2}{m_e}}, \qquad \omega = 2\pi \times 24 \times 10^9 \text{ rad s}^{-1},$$

so that an upper limit for the electron density is

$$N_e = 7 \cdot 10^{13} \text{ cm}^{-3}.$$

Since at $T = 200$ °C there are $\sim 10^{14}$ atoms/cm^3 in the cell, the maximum efficiency for plasma production is

$$\eta = 7\,\%.$$

In fig. 10 the reflected microwave intensity is shown (trace *b*)) as a function of the exciting laser intensity (trace *a*)). From the presence of a laser intensity threshold below which no reflected microwave variation is monitored, we conclude that the plasma production takes place only when the laser power is higher than a certain value.

In fig. 11 the set-up we used with the transmission cell is shown. In this cell the potassium vapour is excited just inside the dielectric wave guide, in the 4 mm hole, and the interaction with the microwave field, which is propagating inside the dielectric wave guide, is stronger. Now we have

$$\Delta S = 2 \text{ mV}, \qquad S_0 = 800 \text{ mV}.$$

It is worthwhile pointing out that in every case it is

$$S_1 - S_0 < 0,$$

S_1 being the d.c. level at the microwave detector when the laser is resonant but not chopped.

[25] See, for example, A. P. THORNE: *Spectrophysics* (London, 1974), p. 348.

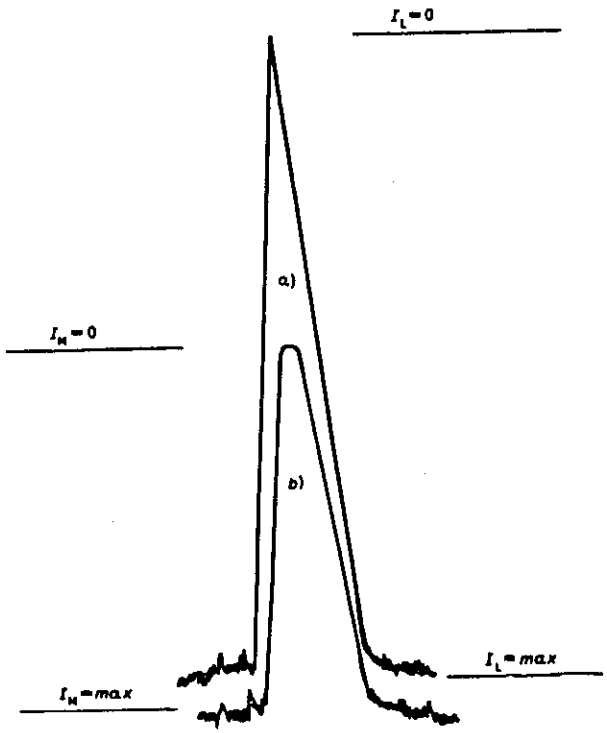

Fig. 10. – Reflected microwave intensity I_M (trace *b*)) as a function of the exciting laser intensity I_L (trace *a*)).

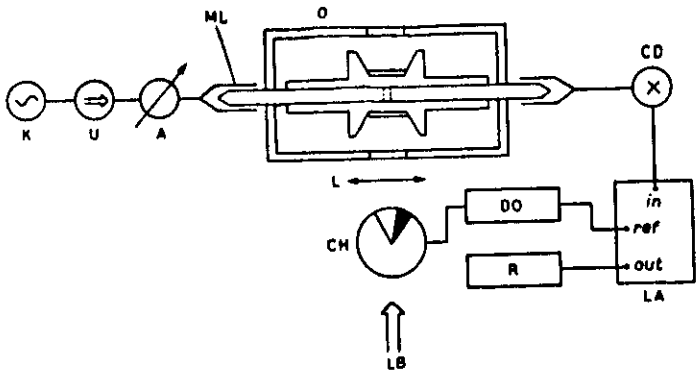

We have not observed any remarkable dependence of the signals upon the polarization of the electric field of the exciting metallic wave guide with respect to the axis of the hole in which the plasma is produced.

If the vapour laser excitation led to a plasma, we should expect the fluorescence of those levels populated by a recombination between ions and electrons be greatly affected by the presence of a voltage across the cell, whilst the fluorescence of those levels mainly populated through energy pooling collisions between two excited K(4*P*) atoms should be almost unaffected by it.

To check this, we constructed a cell with two cylindrical internal parallel electrodes, 5 mm apart, and supplied them with a voltage of ~ 10 V modulated by a lock-in amplifier. At a laser output power of ~ 50 mW and a cell temperature of 200 °C, when the white glow appeared between the electrodes, we recorded, at the same time, the fluorescence signal both directly from the phototube output and after it had been sent through the lock-in amplifier. We were so able to obtain a continuous fluorescence signal and a modulated one showing the influence of the applied voltage on the fluorescence itself.

We observed indeed a difference in the fluorescence of the transition $7S \rightarrow 4P$ in the presence of a voltage at the electrodes, in comparison with what it was in the absence of it, while the fluorescence of the transitions $5P \rightarrow 4S$ and $6S \rightarrow 4P$ did not show such a behaviour.

As a matter of fact, the signals were not good enough to rely upon them to say a definite word about the possible different ways of population of the almost resonant (with $2E(4P)$) levels and the far-away ones; for this reason we performed a different experiment in the same cell which gave definitive indications about this difference existence.

We supplied the electrodes with a continuous voltage of ~ 100 V so that a discharge was just started and a continuous current was measured across the electrodes. We recorded then simultaneously the K fluorescence and the optogalvanic signal [36] when the dye-laser was swept around the D_1 or D_2 resonant K lines and the laser beam ran parallel to the electrodes. Under D_1 excitation, for a laser power of ~ 60 mW and a cell temperature of 200 °C, the ratios between the D_1 fluorescence half-width $\Delta\nu_{D_1}$, the current signal half-width $\Delta\nu_c$ and the fluorescence signal half-width $\Delta\nu_f$ resulted to be

$$\frac{\Delta\nu_{D_1}}{\Delta\nu_c} = \sqrt{2}\,, \qquad \frac{\Delta\nu_c}{\Delta\nu_f} = 1 \quad \text{for the transition } 6S \rightarrow 4P,$$

$$\frac{\Delta\nu_c}{\Delta\nu_f} \neq 1 \quad \text{for the transition } 7S \rightarrow 4P.$$

[36] R. R. Green, R. A. Keller, G. G. Luther, P. F. [illegible]

We also measured, in the same experimental conditions, the current signal intensity as a function of the D_1 laser line intensity and the result is reported, in a bilogarithmic scale, in fig. 12.

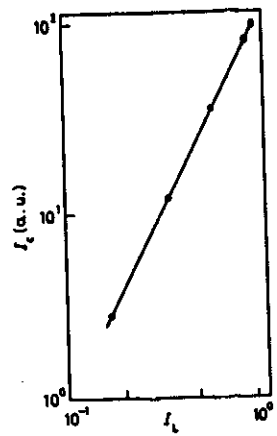

Fig. 12. – Current signal intensity (I_e) *vs.* the laser D_1 resonant line intensity (I_L) in a bilogarithmic scale. The line has a slope equal to 2.

Let us analyse these results:

a) from the $\Delta\nu_{e_1}/\Delta\nu_{e_2}$ value and from the diagram of fig. 12, it comes out that the current signal has a quadratic dependence on the resonant line intensity, which means the mechanism producing electrons must involve two excited atoms or two resonant photons; these electrons, once superelestically heated, may contribute to the plasma generation.

b) From the $\Delta\nu_e/\Delta\nu_L$ values for either the $6S \to 4P$ or the $7S \to 4P$ transition, it can be inferred that the population of the levels near twice the K($4P$) energy has a quadratic dependence on the resonant line intensity, while this is not true for levels very distant in energy from the $2E(4P)$ value. This is a further demonstration that, among all the processes that may populate the highly excited levels, the energy pooling collisions between two excited K($4P$) atoms have the largest cross-section for what concerns the almost resonant levels, while for the distant ones other processes become more relevant.

To conclude, we would like to stress the point that, to our knowledge, this is the first time an optogalvanic detection is applied to the study of collisions

5. – Conclusions.

To conclude this report, let us make a few comments. So far collisions between excited atoms have been studied in two typical situations:

1) low vapour density (down to 10^{12} atoms/cm^3) and a strong exciting laser power density (up to 10^{10} W/cm^2) by which saturation was easily reached;

2) large vapour density (up to 10^{17} atoms/cm^3) and low exciting laser power density (down to 1 W/cm^2), in which case no saturation was possible.

The results obtained in each case were ascribed to different mechanisms apparently in contrast with each other.

To explain the results obtained in this experiment with potassium at intermediate conditions (c.w. laser power density $\sim 10^3$ W/cm^2 and atomic density $\sim (10^{15} \div 10^{16})$ atoms/cm^3), we had to apply to the determinant contribution of either the processes so far considered relevant in the experimental conditions 1) or those considered relevant in the experimental conditions 2). That is to say that all these different mechanisms are always present, their relative contribution depending strongly on the experimental situation.

In particular, from what reported in the preceding paragraphs it follows that two are the leading mechanisms which create a population in the highly excited levels: the energy pooling collisions between two laser-excited atoms for what concerns the levels almost resonant with twice the laser photon energy and the plasma production for all the higher ones. The steps through which this plasma is generated may be several and two new ones are suggested in this report.

* * *

We are grateful to Prof. G. ALZETTA for his useful comments and suggestions and we wish to thank Profs. T. B. LUCATORTO and J. WEINER for communicating the results of their work prior to publication. Thanks are also due to Mssrs. M. BADALASSI and F. PAPUCCI for their technical assistance.

● RIASSUNTO

Quando vapori di potassio sono illuminati dalla luce di un laser a colorante risonante con la transizione fondamentale $4S \to 4P$, si osservano transizioni sia da livelli atomici molto alti, sia da livelli molecolari. In questo articolo si descrive uno studio spettroscopico di questi fenomeni e si dà la prova sperimentale che il meccanismo responsabile della popolazione di alcuni dei livelli non direttamente eccitati dal laser richiede la creazione di un plasma nel vapore.

Резонансное лазерное возбуждение паров калия: экспериментальное исследование соударений, сопровождающихся группировкой, и образование плазмы.

Резюме (*). — Облучение паров калия лазером на красителях с основными переходами $4S \rightarrow 4P$ приводит к возбуждению высоколежащих атомных и молекулярных состояний. В этой работе мы сообщаем результаты спектроскопических исследований этого явления и экспериментальное подтверждение, что механизм, ответственный за заселение некоторых уровней, в результате не прямого возбуждения лазером, включает образование плазмы в паре.

(*) *Переведено редакцией.*

PHOTON-ASSISTED COLLISIONS AND RELATED TOPICS

Edited by
N.K. Rahman and C. Guidotti
I.C.Q.E.M. - C.N.R.
Pisa, Italy

harwood academic publishers
chur • london • new york

COLLISIONAL SPECTROSCOPY OF LASER EXCITED ALKALI VAPOURS

MARIA ALLEGRINI and PAOLA BICCHI[+]
Istituto di Fisica Atomica e Molecolare del C.N.R., Pisa, Italy
[+]Also at Istituto di Fisica dell'Università, Siena, Italy

Abstract Laser excitation of a resonance atomic transition leads to substantial population of highly-excited atomic and molecular levels and to nearly complete ionization. A large number of experiments has been done during the last few years in alkali vapors at laser irradiances in the range $\sim 0.5\text{-}10^{10}$ W/cm^2 and atomic density in the range $\sim 10^{12}\text{-}10^{17}$ cm^{-3}. Here we briefly review the experiments performed with cw laser excitation at low power density $\leqslant 10^{3}$ W/cm^2 and low atomic density $\leqslant 10^{14}$ cm^{-3}, with special emphasis to the recent results obtained in potassium vapor.

EARLY OBSERVATIONS AND EXPERIMENTS IN SODIUM

Resonant laser-excitation of alkali vapors can easily produce a density of atoms in the excited level comparable to the density in the ground state and allows the observation of collisional processes between excited partners. Before the use of the lasers the experiments dealing with collisions between excited atoms were usually restricted to metastable states or to states populated in the afterglow of a discharge. In the early seventies, however, Klyucharev and coworkers in their extensive studies of the associative ionization in

sions between two ^2P-excited atoms as a possible channel for populating an upper level[2]. No further studies of this process were done until 1976 when Allegrini et al.[3] observed fluorescence from highly-excited states in sodium vapor irradiated by a cw dye laser tuned to the D_1 or D_2 resonance lines.

The laser power density achievable in the experiment was so low, $\sim$0.5-10 W/cm^2, that all the multiphoton processes that require a high power to occur were neglected. The intensity of the fluorescence from the states ^2S, ^2P and ^2D lying higher than the photoexcited 3^2P level was measured as a function of the laser power and the temperature of the cell that is related to the atomic density. The results showed a quadratic dependence upon both the laser power and the atomic density, as shown in figs. 2 and 3 of ref. 3. According to these dependences the authors suggested the electronic energy transfer induced in a collision between two excited atoms as a possible mechanism of populating the upper levels

$$Na^*(3P) + Na^*(3P) \rightarrow Na^{**}(nX) + Na(3S) \pm \Delta E \qquad (1)$$

where (nX) indicates any of the high-lying levels from which fluorescence was observed and ΔE the difference between the energy of each (nX) level and twice the energy of a 3P-level. A simple model based on the rate equations gives the relation between the population N_{nX} of the upper levels and N_{3P} as

N_{nX} N_{nX} N_{3P} N_{nX}
level (nX) and K the rate constant of process (1). Since the fluorescence intensity I_{nX}, which is the parameter measured in the experiment, is $I_{nX} = N_{nX}/\tau_{nX}$ the process (1) gives a quadratic dependence between I_{nX} and I_{3P}. This fact was proved in the experiment by simultaneous recording of I_{nX} and I_{3P} as a function of the laser wavelength swept around the excitation line (see fig. 4 of ref. 3). Thus all the results of the experiment gave evidence that the upper levels (nX) were populated as a consequence of processes involving two atoms in the state excited by the laser. The energy defect or excess ΔE of reaction (1) should come from the kinetic energy of the reactants. A third atom such as a foreign gas can contribute to the collision with its kinetic energy and indeed in the experiment it was tested that the transitions involving large values of ΔE were the most affected by the presence of the buffer gas. The kinetic energy of the colliding partners is determined by the cell temperature and process (1) is expected to have an appreciable cross section only for those states lying within a few kT the sum of the internal energy of the two Na(3P) atoms. However, working at temperatures higher than in the first experiment, Allegrini et al.[4] observed fluorescence from levels lying $\simeq$13 kT above the sum energy of the two 3P-atoms and processes other than (1), involving secondary collisions or absorption of one photon from higher levels, were suggested.

An attempt to give a value to the rate constants K or

the results are in agreement with the theoretical calculations of Kowalczyk[7], but are different from the values measured by Kushawaha and Leventhal[8]. However the experimental values are affected by the uncertainty in the determination of the small volume (usually less than 1 mm^3) of laser-vapor interaction and in the measurement of the number of the excited 3P-atoms in this volume; on the other hand, the theoretical values are affected by the uncertainty in the interaction potentials involved in the collision. For atoms in an excited state this calculation is often approximate so the large discrepancy between the experimental and the theoretical rate constants of process (1) may be not too surprising. It remains a crucial problem to be solved and work is in progress in our as well as in other laboratories*. Another process involving two excited atoms and energetically allowed in sodium is the associative ionization which gives the molecular ion:

$$Na^*(3P) + Na^*(3P) \rightarrow Na_2^+ + e^- \qquad (2)$$

This process has been thoroughly investigated by Leventhal and coworkers[9] in experimental conditions similar to those of refs. 3 and 4, i.e. cw dye laser excitation at power density ≤ 10 W/cm^2 and atomic density $\approx 10^{12} - 10^{13}$ cm^{-3}. They have also introduced the notation "energy pooling collisions", comprehensive of both processes (1) and (2) and an extensive report on this subject is given in this book.

Another important result of the resonant laser excitation of alkali atoms is the nearly complete ionization of the vapor. It was observed for the first time in 1976 by Lucatorto and McIlrath[10] in sodium and it has been widely investigated by several groups in lithium, sodium and cesium[11]. The experiments are usually performed with pulsed lasers at laser irradiances $\geq 10^6$ W/cm^2. It is outside the aim of this paper to review the extensive studies done at high laser power densities; let us only remark that, contrary to the cw excitation where the steady state regime can be studied, in the experiments with pulsed lasers each mechanism may be followed on separated time scales. Although several processes contribute to the final result the whole phenomenon is well understood[12-13], with the multiphoton processes dominating at high laser power density and the collisional processes at high atomic densities.

For the low power density available with the cw dye lasers the picture is not so clear and the interpretations are quite different[6-8-9-14-15]. However, evidence of the main role played by the collisions involving laser-excited atoms has been found also in an experiment on a mixture of sodium and potassium contained in the same cell[16]. The sodium atoms, at a concentration $\approx 10^{11} - 10^{12}$ cm^{-3}, were selectively excited to the $3P_{1/2}$ or $3P_{3/2}$ level with a dye laser of ≈ 40 mW modulated at low frequency and the potassium atoms, at a concentration $\approx 10^{13} - 10^{14}$ cm^{-3}, were laser excited to the $4P_{1/2}$ or $4P_{3/2}$ level in cw regime. The fluorescence spec

beam was recorded at the modulation frequency of the laser resonant with the sodium atoms in such a way that only the levels populated through processes involving Na excited atoms could be detected. It was expected to observe fluorescence from the atomic levels of sodium and potassium with energy near the sum energy of the colliding $Na^*(3P)$ and $K^*(4P)$ atoms, while only the resonance D-lines of the two alkalis and the transitions from the 5P, 6S and 4D levels of potassium were observed. Although an interpretation has been proposed, there is no simple model which can explain this result; we think that a recent experiment in potassium[17-18], at intermediate laser irradiances and atomic density, is of extreme importance to the understanding of the phenomenon.

RECENT RESULTS IN POTASSIUM

In this experiment a cell containing potassium vapor was illuminated with resonant laser light and the observations were directed towards two different channels: a detailed examination of the fluorescence spectrum and at the same time a check of the presence of a plasma in the region crossed by the resonant beam. A sketch of the experimental apparatus is given in fig. 2 of ref. 18; essentially, the output of a cw multimode dye laser (Oxazine 1 Perchlorate) of power density $\lesssim 10^3$ W/cm^2 is sent into a cell with potassium vapor inside, kept at a temperature variable in the range 150÷230°C which corresponds to an atomic density of $\simeq 10^{13} \div 10^{14}$ atoms/cm^3. The fluorescence is monitored by a monochromator at right

angles to the laser beam, connected with a photomultiplier in the range 3400÷8200 Å. The fluorescence spectrum, a portion of which, uncorrected, is reported in fig. 4 of ref. 18, is a very rich one, containing a large number of atomic lines as well as some molecular bands[19], the most interesting of which is shown in fig. 5 of ref. 18. It is a diffuse band which peaks at ∿5725 Å, very similar to one observed in potassium discharges[20]. It is to underline that it is present even when the laser is out of resonance, in contrast with the rest of the atomic or molecular transitions. The atomic lines come from transitions from the highly excited levels, see fig. 1, up to the 12S, whose energy differences ΔE are listed in Table 1 together with their wavelenghts and intensities for a cell containing potassium and 5 torr of Ar as buffer gas at a temperature of 200°C upon excitation of the $4S_{1/2} \rightarrow 4P_{3/2}$ K resonance line. A population in such highly excited levels cannot be explained by the mechanisms reported in the literature. In fact the Penning ionization and the two photon ionization are to be disregarded in such experimental conditions, their cross sections being extremely low, $\sim 5 \times 10^{-22}$ cm^2 at 10^3 W/cm^2, as estimated by Geltman[12]. On the other hand neither the energy-pooling processes alone can explain these results, as the energy-excitation transfer can populate only the levels whose ΔE is a few kT and the associative ionization may be responsible for the population of the highly excited levels only at rather high temperatures, when the superelastic collisions[13] of the electrons with the

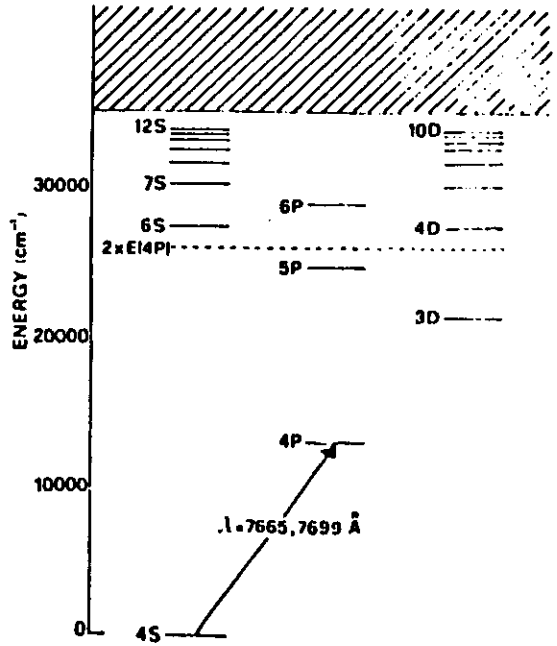

FIGURE 1. Sketch of the energy levels of K from which fluorescence is monitored. Taken from ref. 18.

K^* atoms can supply the needed energy. For potassium this process begins to be appreciable at temperatures larger than 200°C.

To summarize, with potassium, which has been studied in this experiment for the first time, a rather strange situation appears: the presence of K^+ ions is needed to justify the transitions from the highly excited levels, which would be populated by the balance of ion-electron recombination and electron-impact excitation, and, on the other hand, the ionization processes so far proposed cannot be applied to.

TABLE I

Transition	Wavelenght (Å)	Relative Intensity[a]	ΔE (kT units)
4P → 4S	7665-7699	1	
5P → 4S	4044-4047	10^{-4}	+4
6P → 4S	3446-3447	10^{-6}	-9
6S → 4P	6911-6939	5×10^{-4}	-4
7S → 4P	5782-5802	10^{-5}	-13
8S → 4P	5323-5340	2×10^{-6}	-17
9S → 4P	5084-5099	10^{-6}	-20
10S → 4P	4942-4956	10^{-7}	-22
11S → 4P	4850-4864	3×10^{-8}	-23
12S → 4P	4787-4800	10^{-8}	-24
4D → 4P	6936-6965	6×10^{-6}	-4
5D → 4P	5812-5832	6×10^{-6}	-12
6D → 4P	5343-5360	10^{-6}	-17
7D → 4P	5097-5112	8×10^{-7}	-20
8D → 4P	4951-4965	2×10^{-7}	-22
9D → 4P	4856-4870	6×10^{-8}	-23
10D → 4P	4791-4804	10^{-8}	-24
3D → 4S[b]	4642	10^{-6}	

a) The intensities are corrected according to the response of the elements of the detection apparatus. The relative intensities depend strongly upon the laser power, the temperature of the cell and the pressure and kind of buffer gas. These values have to be considered approximate.

b) Quadrupole allowed transition.

In addition the looked for mechanism cannot be unique; that is evident in fig. 2 where the intensity of the transitions

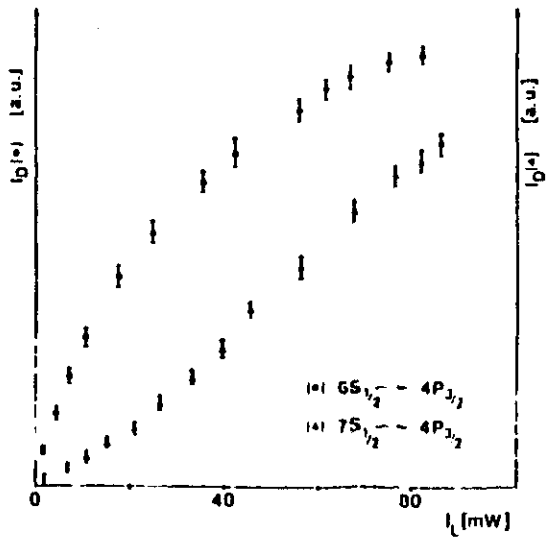

FIGURE 2. Plot of the intensities of the $6S_{1/2} \rightarrow 4P_{3/2}$ (●) and $7S_{1/2} \rightarrow 4P_{3/2}$ (▲) transitions versus the exciting laser power. The relative intensities are not comparable each-other. Taken from ref. 18.

$6S_{1/2} \rightarrow 4P_{3/2}$ ($\Delta E \simeq -4kT$) and $7S_{1/2} \rightarrow 4P_{3/2}$ ($\Delta E \simeq -13kT$) are reported as a function of the laser intensity. There is a clear difference between the two plots, which means that the population of the $6S_{1/2}$ and $7S_{1/2}$ levels are achieved through different paths. To overcome these difficulties and to find out which these paths were an optogalvanic detection[21] of the fluorescence signals was performed. The 4P→4S, 6S→4P, 7S→4P K fluorescences and the optogalvanic signal were si-

around the D_1 or D_2 K resonance lines. Fig. 3 shows the results for the D_1 excitation.

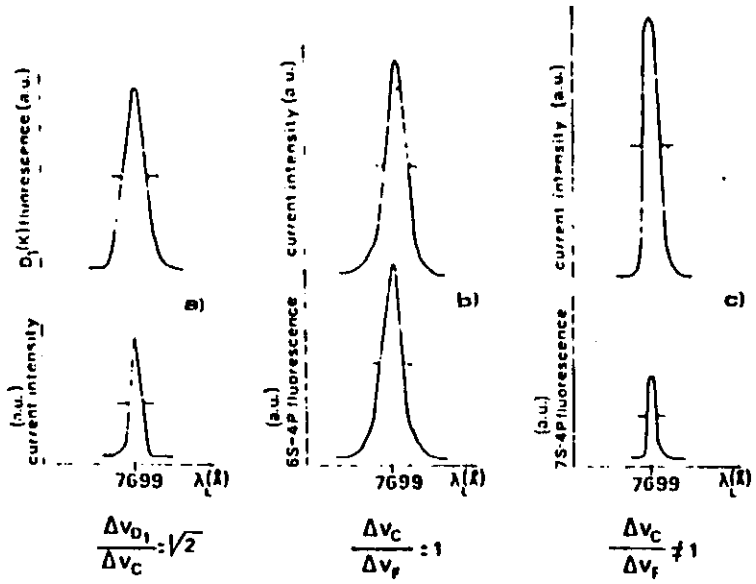

FIGURE 3. Traces of the optogalvanic and the $4S_{1/2} \rightarrow 4P_{1/2}$ fluorescence signals (a), of the optogalvanic and the 6S → 4P fluorescence signals (b) and the optogalvanic and the 7S → 4P fluorescence signals (c), as the laser output is scanned around the 7699 Å line. The ratios between the relative widths at half maximum are also reported for each couple of signals.

The first striking result is evident in fig. 3a. The half-width of the 4P → 4S fluorescence signal is in the ratio $\sqrt{2}$ with that of the optogalvanic signal, which means

line intensity. To verify that we also measured the current intensity as a function of the laser intensity and again we found a quadratic dependence. These results indicate that the mechanisms producing electrons must involve two excited atoms or two resonant photons. In fig. 3b and 3c the half-widths of the optogalvanic signals are compared with those of the 6S $\rightarrow$ 4P and 7S $\rightarrow$ 4P fluorescence signals and their ratios are, respectively, equal to one and different from one. This demonstrates that the population of the excited levels whose energy is near twice the energy of the 4P level has a quadratic dependence on the laser intensity, whilst this isn't true for the levels of much higher energy. In other words, the former are populated through energy-pooling collisions between two K(4P) atoms, while for the latter other processes, involving the production of K^+ ions even at such laser power density, should be more important. A plasma production had already been observed in Cs by Tam and Happer[22] in 1977.

To check for the presence of the plasma in this experiment, two special cells were constructed and an apparatus was realized for a microwave diagnosis. The apparatus, the cells and the procedure are detailed in ref. 18. The result was that a plasma was effectively evidenced and a proposal for its formation was put forward. According to it the plasma could be produced by the atomic ionization in energy-pooling collisions of three excited atoms:

$$K^* + K^* \rightarrow K^{**} + K$$
$$\quad\quad \hookrightarrow + K^* \rightarrow K^+ + K + e^-$$

or by the absorption of a photon and photoionization from a high-lying state:

$$K^* + K^* \rightarrow K^{**} + K$$
$$\quad\quad \hookrightarrow + h\nu \rightarrow K^+ + e^-$$

In the latter case K^{**} represents a potassium atom in the 6S, 4D or 5P level. The same result would be achieved if the intermediate step was a molecular state:

$$K^* + K^* \rightarrow K_2^{**} + B$$
$$\quad\quad \hookrightarrow + K^* \rightarrow K_2^+ + K + e^-$$
$$\quad\quad\quad\quad \hookrightarrow K^+ + K$$

$$K^* + K^* \rightarrow K_2^{**} + B$$
$$\quad\quad \hookrightarrow + h\nu \rightarrow K_2^+ + e^-$$
$$\quad\quad\quad\quad \hookrightarrow K^+ + K$$

Here B represents a third atom, essential for the formation of the molecule; it may be a buffer gas atom or a K ground state one. For energy reason the excited molecular state has a large probability of being a triplet one[23] which dissociates with the formation of an atomic ion. This proposal seems to be in agreement with some further experimental observations which are shown in fig. 4.

Here the intensities of the transitions $6S_{1/2} \rightarrow 4P_{3/2}$ (a) and $7S_{1/2} \rightarrow 4P_{3/2}$ (b) are plotted as function of the

laser intensity in a bilogarithmic scale. As can be seen there is a negative deviation of curve (a) from the quadratic dependence that could be expected (dashed line c) in favour of an increase in the slope of curve (b).

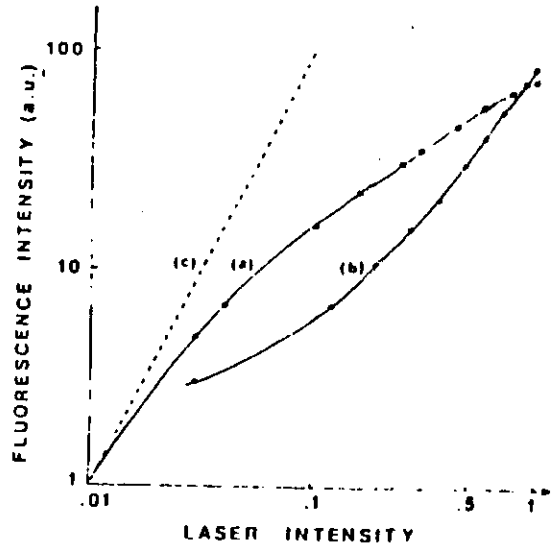

FIGURE 4. Fluorescence intensity of the $6S_{1/2} \rightarrow 4P_{3/2}$ (a) and the $7S_{1/2} \rightarrow 4P_{3/2}$ (b) transitions versus the laser intensity in a bilogarithmic scale. The dashed curve (c) has a slope 2 and it is used as a reference. Taken from ref. 18.

As a matter of fact, if the processes indicated are the right ones, when the laser power increases, they become more and more effective and the level 6S is depopulated to the advantage of the higher ones and its population is no more quadratic with the resonant photons. These processes have been taken into account also theoretically[24] and the experimental data have been compared with the theoretical ones.

REFERENCES

1. A. Klyuckarev, V. Sepman and V. Vuinovich, Opt. Spectrosc. 42, 336 (1977) and early references there cited.
2. A. N. Klyuckarev and A. V. Lazarenko, Opt. Spectrosc. 32, 576 (1972).
3. M. Allegrini, G. Alzetta, A. Kopystyńska, L. Moi and G. Orriols, Opt. Commun. 19, 96 (1976).
4. M. Allegrini, G. Alzetta, A. Kopystyńska, L. Moi and G. Orriols, Opt. Commun. 22, 329 (1977).
5. M. Allegrini, G. Alzetta, A. Kopystyńska, L. Moi and G. Orriols, Lett. Nuovo Cimento 31, 78 (1981).
6. D. J. Krebs and L. D. Schearer, J.Chem.Phys. 75,3340 (1981)
7. P. Kowalczyk, Chem. Phys. Letts. 68, 203 (1979); 74, 80 (1980).
8. V. S. Kushawaha and J. J. Leventhal, Phys. Rev. A 22, 2468 (1980) and Phys. Rev. A 25, 570, (1982).
9. G. H. Bearman and J. J. Leventhal, Phys. Rev. Letts. 41, 1227 (1978); V. S. Kushawaha and J. J. Leventhal, Phys. Rev. A 25, 346, (1982).
10. T. B. Lucatorto and T. J. McIlrath, Phys. Rev. Letts. 37, 428 (1976).
11. For a recent review and references see:
    a) T. B. Lucatorto and T. J. McIlrath, Appl. Opt. 19, 3948 (1980)
    b) J. Weiner in this book
    c) G. Spiess et al. in this book.
12. S. Geltman, J. Phys. B: Atom. Molec. Phys. 15, 3057 (1977); 13, 115 (1980).
13. R. M. Measures and P. G. Cardinal, Phys. Rev. A 23, 804 (1981) and previous references there cited.
14. J. Krasinski, f. Stacewicz and C. R. Stroud Jr., Opt. Commun. 33, 158 (1980).
15. S. G. Leslie, J. T. Verdeyen and W. S. Millar, J. Appl. Phys. 48, 4444 (1977).
16. M. Allegrini, P. Bicchi, S. Gozzini and P. Savino, Opt. Commun. 36, 449 (1981).

17. M. Allegrini, P. Bicchi, S. Gozzini and P. Savino, in Laser Spectroscopy V, edited by A.R.W. Mc Kellar, T. Oka and B.P. Stoicheff (Springer-Verlag, Berlin Heidelberg New York, 1981) p.204.
18. M. Allegrini, P. Bicchi, S. Gozzini, I. Longo and P. Savino, Il Nuovo Cimento D 1, 49 (1982).
19. M. Allegrini, G. Alzetta, P. Bicchi and S. Gozzini, Proc. XII ICPEAC, edited by S. Datz (Gatlinburg July 1981) p. 1103.
20. M. M. Rebbeck and J. M. Vaughan, J. Phys. B: Atom. Molec. Phys. 4, 25 (1971).
21. R. B. Green, R. A. Keller, G. G. Luther, P. K. Shenck and J. C. Travis, Appl. Phys. Letts. 29, 727 (1976).
22. A. C. Tam and W. Happer, Opt. Commun. 21, 403 (1977).
23. A. Valance, J. Chem. Phys. 69, 335 (1978).
24. F. Giammanco and S. Gozzini, Il Nuovo Cimento 66B, 47 1981.
25. M.Allegrini, P.Bicchi and L.Moi to be published.

---

*Note added: preliminary results[25] for the cross-section of both the 5S and the 4D state indicate that $\sigma \geq 10^{-16}$ cm^2.

Ion formation in laser-irradiated sodium vapor

M. Allegrini,* W. P. Garver, V. S. Kushawaha, and J. J. Leventhal
Department of Physics, University of Missouri—St. Louis, St. Louis, Missouri 63121
(Received 7 February 1983)

The formation of Na^+ and Na_2^+ in laser-irradiated sodium vapor has been studied using a nitrogen-laser-pumped dye laser. The effects of irradiation by this pulsed laser are substantially different from those reported previously using a cw device, but otherwise identical experimental conditions. In contrast to the earlier experiments, in which ions were observed only when the cw laser was tuned to a D line, relatively large "background" ion signals are observed at all excitation wavelengths, a result of multiphoton processes involving the Na_2 component of the vapor. It is shown that the laser bandwidth and pulse duration are extremely important parameters; a wide bandwidth effectively magnifying the importance of the dimer component of the vapor and a short pulse duration minimizing the effects of interactions between excited atoms and molecules.

I. INTRODUCTION

During the past few years there has been a great deal of interest in the production of plasmas and electrical discharges by laser irradiation of vapors, especially sodium. Lucatorto and McIlrath[1] have shown that irradiation of a rather dense column of Na vapor ($\sim 10^{16}$ cm^{-3}) with a dye laser tuned to a D line can cause complete ionization of the vapor. In addition to the intrinsic interest of this phenomenon the laser-produced plasma has been exploited as a new tool for absorption spectroscopy.[2] Stwalley and his co-workers have also produced plasmas by laser irradiation.[3] However, in their experiments the laser wavelength was not restricted to the D line; several wavelengths in the yellow region of the spectrum were employed. Since some of these wavelengths do not correspond to atomic resonances it is clear that excitation of the dimer component of the vapor, Na_2, plays a role.

Hertel and co-workers[4] have used laser-irradiated sodium vapor to produce infrared (ir) laser emissions. In this work yellow light from a pulsed dye laser was used to activate the vapor to form the required population inversion. While ir laser action was achieved when the excitation laser was tuned to a D line, it was also achieved when the excitation laser was tuned to optical wavelengths that do not coincide with *atomic* resonances. This again indicates participation by the neutral-dimer component of the vapor.

Because of the interest in laser-produced phenomena of this type several experiments have been performed that are directed toward study of the microscopic processes[5–31] that occur in laser-irradiated sodium vapor. These microscopic processes dictate the collective behavior of the plasma or discharge and are therefore important for a complete understanding of the phenomena. Among the interactions that contribute to this complex environment are those involving photons directly, such as $\hbar\omega + Na$ and $\hbar\omega + Na_2$, and indirectly, for example Na $3p$-Na $3p$ collisions.

The experiments that have been designed to investigate these microscopic processes have been performed under a variety of conditions. Vapor densities have been varied from $\sim 10^9$ cm^{-3}, characteristic of atomic beams,[12] to $\sim 10^{14}$–10^{15} cm^{-3} in cell experiments.[7,10] Of course, the relative concentrations of the dimer ions differ as well since that concentration is temperature dependent. The lasers that have been employed have included both cw and pulsed; because of the characteristics of different pulsed lasers the pulse durations have ranged from ~ 10 nsec to greater than 1 μsec. Laser bandwidths have varied from those associated with multimode lasers to the narrow values achievable with single-frequency devices. Laser power densities have ranged from the low values associated with cw lasers (~ 1 W/cm^2) to the considerably higher values achievable with focused pulsed lasers (up to $\sim 10^9$ W/cm^2). Although there is some disagreement over various aspects of the individual processes involved, no doubt due at least in part to the different experimental parameters employed, a great deal has been learned. The work that is described in this paper is intended to further clarify the situation.

Our approach has been to study the fundamental atomic and molecular collision processes that can occur in laser-irradiated sodium vapor by performing experiments at relatively low density $\sim 10^{11}$–10^{13} cm^{-3} using the inherently low power of cw lasers. In this way multiphoton effects could be virtually eliminated, and interactions involving state-selected excited species studied with minimum interference. Using cw lasers we have studied ionization processes[16] such as

$$Na(3p) + Na(3p) \rightarrow Na_2^+ + e \quad (1)$$

and

$$Na(4d) + Na(3s) \rightarrow Na_2^+ + e \, . \quad (2)$$

In addition to the associative-ionization channel represented by Eq. (1) we have also studied excitation-transfer processes in energy-pooling $3p$-$3p$ interactions[17] such as

$$Na(3p) + Na(3p) \rightarrow Na(4d) + Na(3s) \, . \quad (3)$$

In this earlier work only minor effects were observed if the lasers were not tuned to real atomic resonances. This is doubtless because the low-power density of the cw laser precluded multiphoton effects involving either the atomic or dimer components of the vapor.

This paper presents the results of experiments on ion formation in laser-irradiated sodium vapor using a rather common pulsed laser to investigate higher-power regimes than studied in our previous work using cw lasers. The results demonstrate that dramatic differences occur under otherwise identical experimental conditions when the pulsed laser is substituted for the cw device. In particular, it is shown that the broadband nature of the pulsed-laser light together with the higher-power density effectively magnifies the importance of the dimer concentration so that the ionization process involving dimers obscures ionization from atomic interactions, even when the laser is tuned to a real atomic resonance such as the D line. This is in marked constrast to the cw case where the dimers were found to be virtually unimportant. The data to be presented here strongly suggest that it is two-photon excitation followed by single-photon ionization of the dimers that leads to copious yields of both Na^+ and Na_2^+ at all laser wavelengths employed in this study.

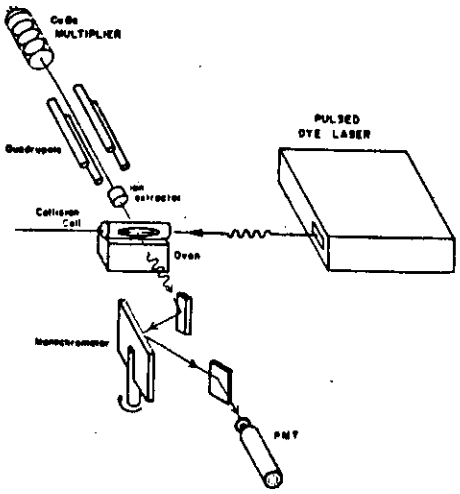

FIG. 1. Schematic diagram of the apparatus.

II. EXPERIMENTAL

The experiments reported in this paper were performed with apparatus that is essentially the same as that used previously[17] with a pulsed laser substituted for the cw laser; a schematic diagram is shown in Fig. 1. An oven consisting of a resistance heater imbedded in a Cu block vaporizes the sodium which effuses into the cylindrical collision cell through a slot in one side of the cylinder; 2-mm-diam apertures in the end caps permit entrance and exit of the laser beam. There is a 2-mm×2-cm window on one side for observation of photons and a 5-mm aperture on the other side for extraction of ions. The vapor density in the cell can be varied over the approximate range 10^{11}–10^{13} atoms/cm^3, however, it is difficult to determine the fractional dimer concentration. If thermodynamic equilibrium were established then the dimer concentration at these temperatures would be on the order of 1%. However, equilibrium has clearly not been established in this setup so the dimer concentration is likely to be greater than this value.

TABLE I. Dye laser characteristics at 5900 Å.

	Power (W)	Bandwidth GHz	Bandwidth Å
Pulsed dye laser	$\simeq 3.5\times10^3$	86	1
cw dye laser (multimode)	$\simeq 1.0$	43	0.5
cw dye laser (single frequency)	$\simeq 0.12$	0.015	1.5×10^{-4}

The pulsed dye laser NRG-Model-DL-03, operated with Rhodamine-6G dye, was pumped with an NRG-Model-0.5 N_2 laser. The laser beam was focused inside the collision cell with a diameter ~ 1 mm. The characteristics of this laser, together with those of the cw lasers used in the related work, are listed in Table I.

Photons emanating from the collision cell were dispersed with a 0.25-m scanning monochromator and detected with a cooled photomultiplier tube (PMT). Ions were extracted from the cell with a set of electrostatic lenses, analyzed by a quadrupole mass filter, and detected with a CuBe particle multiplier. The relative transmission of this system was determined by replacing the oven-cell combination with an electron-impact ion source and comparing the fragment ion yields from various gases with the fragmentation patterns listed in standard tables.[22]

The charge output of either the PMT or the CuBe particle multiplier that resulted from each laser pulse was integrated with a charge-sensitive amplifier and stored in a pulse-height analyzer. After a preset number of pulses (typically 200) the computer read the total charge. Two modes of operation were employed. In one the laser wavelength was fixed and mass scans and/or spectral scans taken. The mass and emission spectra could be acquired simultaneously. In the other mode of operation the settings of the quadrupole mass filter and the monochromater were fixed and the laser wavelength scanned. In either mode the computer controlled operation of the apparatus and stored the data. When photon and ion signals were acquired simultaneously the output of the PMT was fed into a fast counter, the output of which was stored by the computer. Because of the pulsed nature of the experiment this technique does not give reliable absolute photon signals; however, it was used primarily as a wavelength marker.

III. RESULTS

Mass scans were taken at a variety of different wavelength settings λ_L of the pulsed laser. Figure 2 shows three such scans, each taken with λ_L fixed at a different wavelength, one of which was the D_2 line. It is important to note that the ordinate scale, although arbitrary, is the same for each scan; these data therefore show no enhancement of either the Na^+ or the Na_2^+ signals when the laser is tuned to a D line.

Figure 3 shows data analogous to those shown in Fig. 2, but taken with the cw laser. In contrast to the data ac-

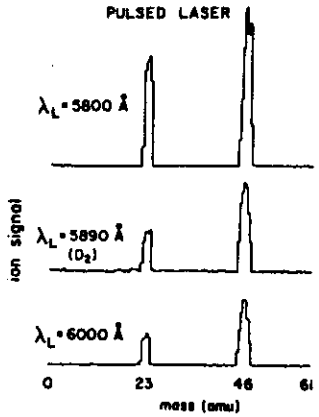

FIG. 2. Mass spectra taken at three different wavelength settings of the pulsed laser. Spectra have been corrected for relative transmission as a function of mass. Ordinates are in arbitrary units, but the three spectra are plotted on the same scale.

quired with the pulsed laser, ions are observed *only* when the cw laser is tuned to a *D* line. The Na_2^+ ions are from $3p+3p$ associative ionization,[4,6,9,16] while the small Na^+ signal is from photodissociation[6,15] of the incipient Na_2^+.

The surprising conclusion that the ion yields do not increase when the pulsed laser is tuned to a *D* line is clearly shown in Figs. 4 and 5. Figure 4 shows the Na^+ and *D*-line fluorescence signals (taken simultaneously) as functions of λ_L. The axes shown in the figure are included to emphasize the relatively large "background" ion signal at all wavelengths. The *D*-line fluorescence trace establishes that indeed Na $3p$ are being formed at the appropriate settings of λ_L, and serves as a wavelength marker in the scan. Figure 5 shows traces of the Na_2^+ ion signal and

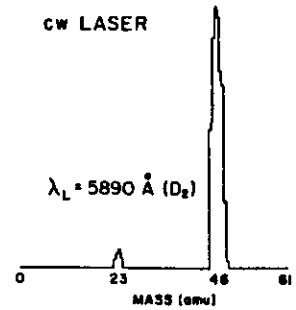

FIG. 3. Mass spectrum taken with a multimode cw laser tuned to the D_2 line. No ions were observed when the cw laser was detuned from a *D* line. This spectrum, which is shown primarily for comparison with those produced by pulsed laser excitation (Fig. 2), has also been corrected for relative transmission as a function of mass. Ordinate scale is in arbitrary units.

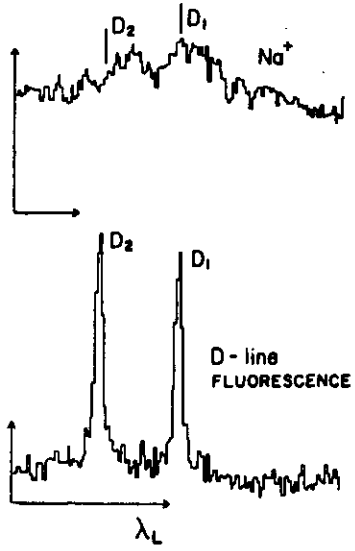

FIG. 4. Na^+ signal and *D*-line fluorescence (from both *D* lines) as functions of λ_L, the wavelength of the pulsed laser. Two sets of axes are shown to indicate the relative magnitudes of the background levels. Both ordinates are in arbitrary units.

$4p \rightarrow 3s$ fluorescence signal (3302 and 3303 Å) as functions of λ_L. No significant enhancement of this ion signal occurs at the *D* lines, but enhancement of the fluorescence is observed, a result of $3p+3p$ energy-pooling excitation transfer.[6,9,17] The axes in this figure again indicate that ions are produced at all wavelengths.

Since substantial enhancements of the Na^+ and Na_2^+

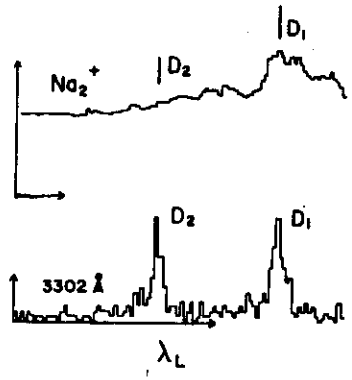

FIG. 5. Na_2^+ signal and $4p \rightarrow 3s$ fluorescence (3302 and 3303 Å) as functions of λ_L, the wavelength of the pulsed laser. Two sets of axes are shown to indicate the relative magnitudes of the background levels. Both ordinates are in arbitrary units.

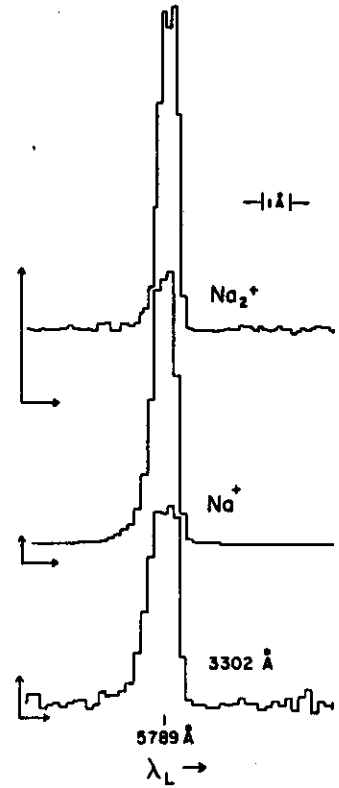

FIG. 6. Na_2^+, Na^+, and $4p \rightarrow 3s$ fluorescence (3302 and 3303 Å) as functions of λ_L, the wavelength of the pulsed laser. Ordinate scales are in arbitrary units, and are unrelated to each other. Three sets of axes are shown to indicate the relative magnitudes of the background levels.

signals were expected when the pulsed laser was tuned through the *D* lines it was considered important to find some condition under which ion peaks could be observed as λ_L was varied in order to establish proper operation of the apparatus. Assurance of proper operation was achieved by tuning the pulsed laser through either the $3s \rightarrow 4d$ or $3s \rightarrow 5s$ two-photon resonances at 5789 and 6024 Å, respectively. Figure 6 shows the Na^+, Na_2^+, and 3302-Å signals as λ_L is scanned through a very small range that includes the $3s \rightarrow 4d$, two-photon atomic resonance. The Na^+ ions are from three-photon resonance-enhanced ionization; the origin of the Na_2^+ will be discussed in Sec. IV. The 3302-Å $4p \rightarrow 3s$ fluorescence is a result of the cascade from the $4d$ state via the $4d \rightarrow 4p$ infrared transition. These data unequivocally establish that the apparatus is indeed operating properly. Similar observations were made as the pulsed laser was scanned

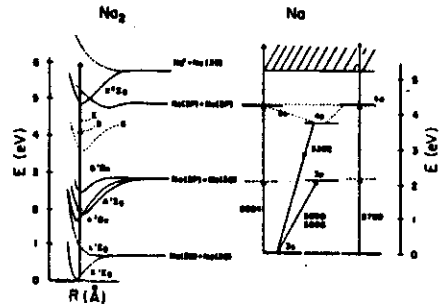

FIG. 7. Partial term diagram for the Na atom showing transitions that can be excited by absorption at the laser wavelengths of these experiments. Also shown in the 3302-Å $4p \rightarrow 3s$ emission detected in the experiments. Dashed line between the $5s$ and $5d$ levels is drawn at twice the energy of the $3p$ state. Also shown are several potential-energy curves of the Na_2 molecule. Vertical arrows on these curves are drawn to indicate the approximate energy of each photon from the excitation laser that may be absorbed by the molecule (each photon has energy in the range 2.05–2.11 eV). Right and left ordinate scales are adjusted so that zero on the right corresponds to Na $3s$ and zero on the left to the bottom of the Na_2 $X\,^1\Sigma_g$ potential-energy well.

through the 6024-Å, $3s$-$5s$, two-photon atomic resonance.

IV. DISCUSSION

The laser wavelengths used in these experiments, 5750–6050 Å, make it possible to access a number of Na and Na_2 states by both one- and two-photon absorption. This is illustrated in Fig. 7 which shows a partial term diagram for Na and potential-energy curves for several Na_2 states. Some of the transitions that can be excited with laser light in the range of wavelengths used in this work are shown in the figure. Also shown are the transitions from the $4d$ level that lead to 3302-Å radiation by cascading.

A number of two-photon absorptions in Na_2 have recently been reported[23–27] for the same wavelength range as that employed in our experiments. These two-photon absorptions can serve as the first step in resonance-enhanced three-photon ionization. We believe that these resonances are important steps in the multiphoton ionization of Na_2 to both bound and repulsive states of Na_2^+. This conclusion is consistent with one reached by Wu *et al.* in a recent paper.[28]

The most unexpected feature of the data presented here is the absence of significant enhancement of either ion signal when the pulsed laser is tuned to a *D* line. Enhancement of the Na^+ signal might have resulted from three-photon resonance-enhanced ionization of sodium atoms, and that of Na_2^+ from $3p+3p$ associative ionization. Obviously these two processes are occurring, however, because the Na_2 molecules absorb at essentially all wavelengths in this range, including those corresponding to atomic resonances; Na^+ and Na_2^+ are copiously produced

from the dimer. These ions are presumably obscuring the Na^+ and Na_2^+ that result from interactions involving atoms when the laser is tuned to a D line. The fact that dimer molecules lead to ion formation with the pulsed laser, but not with the relatively low-power cw laser, suggests that two-photon excitation of high-lying molecular states, via virtual intermediate states, rather than sequential excitation, via a real intermediate state, is the first step in the multiphoton ionization of the dimer. Although significant enhancement of the ion signals was not observed at the D line we do see relatively large increases in both Na^+ and Na_2^+ at the $3s \rightarrow 4d$ and $3s \rightarrow 5s$ two-photon atomic resonances. The increased Na^+ signal is almost certainly from three-photon resonance-enhanced ionization via the $4d$ (or $5s$) level, a process that is expected to be orders of magnitude larger than three-photon resonance-enhanced ionization via the $3p$ level.[29] In fact, our data confirm this.

As noted above it was anticipated that $3p + 3p$ associative ionization would cause the Na_2^+ signal to increase dramatically as the laser was scanned through the D lines. Unlike three-photon ionization, associative ionization requires a heavy-body—heavy-body collision. Since the heavy bodies in this case must *both* be Na $3p$, associative ionization can occur only during the time interval in which these excited atoms are present. Because the laser pulse is shorter than the 16-nsec natural lifetime of the $3p$ state it is the lifetime of this state that dictates the temporal dependence of the potential reactants. (If radiation trapping is considered then the expanding reaction volume must also be taken into account so that this complication will be neglected for the purpose of this discussion.) Because significant enhancement of the Na_2^+ signal is not observed at the D lines it is apparent that the cross section for $3p + 3p$ associative ionization[8,16] ($\sim 10^{-17}$ cm^2) is insufficient to produce an Na_2^+ signal (during the time that Na $3p$ are present) that is measurable above the ion background from processes involving the dimers. This is in contrast to our earlier work with cw lasers, in which the dimers were found to be unimportant. Recall that no signals, photon or ion, were observed when the cw laser was tuned off a D line so there was no background signal from dimer ionization. Furthermore, in the cw case there is a continuous supply of potential reactants, the Na $3p$ atoms.

We do, however, observe enhancement of the Na_2^+ signal as the pulsed laser is scanned through the two-photon atomic resonances. There are two possible sources of these increased Na_2^+ yields. Since the ionization potential of atomic sodium (5.1 eV) is greater than the ionization potential of the dimer (4.9 eV), charge exchange in Na^+-Na_2 collisions can contribute to the Na_2^+ yield. If this is the case then the increased Na^+ concentration at these wavelengths is directly responsible for the observed Na_2^+ increase. To our knowledge there are no data available on this charge-transfer process.

A second possible source of Na_2^+ at the two-photon atomic resonances is $3s + 4d$ or $3s + 5s$ associative ionization.[16] Although $3p + 3p$ associative ionization could not be detected above the dimer-produced Na_2^+ signal, there are several factors that could permit the observation of $3s + 4d$ and $3s + 5s$ processes, especially the former. First, the lifetimes of the $4d$ and $5s$ states are longer than that of the $3p$ state, 55 and 80 nsec, respectively.[30] Second, in each of these procedures, Na $3s$, which is the major component of the vapor, is one of the reactants and is of course continuously present. Thus, although the $4d$ or $5s$ concentration is no doubt lower at the respective laser wavelengths than is the $3p$ concentration at the D lines, the significantly larger concentration of Na $3s$, together with the longer lifetimes, may conspire to make these associative-ionization processes observable while that from $3p + 3p$ collisions is not.

We have also observed that the ion signal due to the dimers tends to decrease with increasing wavelength. That is, the dimer-produced background is greater at the $3s \rightarrow 4d$ wavelength 5789 Å than at the D lines (or the $3s \rightarrow 5s$ wavelength 6024 Å). Although this background is higher, by about a factor of 2, the $3s + 4d$ associative-ionization cross section is about 60 times larger[16] than that for $3p + 3p$. However the $3s + 5s$ cross section is about 40 times *lower*[16] than that for $3p + 3p$; yet an enhancement of the Na_2^+ signal is observed at 6024 Å. These observations suggest that Na^+-Na_2 charge transfer discussed above plays a major role in the production of Na_2^+ at the wavelengths of the two-photon atomic resonances, especially the $3s \rightarrow 5s$ transition.

The results presented here are in contrast to those of Roussel *et al.*[12] who have reported data for Na_2^+ production as a function of pulsed-laser wavelength at vapor densities comparable to those employed in our experiments. While, in agreement with our data, they observe an enhancement of the Na_2^+ signal at 6024 Å (they did not report data for λ_L as short as 5789 Å), they also observe significant enhancement of the Na_2^+ signal at the D lines. The major difference between their experiment and ours is that they used a flashlamp pumped pulsed laser, for which the pulse length is ~ 1 μsec, approximately 100 times longer than that of the laser used in our experiments. Thus it seems likely that this pulse length permits the active medium for production of Na_2^+ by associative ionization, the Na $3p$ atoms, to survive for a sufficient time to permit reaction.

The observation by Lucatorto and McIlrath[1] that a column of Na vapor could be completely ionized when irradiated by ~ 1 MW of laser light tuned to a D line has been attributed to ionization by superelastically heated electrons,[31-35] electrons that have acquired kinetic energy in e-Na $3p$ quenching collisions. These hot electrons are then capable of ionizing Na $3p$ or even Na $3s$. Each ionization event adds to the electron inventory so that a cascading process results. It has been proposed that the "seed" electrons for this avalanche are provided by $3p + 3p$ associative ionization,[8,9,18,35] so that our data, together with those of Roussel *et al.*,[12] suggest that the use of a flashlamp pumped laser may have been an important aspect of the experiments of Lucatorto and McIlrath.[1] However, based on our data, it seems likely that even if a laser of much shorter pulse duration, such as one that is pumped by either an N_2 or a Q-switched Nd:YAG laser, is used, seed electrons could be produced by ionization of the dimer component of the vapor. Such effects would be magnified at the higher densities employed by Lucatorto and McIlrath because the fractional dimer concentration is higher than in our experiments. In any case our data show that dimer ionization contributes substantially to the electron concentration in laser-irradiated vapor.

Although we were unable to detect Na_2^+ from $3p + 3p$ collisions above the dimer-produced background, our observation of 3302-Å radiation as the pulsed laser was scanned through the D lines shows clearly that $3p + 3p$ energy-pooling excitation transfer is occurring. Previously we have shown that the primary products of such excitation transfer are Na $4d$ and Na $5s$,[17] and that the 3302-Å radiation is indicative of the formation of these states. Given that we were unable to detect $3p + 3p$ associative ionization in this work how then were we able to detect $3p + 3p$ excitation transfer? Of course, the relative magnitudes of the cross sections for each of these processes is important, but there is disagreement in the literature over the cross sections for $3p + 3p$ excitation transfer.[14,16,20,21] The reported values range from about an order of magnitude larger than our previously measured $3p + 3p$ associative-ionization cross section to about three orders of magnitude lower than the associative-ionization cross section. However, from an experimental point of view the reason that 3302 Å can be measured, while Na_2^+ produced by associative ionization cannot, is simply that there is little or no 3302 Å background, but the dimer-produced ion signal is sufficient to obscure the Na_2^+ signal from $3p + 3p$ associative ionization. The data in Fig. 5 illustrate this point.

Finally, it is worthwhile to consider the mechanisms by which the dimer component of the vapor produces so many ions. As discussed previously it is difficult to reliably estimate the dimer fraction of the vapor due to the nonequilibrium nature of the reaction cell. Our data suggest however that this fraction may be considerably higher than 1%, the fraction calculated under the assumption of thermodynamic equilibrium. Nevertheless, while only a small fraction of the photons from a broadband laser, such as the one used in this work, can excite an atomic transition, virtually all of the photons in the laser beam can excite Na_2. This effectively magnifies the Na_2 concentration relative to that of the atoms so that the ratio of excited Na_2 molecules to excited atoms can be significantly greater than the ratio of ground state species.

Wu and Judge, in collaboration with Roussel and coworkers,[28] have reached the conclusion that in the earlier work of Roussel *et al.*[12] the production of Na_2^+ at laser wavelengths that do not coincide with atomic resonances was due primarily to the dimers. This conclusion is of course consistent with the main theme of the discussion in this paper. They suggest that Na_2^+ results from two-photon absorption by the Na_2 molecules, followed by single-photon photoionization, as we suggest in this paper. Further, Muller and Hertel[4] suggest that two-photon excitation of the dimers is the primary excitation mechanism that leads to the infrared laser emission in their experiments.

It is possible that ions are being produced by interactions that are driven by the presence of the strong electromagnetic field associated with the laser, so-called laser-induced reactions. This possibility was precluded in the cw experiments, but it must be considered when pulsed lasers are employed. Although there have been some recent experiments on laser-induced processes in sodium vapor,[11-13,36] the picture is unclear at this time. Despite the potential complications introduced by the presence of neutral dimers, studies of laser-induced effects in sodium vapor are continuing[37,38] in several laboratories, including our own.

ACKNOWLEDGMENTS

The authors would like to thank E. Arimondo, C. E. Burkhardt, P. L. DeVries, M. H. Nayfeh, and W. C. Stwalley for helpful discussions. This work was supported by the U. S. Department of Energy, Division of Chemical Sciences, under Contract No. DE-AS02-76-ER02718 and a North Atlantic Treaty Organization Grant No. 101.82 for collaborative research (M.A. and J.J.L.).

---

[a]Permanent address: Laboratorio di Fisica Atomica e Molecolare del Consiglio Nazionale delle Richerche, I-56100 Pisa, Italy.

[1]T. B. Lucatorto and T. J. McIlrath, Phys. Rev. Lett. 37, 428 (1976).

[2]T. B. Lucatorto and T. J. McIlrath, Appl. Opt. 19, 3948 (1980).

[3]M. E. Koch, K. K. Verma, and W. C. Stwalley, J. Opt. Soc. Am. 70, 627 (1977) and private communication.

[4]W. Muller and I. V. Hertel, Appl. Phys. 24, 33 (1981); and private communication.

[5]M. Allegrini, G. Alzetta, A. Kopystynska, L. Moi, and G. Orriols, Opt. Commun. 22, 329 (1977).

[6]G. H. Bearman and J. J. Leventhal, Phys. Rev. Lett. 41, 1227 (1978).

[7]A. Kopystynska and P. Kowalczyk, Opt. Commun. 23, 351 (1978).

[8]A. de Jong and F. van der Valk, J. Phys. B 12, L561 (1979).

[9]V. S. Kushawaha and J. J. Leventhal, Phys. Rev. A 22, 2468 (1980).

[10]F. Roussel, P. Breger, G. Spiess, C. Manus, and S. Geltman, J. Phys. B 13, 631 (1980).

[11]B. Carre, F. Roussel, P. Breger, and G. Spiess, J. Phys. B 14, 4271 (1981).

[12]F. Roussel, B. Carre, P. Breger, and G. Spiess, J. Phys. B 14, L313 (1981).

[13]J. Weiner and P. Polak-Dingles, J. Chem. Phys. 74, 508 (1981).

[14]D. J. Krebs and L. D. Schearer, J. Chem. Phys. 75, 3340 (1981).

[15]V. S. Kushawaha and J. J. Leventhal, J. Chem. Phys. 75, 5966 (1981).

[16]A. Z. Devdariani and A. L. Zagrebin, Khim. Fiz. 1, 947 (1982), and references contained therein.

[17]V. S. Kushawaha and J. J. Leventhal, Phys. Rev. A 25, 570 (1982).

[18]J. L. Le Gouet, J. L. Picque, F. Wuilleumier, J. M. Bizau, P. Dhez, P. Koch, and D. L. Ederer, Phys. Rev. Lett. 48, 600 (1982).

[19]J. G. Kircz, R. Morgenstern, and G. Nienhuis, Phys. Rev. Lett. 48, 610 (1982).

[20]M. Allegrini, P. Bicchi, and L. Moi (unpublished).

[21]J. Huennekens and A. Gallagher, Phys. Rev. A 27, 771 (1983).

[22]E. Stenhagen, S. Abrahamsson, and F. W. McLafferty, *Registry of Mass Spectral Data* (Wiley, New York, 1974).

[23]J. P. Woerdman, Chem. Phys. Lett. 43, 279 (1976).
[24]A. J. Taylor, K. M. Jones, and A. L. Shawlow, Opt. Commun. 39, 47 (1981).
[25]N. W. Carlson, A. J. Taylor, K. M. Jones, and A. L. Shawlow, Phys. Rev. A 24, 822 (1981).
[26]G. W. King, I. M. Littlewood, and N. T. Littlewood, Chem. Phys. Lett. 80, 215 (1981).
[27]R. Vasudev, T. M. Stachelek, W. M. McClain, and J. P. Woerdman, Opt. Commun. 38, 149 (1981).
[28]C. Y. R. Wu, D. L. Judge, F. Roussel, B. Carre, P. Breger, and G. Spiess, in *Laser Techniques for Extreme Ultraviolet Spectroscopy*, edited by T. J. McIlrath and R. R. Freeman (AIP, New York, 1982).
[29]M. H. Nayfeh (private communication).
[30]P. F. Gurzdev and N. V. Afanaseva, Opt. Spektrosk. 49, 625 (1980) [Opt. Spectrosc. 49, 341 (1980)].
[31]R. M. Measures, J. Quant. Spectrosc. Radiat. Transfer 10, 107 (1970).
[32]R. M. Measures, J. Appl. Phys. 48, 2673 (1977).
[33]S. Geltman, J. Phys. B 10, 3057 (1977).
[34]T. J. McIlrath and T. B. Lucatorto, Phys. Rev. Lett. 38, 1390 (1977).
[35]R. M. Measures and P. T. Cardinal, Phys. Rev. A 23, 804 (1981).
[36]*Photon-Assisted Collisions and Related Topics*, edited by N. K. Rahman and C. Guidotti (Harwood, New York, 1982).
[37]J. Weiner (private communication).
[38]F. Roussel and B. Carre (private communication).

PHYSICAL REVIEW A VOLUME 28, NUMBER 3 SEPTEMBER 1983

Cross-section measurement for the energy-transfer collisions $Na(3P) + Na(3P) \rightarrow Na(5S,4D) + Na(3S)$

M. Allegrini
Istituto di Fisica Atomica e Molecolare del Consiglio Nazionale delle Richerche, Via del Giardino, 3-56100 Pisa, Italy

P. Bicchi
Istituto di Fisica Atomica e Molecolare del Consiglio Nazionale delle Richerche, Via del Giardino, 3-56100 Pisa, Italy and Istituto di Fisica dell'Università di Siena, Via Banchi di Sotto, 57-53100 Siena, Italy

L. Moi
Istituto di Fisica Atomica e Molecolare del Consiglio Nazionale delle Richerche, Via del Giardino, 3-56100 Pisa, Italy

(Received 15 September 1982)

We report our measurements of the cross sections σ_{5S} and σ_{4D} for the electronic-energy-transfer process $Na(3P) + Na(3P) \rightarrow Na(5S,4D) + Na(3S)$. To obtain these cross sections we have measured the fluorescence intensity for the transitions $5S \rightarrow 3P$, $4D \rightarrow 3P$, and $3P \rightarrow 3S$ in sodium vapor excited with a cw dye laser. The study of this electronic energy transfer is complicated and there is a large disagreement ($\geq 10^4$) among reported measurements. We believe we have avoided most of the difficulties of previous experiments. Our results are $\sigma_{5S} = (2.0 \pm 0.7) \times 10^{-15}$ cm^2 and $\sigma_{4D} = (3.2 \pm 1.1) \times 10^{-15}$ cm^{-2}, and they are compared with the results of other experiments.

I. INTRODUCTION

There is lively theoretical and experimental interest in understanding phenomena arising from resonance laser excitation in a dense vapor.[1] Most of the experiments concern sodium atoms excited to the $3P$ level by pulsed or cw dye lasers over a wide range of atomic density. If the laser power density is less than 10^2–10^3 W cm^{-2}, atomic multiphoton excitation and ionization can be neglected and the main mechanisms for production of ions and highly excited atoms are the associative ionization

$$Na(3P) + Na(3P) \rightarrow Na_2^+ + e^- \quad (1)$$

and the energy-transfer collision process

$$Na(3P) + Na(3P) \rightarrow Na(nl) + Na(3S) . \quad (2)$$

There have been a number of experimental determinations of the rate constant for reaction (2), but there is a surprisingly large disagreement. As Table I reveals, the reported values differ by as much as a factor of 10^5. We present here the results of a new determination which avoids a number of important source of systematic errors in previous experiments, and which we believe is reliable to 30%.

We believe that two sources of systematic errors contributed to the discrepancies between the previous measurements. First is the problem of accurately determining the effective volume of the laser-vapor interaction region. Second is the problem of controlling and measuring the density of excited $Na(3P)$ atoms. We have largely overcome these problems with the use of a "capillary cell," a 7-cm long cylindrical cell of small (0.9 mm) radius connected to a sealed-off Na reservoir. The laser illuminates the entire volume of the cell through end windows of highly optical quality. The interaction volume is determined by the diameter of the cell and a carefully designed slit which accepts radiation only up to a distance of 150 μm from the entrance window. These procedures assure that the interaction volume is accurately determined and that it is insensitive to variation in the optical-absorption length due to changes in the atom density or to laser intensity. The density of $Na(3P)$ atom is determined by a novel calibration method which is discussed in detail below.

II. APPROACH

The experiment involves continuously exciting Na to the $3P$ state with a cw dye laser, and observing

TABLE I. Measured rate coefficients k_{nl} and derived collision cross section σ_{nl} for $nl = 5S$ and $4D$.

Level	T (°C)	k_{nl} ($cm^3 sec^{-1}$)[a]	σ_{nl} (cm^2)[a]	Reference
4D	397	1×10^{-12}	9.0×10^{-18} [b]	12
	227	4.5×10^{-15}	4.7×10^{-20} [b]	11
	307[d]		$\sim10^{-14}$ [c]	14
	~324	$2.46\times10^{-10}\pm35\%$	$2.3\times10^{-15}\pm35\%$	16
	210	$(3.0\pm0.9)\times10^{-10}$	$(3.2\pm1.1)\times10^{-15}$	this work
	277	2.2×10^{-11} [b]	2.3×10^{-16}	13 theoretical
5S	227	7.0×10^{-15}	7.3×10^{-20} [b]	11
	~324	$1.63\times10^{-10}\pm35\%$	$1.6\times10^{-15}\pm35\%$	16
	210	$(1.9\pm0.6)\times10^{-10}$	$(2.0\pm0.7)\times10^{-15}$	this work

[a]Experimental errors are shown whenever they are given by the authors.
[b]Calculated from the relation $k_{nl}=\sigma_{nl}\bar{v}$ with $\bar{v}=(8kT/\pi\mu)^{1/2}$.
[c]This value is derived from a measurement on the number of seed electrons produced via collisional ionization from the energy-pooling-populated $4D$ state.
[d]The experiment used a weakly collimated effusive sodium beam. The oven temperature $T=307$°C corresponds to an average relative velocity of the atoms in the beam of $\simeq4\times10^4$ cm/sec.

the fluorescence from atoms in the $3P$ state and also from the $4D$ and $5S$ states. From the ratio of these intensities the rate constants k_{nl} for reaction (2) are determined.

For our sodium densities the general evolution of the atomic system is governed by laser excitation, collisional transfer, and spontaneous emission. The rate equations are of the form

$$\dot{N}_{3P}=F-A(3P,3S)N_{3P}-\sum_{n'l'}k_{n'l'}N_{3P}^2+\sum_{n''l''}A(n''l'',3P)N_{n''l''}\,, \tag{3}$$

$$\dot{N}_{nl}=k_{nl}N_{3P}^2-\sum_{n'l'}A(nl,n'l')N_{nl}+\sum_{n''l''}A(n''l'',nl)N_{n''l''}\,, \tag{4}$$

where F is the number of atoms excited per second from the $3S$ to the $3P$ level and $A(nl,n'l')$ is the spontaneous transition probability for $|nl\rangle\rightarrow|n'l'\rangle$. In Eq. (3) we have neglected stimulated emission because of the low laser power available in our experiment. However, we will not need to use this equation explicitly.

The rate constant k_{nl} for process (2) can be derived by solving Eq. (4) for N_{nl} in the steady-state condition. The general result is

$$k_{nl}=\frac{1}{N_{3P}^2}\left[\sum_{n'l'}A(nl,n'l')N_{nl}-\sum A(n''l'',nl)N_{n''l''}\right], \tag{5}$$

where the sum extends in principle to all levels allowed by the dipole selection rules. In practice, however, the equation can be considerably simplified. The energy pooling collisions are "pure" inelastic processes whose cross section rapidly vanishes as the energy defect $\Delta E_{nl}=(2E_{3P}-E_{nl})$ increases beyond a few kT.

As shown in Fig. 1, the only levels which play important roles are $5S$, $4D$, and $4F$. Unfortunately, the $4F$-level fluorescence is at 1.8 μm and cannot be detected by our apparatus. However, evidence of the $4F$ populating process is given by the fluorescence intensity of the $3D\rightarrow3P$ transition;[2] that is surprisingly high with respect to the large energy defect of the $3D$ level ($\Delta E_{3D}\simeq12\,kT$). This peculiarity can be justified assuming a cascade transition from the $4F$ level.

Therefore we have restricted our analysis to the $5S$ and $4D$ states.

For these two levels we can neglect in Eq. (5) the second term representing the cascade radiation from the higher levels, without introducing appreciable error. Thus we can rewrite Eq. (5) as

$$k_{nl}=\frac{A(nl,3P)N_{nl}}{N_{3P}^2}\left[1+\sum_{n'l'\neq3P}\frac{A(nl,n'l')}{A(nl,3P)}\right], \tag{6}$$

where we emphasize the dominant term connecting the $|nl\rangle$ and the $|3P\rangle$ levels. The factor

$$\gamma_{nl}=\left[1+\sum\frac{A(nl,n'l')}{A(nl,3P)}\right] \tag{7}$$

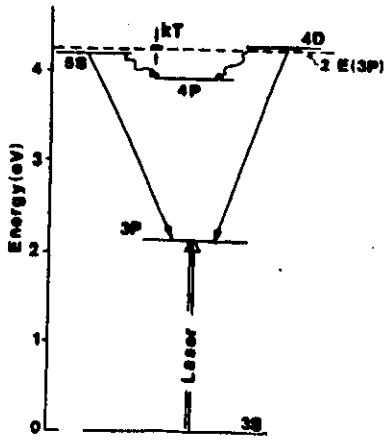

FIG. 1. Na energy-level diagram with the involved levels and transitions. The horizontal line represents the double of the $3P$-level energy.

is a number expressing the branching ratio of the analyzed transition.[3] In our case each sum is reduced to a single term with the result $\gamma_{4D}=1.51$ and $\gamma_{5S}=1.74$.

The measured quantities in our experiment are the intensities of the fluorescence lines. It is therefore convenient to use the relation between the transition probabilities and the line intensities (see, for example, Ref. 3) and to express k_{nl} as

$$k_{nl}=\alpha_{nl}\gamma_{nl}\frac{\omega_{3P\rightarrow3S}}{\omega_{nl\rightarrow3P}}\frac{I_{nl\rightarrow3P}}{I_{3P\rightarrow3S}}\frac{1}{N_{3P}\tau^*}\,, \tag{8}$$

where α_{nl} is a factor which takes into account the instrumental response of the detecting apparatus and the calibration, I is the intensity of the detected transition, and τ^* is the lifetime of the $3P$ level in the presence of the radiation trapping. Radiation trapping for the $4D$, $5S\rightarrow3P$ transitions at our densities is negligible. From Eq. (8) it is clear that in order to determine k_{nl}, great care must be used in measuring N_{3P} and τ^*.

To evaluate the N_{3P} density we make an absolute calibration of our apparatus by observing saturation fluorescence signals at fixed temperature but varying the intensity of the laser tuned to the $3S_{1/2}\rightarrow3P_{3/2}$ transition. To obtain the saturation of the fluorescence with the low-laser intensity available in our experiment, we need a relatively low atomic density. According to Cardinal and Measures,[4] at saturation the $P_{3/2}$ and the ground-state $S_{1/2}$ population densities are locked in the ratio of their degeneracies,[5] i.e.,

$$N_{3P_{3/2}}\simeq\frac{N_{at}}{1+(g_{3S_{1/2}}/g_{3P_{3/2}})}=\frac{1}{3}N_{at}\,.$$

The behavior of the fluorescence intensity $I_{3P\rightarrow3S}$ versus the laser intensity I_L is complicated by the fact that the fluorescence intensity for an inhomogeneously broadened line varies as

$$\frac{I_L/I_S}{(1+I_L/I_S)^{1/2}}=A(I_L)\,, \tag{9}$$

whereas for a homogeneously broadened line it varies as

$$\frac{I_L/I_S}{1+I_L/I_S}=B(I_L)\,, \tag{10}$$

where I_S is the saturation parameter.[6] We use a multimode dye laser to excite the atoms. The mode spacing (~290 MHz) is small compared to the Doppler width (~1 GHz) and when the laser intensity is so high that the power broadening is comparable to or larger than the mode spacing this assures that the line is homogeneously broadened and that the power dependence is described by Eq. (10). At low power, however, one expects the power dependence to be given by Eq. (9).

Because the experimental results are very sensitive to the assumed power dependence of the line, we have carried out numerical studies of the fluorescence intensity over a wide range of parameters. The results could in all cases be accurately described by a linear combination of Eqs. (9) and (10) in the form

$$I_{3P\rightarrow3S}=e^{-\zeta I_L}A(I_L)+(1-e^{-\zeta I_L})B(I_L)\,, \tag{11}$$

where ζ is an adjustable parameter and $A(I_L)$ and $B(I_L)$ are independently normalized. Consequently, we have used this form to analyze our experiment, fitting the fluorescence line intensity to Eq. (11).

The evaluation of τ^* will be described in Sec. IV.

III. APPARATUS

A sketch of the experimental apparatus is shown in Fig. 2. The $3P_{3/2}$ state is excited with a cw dye laser with a density power $\lesssim10\ W\,cm^{-2}$. The bandwidth could be varied between 0.3 and 0.03 Å by using different intracavity etalons. The laser beam illuminates the principal axis of a cylindrical capillary cell whose internal radius is 0.9 mm. This cell is made in our laboratory utilizing as windows slices of glass rods flattened on the internal side and welded with the capillary tube. After welding, the ends of the cell also are optically flattened. A sidearm of the cell contains the sodium. Before loading, the cell is cleaned and baked for many hours on a vacuum

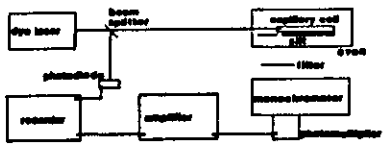

FIG. 2. Sketch of the experimental apparatus.

um system at a pressure of 10^{-7} torr. No buffer gas is used. Because the cell is sealed and the vapor is saturated the atomic density N_{at} can be accurately determined from the temperature using the Nesmeyanov tables.[7]

The cell is placed in an oven in which a small temperature gradient is created in order to prevent window contamination. The temperature of the sodium reservoir is controlled to 0.1°C and it is varied between 190°C and 210°C, corresponding to an atomic density $N_{at} \simeq (1-6)\times 10^{12}$ cm^{-3}. Close to the input window a narrow slit ($\simeq 150$ μm) is placed near to the cell to reduce the observation volume from which fluorescence is detected. The effective volume is 4×10^{-4} cm^3.

The laser beam is focused to the diameter of the cell window so as to illuminate the whole cross section of the cell uniformly. To measure directly the laser intensity a beam splitter directs a small fraction of the laser beam into a photocell. The fluorescence is analyzed at right angles by a 0.35-m monochromator and is detected by a photomultiplier with an S-20R cathode response.

To further minimize effects present in high vapor pressure, such as strong radiation trapping, collisional heating[1,4] of electrons produced by photoelectric effect in laser-wall interaction or by associative ionization, secondary collisional processes[1] etc., the experiment is performed at the lowest temperatures. Although this low atomic density decreases the intrinsic signal-to-noise ratio, this disadvantage is more than offset by the elimination of systematic errors which are the major problem in such experiments.

IV. EXPERIMENTAL PROCEDURE AND RESULTS

The experiment involves determining the rate constants k_{nl} using Eq. (8). The measured quantities are the principal fluorescence intensity $I_{3P\to 3S}$, the transfer fluorescence intensity $I_{nl\to 3P}$, and the excited-state density N_{3P}. The effective lifetime τ^* is also required. Because the problem of radiation self-trapping is so complex and potentially troublesome,[8] we avoid measuring τ^* directly. Instead we measure the product $k_{nl}\tau^*$ which is equal to

$$\alpha_{nl}\gamma_{nl}\frac{\omega_{3P\to 3S}}{\omega_{nl\to 3P}}\frac{I_{nl\to 3P}}{I_{3P\to 3S}}\frac{1}{N_{3P}} \tag{12}$$

and from it determine k_{nl}, as described below.

The excited-state density N_{3P} is determined by observing the fluorescence at low temperature, where the line can be completely saturated and Eq. (11) can be mapped over its full range of variation. Typical results are shown in Fig. 3. The observed fluorescence intensity in all cases agrees with Eq. (11) within the experimental errors, namely, 5% or less. This operation is carried out before each determination of the rate constants.

Once the excited-state density is known at low temperature, the temperature is increased to the point where the fluorescence from the collisionally excited states becomes visible. At each temperature the line intensities $I_{3P\to 3S}$ and $I_{5S\to 3P}$, $I_{4D\to 3P}$ are measured. To avoid operating the photomultiplier over a wide dynamic range, an optical attenuator is used to reduce the intense signal from the principal transition. The density at high temperature is found from the ratio of the accurately measured fluorescence intensity at high (T') and low (T^0) temperature,

$$N_{3P}(T')=N_{3P}(T^0)\frac{I(T')}{I(T^0)}\frac{\tau^*}{\tau_0}\,, \tag{13}$$

where τ^* is the trapped lifetime of the $3P$ level at high temperature and τ_0 the natural lifetime at low temperature, and where the contribution of the $P_{1/2}$ level to $I(T')$ is taken into account. This method avoids the need to measure absolutely the system response effeciency α_{nl} and requires only trivial corrections for such things as amplifier gain and possible nonlinearities.

We made a number of searches for fluorescence from higher-lying levels, but could not observe any

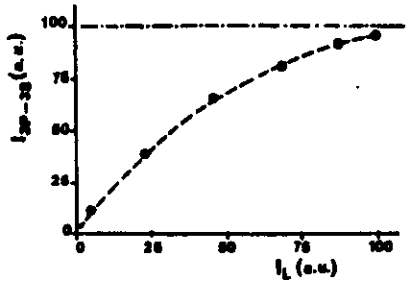

FIG. 3. Na $3P$-$3S$ fluorescence versus the laser intensity. The dashed curve represents the fit obtained by calculating the expression (11). The reported example was taken at $T=150$°C and $W_{Laser}\simeq 300$ mW. The errors are given by the size of the dots.

over our temperature range, validating the simplifying assumptions made in Eq. (8). At higher temperatures, however, contribution from high-lying states are easily observable.[2] Avoiding such contribution eliminates cascade transitions as a possible source of systematic errors.

Using these procedures the density N_{3P} was determined over a temperature range in which the atomic density varied by a factor ~ 6. Substitution of $N_{3P}(T')$ in expression (12) provides the products $k_{nl}\tau^{*2}/\tau_0$. Results for $k_{5S}\tau^{*2}/\tau_0$ are shown in Fig. 4. Over this small temperature range k_{5S} is expected to be constant because the relative energy of the colliding atoms remains constant to a few % as does the collisional frequency. Thus the temperature dependence is dominated by radiation trapping.

We have found that Milne's theory[8] of radiation trapping at low density is in good agreement with our data. We have solved the general equation of Milne for an optical depth $d=0.35$ mm and have found values of τ^* such that k_{5S} is essentially temperature independent. This is shown in Fig. 4, where τ^{*2}/τ_0 versus temperature is reported on the right-hand side. The value $d=0.35$ mm used in the calculation of the τ^* is consistent with the geometrical configuration of our experiment considering that the major escape factor for the photons is through the entrance window. The fact that Milne's theory has been confirmed in the early experiment of Kibble *et al.*,[9] and the recent one of Garver *et al.*,[10] gives us further confidence in its validity under our conditions. Moreover, in Milne's theory at low temperature, τ^* becomes the natural lifetime while high-temperature theories[8] often fail this simple test when applied to low-temperature data. Using this result we can extract the value for k_{nl} and results for k_{5S} are shown in Fig. 5. It is constant within experimental errors over the entire temperature range studied. The larger error at low temperature is due

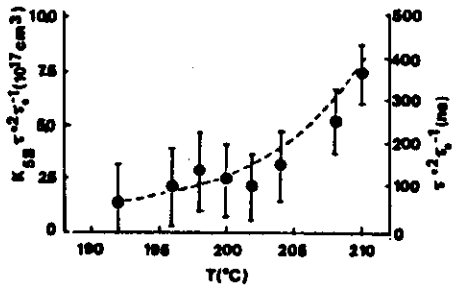

FIG. 4. Plot of $k_{5S}(\tau^{*2}/\tau_0)$ values versus T. The dashed curve represents τ^{*2}/τ_0 with τ^* calculated from Milne's theory for an optical depth $d=0.35$ mm.

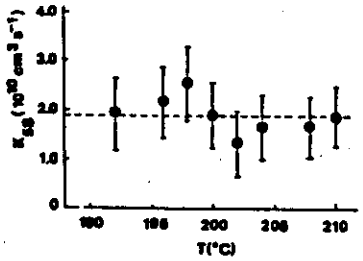

FIG. 5. Rate constant values versus T of the process (2) for the level $5S$.

to the low counting rate. Similar results for k_{4D} are obtained. We estimate our measurements to be reliable within 30%.

Our results are (in cm^3/sec)

$$k_{5S}=(1.9\pm 0.6)\times 10^{-10}\,,$$

$$k_{4D}=(3.0\pm 0.9)\times 10^{-10}\,.$$

The uncertainty, apart from statistical errors, is due to the determination of the ground-state density, to the self-trapping, to the calibration, and such things as laser fluctuations and system shift.

By applying the relation $k_{nl}=\sigma_{nl}\bar{v}_{rel}$ with $\bar{v}_{rel}$ the mean interatomic velocity

$$[\bar{v}_{rel}=(8kT/\pi\mu)^{1/2}]\,,$$

we obtain (in cm^2)

$$\sigma_{5S}=(2.0\pm 0.7)\times 10^{-15}\,,$$

$$\sigma_{4D}=(3.2\pm 1.1)\times 10^{-15}\,.$$

V. DISCUSSION

Our results and the results of previous works are displayed in Table I. Disagreement between many of the measurements are marked. We believe that we have avoided many sources of errors which affected earlier measurements. In their experiment Kushawaha and Leventhal[11] employed an open cell which can be a major source of error in determining the density. In such a case, the actual density can be much lower than calculated. The fact that molecular fluorescence could not be observed suggested that this may have been the case.

The experiment of Krebs and Schearer[12] operated at high temperature ($T\simeq 400$°C) and used a buffer gas at high pressure (~ 1 atm), plus a powerful pulsed laser; all these conditions enhance the processes we have tried to avoid.

Our measurements are in good agreement with the theoretical value of Kowalczyk,[13] particularly

since his value is intended as a lower limit, having neglected curve crossing for internuclear separations $\lesssim 15$ Å.

The experiment of Le Gouet *et al.*[14], which indirectly determines k_{nl}, confirms our values. This is particularly significant because it also supports other measurements[15] on the associative ionization process as in Eq. (1). The excellent agreement between our results and the recent measurements of Huennekens and Gallagher[16] lends added confidence.

ACKNOWLEDGMENTS

We are very grateful to Professor D. Kleppner for many helpful comments on the manuscript. Thanks are also due to Mr. M. Badalassi who prepared the "capillary" cells. One of us (M.A.) wishes to thank Professor A. Gallagher and Dr. J. Huennekens for many enlightening discussions.

[1]For a recent review, see T. B. Lucatorto and T. J. McIlrath, Appl. Opt. 19, 3948 (1980); A. Kopystyńska and L. Moi, Phys. Rep. (in press).

[2]M. Allegrini, G. Alzetta, A. Kopystyńska, L. Moi, and G. Orriols, Opt. Commun. 19, 96 (1976); 22, 329 (1977).

[3]W. L. Wiese, M. W. Smith, and B. M. Miles, Nat. Stand. Ref. Data Ser. Nat. Bur. Stand. 22, 4 (1969); E. M. Anderson and V. A. Zilitis, Opt. Spektrosk. XVI, 177 (1964) [Opt. Spectrosc. (USSR) XVI, 99 (1964)].

[4]R. M. Measures and P. G. Cardinal, Phys. Rev. A 23, 804 (1981).

[5]At these densities the transfer from the $3P_{3/2}$ to the $3P_{1/2}$ level is negligible.

[6]See, e.g., A. Yariv, *Quantum Electronics* (Wiley, New York, 1975).

[7]A. N. Nesmeyanov, *Vapor Pressure of the Chemical Elements* (Elsevier, Amsterdam, 1963). Recent measurements of the atomic density (Ref. 16), carried out around 320 °C, result in values larger than the 2—13 % of Nesmeyanov's.

[8]E. A. Milne, J. London Math. Soc. 1, 40 (1926); T. Holstein, Phys. Rev. 72, 1212 (1947); 83, 1159 (1951); C. van Trigt, *ibid.* 181, 97 (1969); Phys. Rev. A 1, 1298 (1970); 4, 1303 (1971); H. K. Holt, *ibid.* 13, 1442 (1976).

[9]B. P. Kibble, G. Copley, and L. Krause, Phys. Rev. 153, 9 (1967).

[10]W. P. Garver, M. R. Pierce, and J. J. Leventhal, J. Chem. Phys. 77, 1201 (1982).

[11]V. S. Kushawaha and J. J. Leventhal, Phys. Rev. A 25, 570 (1982); J. J. Leventhal, in *Photon Assisted Collisions and Related Topics*, edited by N. Rahman and C. Guidotti (Harwood Academic, Chur, 1982).

[12]D. J. Krebs and L. D. Schearer, J. Chem. Phys. 75, 3340 (1981).

[13]P. Kowalczyk, Chem. Phys. Lett. 68, 203 (1979).

[14]J. L. Le Gouët, J. L. Picqué, F. Wuilleumier, J. M. Bizeau, P. Dhez, P. Kock, and D. L. Ederer, Phys. Rev. Lett. 48, 600 (1982).

[15]V. S. Kushawaha and J. J. Leventhal, Phys. Rev. A 25, 346 (1982).

[16]J. Huennekens and A. Gallagher, in *VIII International Conference on Atomic Physics, Göteborg, 1982, Program and Abstracts*, edited by I. Lindgren, A. Rosen, and S. Svanberg (Wallin and Dalholm, Lund, 1982), and Phys. Rev. A 27, 771 (1983).

COLLISIONS AND HALF-COLLISIONS WITH LASERS

Edited by
N. K. Rahman and C. Guidotti
University of Pisa, Italy

harwood academic publishers
chur · london · paris · utrecht · new york

EXPERIMENTAL METHOD FOR MEASURING ELECTRONIC ENERGY TRANSFER CROSS SECTIONS IN LASER EXCITED ATOMIC VAPORS.

M.ALLEGRINI, P.BICCHI* and L. MOI
Istituto di Fisica Atomica e Molecolare del C.N.R. - Pisa, Italy
* Also at Istituto di Fisica dell'Università-Siena, Italy.

Abstract The electronic energy transfer in collisions between two laser excited atoms is now a widely studied process. Here we present a novel method for the determination of its cross section, which is based on a specially built cell and on an absolute calibration procedure. Experimentally such a method simply requires a broadband, low power, cw dye laser in resonance with an atomic transition. It can be applied to any atomic vapor which may be contained in the sealed cell and it is reliable to ∿30%. Its application to the process Na (3P)+ Na (3P) → Na(5S,4D)+Na(3S)is presented.

INTRODUCTION

The transfer of electronic energy in collisions between two atoms, i.e.

$$A(n\ell) + B(\text{ground}) \rightarrow A(\text{ground}) + B(n'\ell') \qquad (1)$$

is a well known process, widely studied in the past by using spectral lamps to excite the atoms[1]. Its cross section σ has been measured for many pairs

of atoms, especially for the alkali atoms. Solution of the rate equations of process (1) is straightforward and, in terms of the intensity of the fluorescence lines I, which is the quantity usually measured in the experiment, σ results

$$\sigma = \frac{\alpha}{\bar{v}} \quad \frac{1}{N_B \tau_A} \quad \frac{I_B}{I_A} \qquad (2)$$

where α is a factor which takes into account the response of the detection apparatus and the characteristics of the transitions (such as frequency factors and braching ratios), $\bar{v} = \sqrt{\frac{8\pi k}{\pi \mu}}$ is the mean velocity of the colliding partners, N_B the density of the B species and τ_A the radiative lifetime of the excited level of the A atoms. The accuracy on σ depends on the accuracy in measuring the density of the atomic species B and the lifetime of the excited state A(nℓ), which may be complicated in presence of radiation trapping.

Recently the laser, owing to the power and frequency selectivity available compared to a spectral lamp, has allowed the observation of many kinds of collisions involving more than one excited atom. In analogy to process (1), known as sensitized fluorescence, also the process[2]

$$A(n\ell)+A(n\ell) \rightarrow A(n'\ell')+A(\text{ground}) \qquad (3)$$

involving collisions between two atoms excited

to the same quantum level, has a cross section which depends on the population $N_{n\ell}$ and the lifetime $\tau_{n\ell}$ as

$$\sigma = \frac{\beta}{\bar{v}} \quad \frac{1}{N_{n\ell}\tau_{n\ell}} \quad \frac{I_{n'\ell'}}{I_{n\ell}} \qquad (4)$$

where the notations have the same meaning of those used in equation (2).

The volume in which the fluorescence appears does not enter specifically in equation (2) because it cancels out in the ratio of the intensities $\frac{I_B}{I_A}$, provided the single fluorescence lines I_A and I_B come out from the same volume and provided the volume remanins constant during the measurements. Also for process (3) the absolute measurement of the laser-vapor interaction volume may be avoided if the population density of the excited state $|n\ell\rangle$ is independently determined (see Equ.(4)). The absolute value of the volume from which $I_{n\ell}$ and $I_{n'\ell'}$ are observed is not important, however it must be well defined and remain constant during the measurements. Unfortunately this in not usually the case because in a vapor the optical absorption length varies considerably with changes in the atom density and/or in the laser intensity, resulting in a variation of the volume of the laser-vapor interaction. Moreover, because of the diffusion, the excited atoms are not confined to the focused

laser column and great care must be taken in the evaluation of the resulting volume of excitation[3].

In spite of these difficulties great effort has been paid to get reliable quantitative results of σ for process (3), at least in the alkali vapors[4-9]. In effect process (3) followed by the photoionization of the highly-excited species A(n'ℓ') has proven to be important for the production of the seed electrons in the experiments where total ionization of the vapor is achieved[10]. Lasing action has recently been observed from one of the A(n'ℓ') level[11], populated through process (3). The interest in collisions between excited atoms is more general since they are certainly involved in stellar processes and in chemical reactions induced by laser radiation. From a theoretical point of view the cross sections of process (3) give informations on the long-range interactions between atoms, in the intersting region where the atoms are not trapped to form the stable neutral dimers but cannot be considered isolated either.

Here we present a novel experimental procedure to measure σ with about 30% accuracy, which avoids most of the error sources responsible for the discrepancies between previous measurements.

EXPERIMENTAL METHOD

The construction of a special capillary cell, sketched in figure 1, has solved the main part the problem mentioned before.

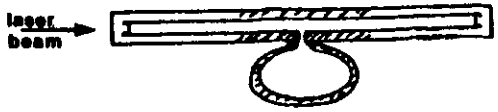

FIGURE 1. Capillary cell (actual dimensions).

The cell body is a pyrex capillary tube of internal radius 0.9 mm and the windows are slides of pyrex rods optically flattened on the internal side before welding to the capillary tube. After welding the ends of the cell are also flattened. The alkali metal is contained in a side arm of the cell and to prevent window contamination there is a small temperature gradient between the cell body and the side arm. The laser is focused to the diameter of the cell and illuminates the entire volume of the cell. To further define the volume from which fluorescence is detected a slit of 150 μm is placed near the input window. The resulting volume is 4×10^{-4} cm^3; however its absolute value is not crucial. The important point is that it is well defined, insensitive to variations in the optical absorption path and uniformly illuminated. Moreover, since the cell is sealed and the vapor

is saturated, the atomic density N_{at}, whose value is necessary to obtain $N_{n\ell}$ can be determined for each temperature from the Nesmeyanov tables[12], without any sophisticated measurement. The accuracy of the Nesmeyanov tables, tested in sodium at ∿100°C higher than the temperature typical of our experiment, has been proved to be ∿2-13%[4].

The density of the excited state $N_{n\ell}$ is determined by an original calibration method based on the saturation of the resonance fluorescence. At low temperature, when the atomic density is also low, it is possible to achieve saturation of the resonance fluorescence transition A(nℓ)→A(ground), as it is shown in figure 2, even if the excitation is made with a low power broadband dye laser.

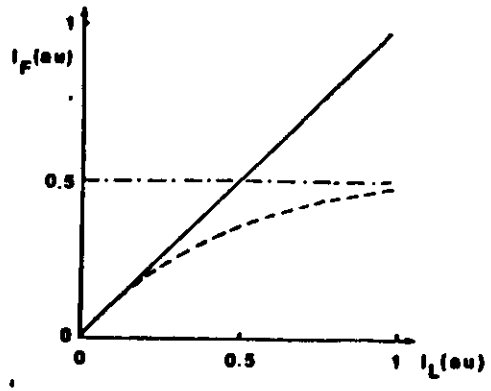

FIGURE 2. Resonance fluorescence signal versus the laser intensity, in absence of saturation (full line) and in presence of saturation (dashedline).

At saturation the ratio between $N_{n\ell}$ and N_{at} is known from the degeneracies of the ground and excited state and in first approximation $N_{n\ell} \simeq \frac{1}{2} N_{at}$ More details on this particular point, including the treatment of the line shape of the saturated fluorescence, are in ref.5. Once the detection apparatus is calibrated ,the resonance fluorescence signals at different atomic densities are compared and the density $N_{n\ell}$ is obtained from the expression

$$N_{n\ell}(T_1) = \frac{I(T_1)}{I(T_o)} \; N_{n\ell}(T_o) \; \frac{\tau^*}{\tau_o} \qquad (5)$$

where τ^* is the trapped lifetime of the state $|n\ell\rangle$ at T_1 and τ_o is the natural lifetime at T_o, when there is not radiation trapping. From equation(5) it is clear that the measurement of τ^* is of primary importance. Once again the system which has been studied in more detail involves the 3P-level of sodium. The experiment of ref. 3 has proved that the complicated mechanism of radiation trapping can be well understood and also controlled; however this is done at the expenses of the simplicity of the experimental set-up. In the application of our method to the process

$$Na(3P) + Na(3P) \rightarrow Na(5S,4D) + Na(3S) \qquad (6)$$

we have avoided the direct measurement of $\tau^*(3P)$

APPLICATION TO SODIUM

The atomic levels of interest in this experiment are sketched in figure 3.

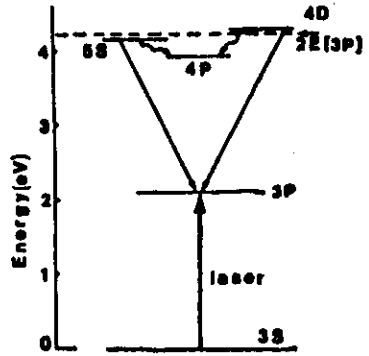

FIGURE 3. Sketch of the atomic sodium levels involved.

The rate constant $k_{n\ell}$ (with $n\ell$ = 5S or 4D) is related to the cross-section so far considered simply through the mean interatomic velocity $k_{n\ell} = \sigma_{n\ell}\bar{v}$. In the experiment we measure the density N_{3P} of the excited 3P-atoms, the intensity of the fluorescence transitions $I_{5S\to 3P}$, $I_{4D\to 3P}$ and $I_{3P\to 3S}$, corrected for the response of the apparatus. These quantities are related to the product $k_{n\ell}\frac{I}{\tau_o}\tau^{*2}$. To minimize effects present in high vapor pressure, which may obscure process (6), the experiment is performed in a range of relatively low densities. Although in this situation the intrinsic signal-to-noise ratio is reduced we take advantage of this

fact by minimizing the self trapping corrections and the contribution of other possible processes enhanched by the high vapour density. At these temperatures the colliding 3P-atoms have thermal energy so that their relative energy remains constant as does the collision frequency. As a consequence $k_{n\ell}$ has to remain constant and the temperature dépendence of $k_{n\ell}\frac{\tau}{\tau_b}\tau^{*2}$ is due only to τ^*. We have checked that in our experiment the Milne theory of radiation trapping[13] satisfies this condition (as shown in figure 4 for the 5S level) and provides the correct value for τ^*.

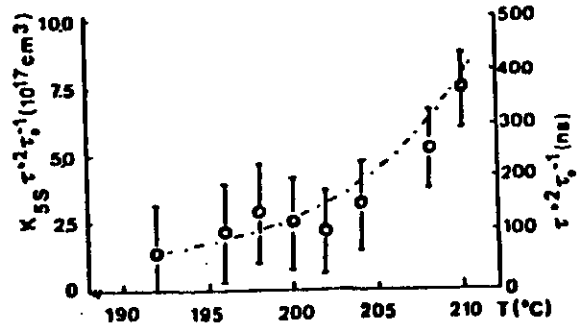

FIGURE 4. The dashed line gives the values of τ^{*2}/τ_o from the Milne theory. The dots represent the experimental values of $k_{5S}\tau^{*2}/\tau_o$.

As an example, the resulting values for k_{5S} is

plotted in figure 5.

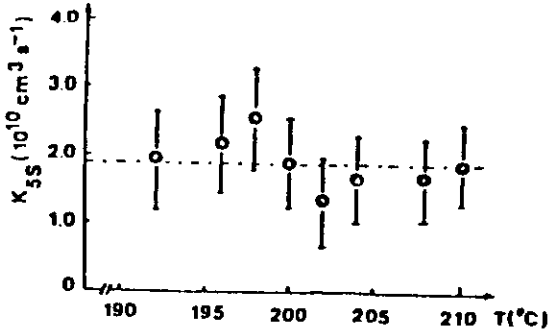

FIGURE 5. Experimental results of k_{5S} versus the temperature.

CONCLUSION

The previous disagreement between the experimental determinations of the rate constants for process (6), as shown in table 1, makes clear the need for reliable methods of measurement. The approach is obviously not unique. Huennekens and Gallagher[4], for example, have demonstrated that using a pulsed dye laser for the excitation and a single mode cw dye laser tuned to the wings of the resonance transition it is possible to measure both the spatial and temporal distribution of the excited atoms. Thus they can control the radiation diffusion and get N(3P) and τ^*(3P) in the changing volume. The special cell designed for our experiment instead, allows us to take constant the excitation volume and to minimize the radiation trapping problems. It is satisfying

that such different approaches give very close values (see table I) for the cross section of process (6).

Table I Rate coefficients k and cross sections σ for the 5S and 4D levels of sodium.

Level	T(°C)	k(cm^{3}sec^{-1})	σ(cm^2)	Ref.
5S	227	7.0 x10^{-15}	7.3x10^{-20}	8,(1982)
	∿324	1.63x10^{-10}	1.6x10^{-15}	4,(1983)
	210	1.9 x10^{-10}	2.0x10^{-15}	5,(1983)
4D	277	2.2x10^{-11}	2.3x10^{-16}	14,(1979)
	397	1 x10^{-12}	9.0x10^{-18}	7,(1981)
	227	4.5x10^{-15}	4.7x10^{-20}	8,(1982)
	307*		∿10^{-14}*	9,(1982)
	∿324	2.46x10^{-10}	2.3x10^{-15}	4,(1983)
	210	3.0 x10^{-10}	3.2x10^{-15}	5,(1983)

* This experiment used a sodium beam: T=307°C is the temperature of the oven and σ≈10-14cm^2 is an indirect measurement.

REFERENCES

1. For a review see M. Elbel "Energy and Polarization Transfer" in Progress in Atomic Spectroscopy, W.Hanle and H.Kleinhoppen Ed. (Plenum Press, 1978) Part.B pag.1299.

2. M.Allegrini, G. Alzetta, A. Kopystyńska, L.Moi and G.Orriols, Opt.Commun.19,96 (1976); 22, 329 (1977). For a review see : A. Kopystyńska and L.Moi; Phys.Rep.92, 135 (1982).

3. J.Huennekens and A.Gallagher, Phys.Rev.A ..., ... (1983) and references there in.

4. J.Huennekens and A.Gallagher, Phys. Rev. A ..., ... (1983)

5. M. Allegrini, P.Bicchi and L. Moi, Phys. Rev. A ..., ... (1983)

6. L.Barbier and M. Chèret in this book

7. D.J. Krebs and L.D. Schearer, J.Chem.Phys. 75, 3340 (1981)

8. V.S.Kushawaha and J.J. Leventhal, Phys.Rev.A 25, 570 (1982)

9. J.L. Le Gouet, J.L.Piqué, F.Wuilleumier, J.M.Bizeau, P.Dhez, P.Kock and D.L.Ederer, Phys. Rev. Lett. 48,600 (1982)

10. T.B.Lucatorto and T.J.Mc.Ilrath, Phys. Rev. Lett. 37, 428 (1976)

11. W. Müller and I.V.Hertel, Appl.Phys. 24,33 (1981);

12. A.N. Nesmeyanov "Vapor Pressure of the Chemical Elements" (Elsevier, Amsterdam 1963)

13. E.A.Milne, J.London Math. Soc.1, 40 (1926)

14. P. Kowalczyk, Chem. Phys. Lett. 68, 203 (1979).

Cross-section measurement and theoretical evaluation for the energy-transfer collision $Na(3P)+Na(3P)\rightarrow Na(4F)+Na(3S)$

M. Allegrini, C. Gabbanini, and L. Moi
Istituto di Fisica Atomica e Molecolare del Consiglio Nazionale delle Ricerche, Via del Giardino 7, I-56100 Pisa, Italy

R. Colle
Scuola Normale Superiore, Piazza dei Cavalieri 5, I-56100 Pisa, Italy

(Received 29 April 1985)

We have measured the cross section $\sigma(4F)$ for the collisional process $Na(3P)+Na(3P)\rightarrow Na(4F)+Na(3S)$. The experiment is based on the measurement of the intensities for $4F$, $4D$, and $3P$ fluorescence emissions in sodium vapor excited with a cw dye laser. $\sigma(4F)$ is determined relative to $\sigma(4D)$, which has been measured in an absolute way in previous experiments. Influence on $\sigma(4F)$ and $\sigma(4D)$ of the energy-transfer process $Na(4F)+Na(3S)\rightleftarrows Na(4D)+Na(3S)$ is also discussed. A theoretical evaluation of $\sigma(4F)$ and $\sigma(4D)$ relative to a chosen molecular channel is given and compared with the experimental determinations.

I. INTRODUCTION

Recently, there has been much interest in energy-transfer collisions (known also as energy-pooling collisions[1,2]) between two laser-excited $3P$ sodium atoms,

$$Na(3P)+Na(3P)\rightarrow Na(nL)+Na(3S)\ , \tag{1}$$

where nL indicates atomic levels lying higher than $3P$. Three of such nL states, namely $5S$, $4D$, and $4F$, are separated from the sum energy of two $3P$ atoms by a few kT (see Fig. 1). For the $5S$ and $4D$ levels there have been a number of experimental determinations of the cross section (updated results have been collected, for example, in Ref. 3). Here we report the first measurement of $\sigma(4F)$, the cross section for the population transfer to the $4F$ state, i.e., for the process

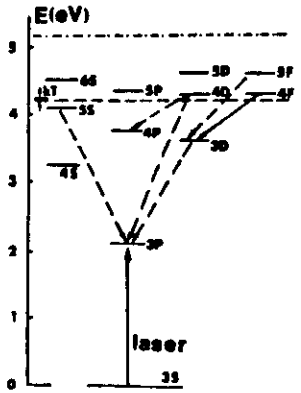

FIG. 1. Simplified energy-level diagram of atomic sodium. The dashed lines indicate the transitions of interest in this experiment and the horizontal line indicates the energy of two $3P$ atoms.

$$Na(3P)+Na(3P)\rightarrow Na(4F)+Na(3S)\ . \tag{2}$$

$\sigma(4F)$ was not measured previously because the $4F$-level fluorescence is in the near infrared, at 1.84 μm, outside the sensitivity of the apparatuses used for the determination of $\sigma(5S)$ and $\sigma(4D)$. The $4F$ state radiatively decays only to the $3D$ level and $\sigma(4F)$ could in principle be indirectly determined from the $3D$-level fluorescence intensity. However, since the $3D$ level is populated also through cascades from levels other than the $4F$, we prefer to modify the apparatus and perform a direct experiment. In this experiment we have also established the contribution of the collisional transfer process

$$Na(4D)+Na(3S)\underset{K}{\overset{K'}{\rightleftarrows}}Na(4F)+Na(3S)\ , \tag{3}$$

where K and K' are the rate coefficients of the reaction in the two directions. Process (3) is expected to be strong since the $4D$ and $4F$ levels lie very close in energy ($\Delta E=38\ cm^{-1}\approx 0.1kT$). However, our experiment has proved that the influence of process (3) on the energy-pooling cross sections $\sigma(4D)$ and $\sigma(4F)$ is only of the order of a few percent. This means that the values of $\sigma(4D)$ (Refs. 4 and 5) obtained in experiments which neglected process (3) remain correct.

To measure $\sigma(4F)$ we first tried the same approach and geometry as in our previous experiment[3] for the absolute determination of $\sigma(5S)$ and $\sigma(4D)$ involving excitation of sodium vapor from the ground state to the $3P$ state by means of a cw dye laser and measurement of the intensity ratio of $4F$-$3D$ to $3P$-$3S$ fluorescence. Unfortunately, the efficiency of the infrared detection apparatus is low compared to that of the visible apparatus and, as a consequence, the signal from the $4F$ level is weak compared to the fluorescence in the visible region of the spectrum from the $4D$ and $5S$ levels. We could easily increase the intensity of the $4F$-$3D$ fluorescence by increasing the laser power density and/or the atom density either by increasing the temperature of the cell or by adding a buffer gas

TABLE I. Fluorescence lines observed.

Transition	λ (μm)	Relative intensity[a] $T=260$°C (cell: no buffer gas)	$T=320$°C (cell: with buffer gas)
$4D$-$4P$	2.33	1.3	1.5
$4F$-$3D$	1.84	1	1
$4P$-$4S$	2.20	2.3	1.7
$4S$-$3P$	1.14	2.9	5.4
$5F$-$3D$	1.26		0.15
$6S$-$4P$	1.63		0.3
$7S$-$4P$	1.28		0.1

[a] The intensities are corrected for the apparatus response and they are normalized to the $4F$-$3D$ emission for each temperature.

(as will be shown later). However, one of our goals was to keep the laser power and the atom density at low values in order to avoid multiphoton and secondary collisional processes. So we took advantage of the fact that the $4D$ level has a fluorescence line, corresponding to the $4D$-$4P$ transition, in the near infrared (see Table I), in the same spectral region as the $4F$-$3D$ transition. By comparing the intensity of the $4D$-$4P$ line with the $4F$-$3D$ line we were able to measure $\sigma(4F)$ relative to the absolute value of $\sigma(4D)$ with an accuracy comparable to that of our previous experiment. In the same way we also determined an upper bound for $\sigma(5F)$.

From an experimental point of view the problems which led to large discrepancies in measured cross sections (see Table I of Ref. 3) have been overcome, while little work has been done from a theoretical point of view. The cross section of process (1) has been calculated only for the $4D$ state[6] by a procedure which does not use good-quality variational wave functions for the excited states and takes into account only the region of large interatomic distances. Here we report the first calculation for $\sigma(4F)$ and with the same approach we also find a value for $\sigma(4D)$ which is in better agreement with the experimental results. The method used and its results and limits will be described in detail in Sec. IV.

II. RATE EQUATIONS

The evolution of the population of the $4D$ and $4F$ levels, in the atomic system irradiated by the cw laser resonant with the $3S$-$3P$ transition, is affected by the energy-pooling collision process (1) and by the exchange process (3). In the conditions of our experiment, where the terms due to Penning ionization, electron collision ionization, and ionic recombination can be neglected, the rate equations have the form

$$\begin{aligned}\dot N(4F)&=-A(4F,3D)N(4F)+N^2(3P)K(4F)\\&\quad+KNN(4D)-K'NN(4F)\ ,\\ \dot N(4D)&=-\sum_{nL}A(4D,nL)N(4D)+K(4D)N^2(3P)\end{aligned} \tag{4}$$

where N is the atom density, $N(nL)$ is the population of the nL level, $A(nL,nL')$ is the spontaneous transition probability for $nL\rightarrow n'L'$, and $K(4F)$ and $K(4D)$ are the rate coefficients for the energy-pooling collisions. Since the collisions are thermal, $K(nL)=v\sigma(nL)$, where $v=\sqrt{8kT/\pi\mu}$ is the mean interatomic velocity. The rate coefficients K and K' for process (3) are connected by the detailed balance principle involving the level degeneracies as follows:[7]

$$K/K'=[g(4F)/g(4D)]\exp(-\Delta E/kT)\ .$$

At the temperature of our experiment $K/K'\simeq 1.26$. Solution of Eqs. (4) and (5) in the steady-state conditions yields the following relation for the population of the $4D$ and $4F$ levels:

$$\frac{N(4F)}{N(4D)}=\frac{[A(4D,3P)+A(4D,4P)+KN]K(4F)+KNK(4D)}{[A(4F,3D)+K'N]K(4D)+K'NK(4F)}\ . \tag{6}$$

by fitting the data to this expression both $K(4F)$ and K can be obtained.

Fluorescence from the $5F$ level has also been observed, under experimental conditions which will be described later. However, energy pooling is not the predominant process that populates the $5F$ level, which has an energy defect of 3150 cm^{-1}. Therefore, in the rate equations describing the population evolution of the $5F$ level, in addition to the radiative decay and

$$Na(3P)+Na(3P)\rightarrow Na(5F)+Na(3S)\ , \tag{7}$$

we must consider the following processes: electron-ion recombination, described by $K(R)$; radiative decay to the $5F$ state from upper levels; electron-impact ionization, described by $K(e)$; photoionization from the $5F$ level; Penning ionization, described by $K(3P,5F)$; associative ionization, described by $K(3S,5F)$; and electron-impact excitation of $5F$ from lower nL states, described by $K(e,nL)$. Taking all of these terms into account, the rate

$$\dot{N}(5F) = -\sum_{nL} A(5F,nL)N(5F) + K(5F)N^2(3P) + K(R,5F)N^2(e) + \sum_{nL} K(e,nL)N(e)N(nL)$$
$$+ \sum_{n'L'} A(n'L',5F)N(n'L') - K(e,5F)N(e)N(5F) - B_l N(5F) I_L$$
$$- K(3P,5F)N(3P)N(5F) + K(3S,5F)N(3S)N(5F) . \quad (8)$$

In the photon ionization term $B_l I_L N(5F)$, I_L is the laser power density and $B_l = \sigma(PI)/h\nu_L$, with $\sigma(PI)$ the photoionization cross section and ν_L the laser frequency. The steady-state solution of Eq. (8) is

$$N(5F) = \frac{K(5F)N^2(3P) + K(R,5F)N^2(e) + \sum_{n'L'} A(n'L',5F)N(n',L') + \sum_{nL} K(e,nL)N(e)N(nL)}{\sum_{nL} A(5F,nL) + K(e,5F)N(e) + K(3P,5F)N(3P) + K(3S,5F)N(3S) + B_l I_L} \quad (9)$$

which suggests the possibility of obtaining $K(5F)$ by a procedure analogous to that used for the $4F$ level. However, it has been difficult to evaluate the influence on $K(5F)$ of the other terms and we have obtained only an upper limit to $K(5F)$ via the ratio $N(5F)/N(4F)$.

III. APPARATUS AND RESULTS

A sketch of the apparatus is shown in Fig. 2. An actively stabilized single-mode cw dye laser ($\Delta\nu \simeq 1$ MHz) excites sodium atoms to the $3P_{3/2}$ level with ~ 10 W/cm^2. The laser beam illuminates the sodium cell placed in a temperature-controlled oven; the temperature is varied between 235°C and 310°C. Since the cell is sealed and the vapor is saturated, the corresponding atomic density is conveniently determined from the Nesmeyanov tables[8] to be 10^{13}–10^{14} cm^{-3}. Two ordinary Pyrex cylindrical cells, prepared with standard vacuum techniques, have been used; one contains only sodium and the second contains sodium plus 10 Torr of He as buffer gas. The fluorescence is analyzed at right angles by a 0.35-m monochromator equipped with a 300-grooves/mm grating for the near infrared. The detector is a photoconductive PbS device sensitive to radiation in the (1–3)-μm region and cooled to dry-ice temperature for a better response. To improve the signal-to-noise ratio the laser beam is modulated at low frequency (481 Hz) by a mechanical chopper, and phase-sensitive detection is used. Typical fluorescence spectra recorded with this configuration are reported in Figs. 3(a) and 3(b).

As expected, the $4F$-$3D$ fluorescence intensity increases

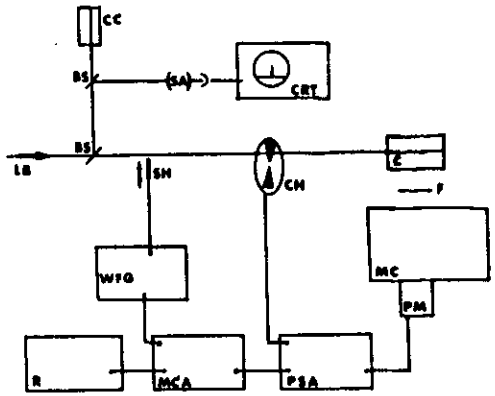

FIG. 2. Sketch of the experimental setup. LB, laser beam; BS, beam splitter; CC, control cell; SA, spectrum analyzer; CRT, cathode-ray tube; SH, shutter; CH, chopper; C, collision cell; F, filter; MC, monochromator; PM, photomultiplier; WFG, wave-function generator; R, recorder; MCA, multichannel analyzer; PSD, phase-sensitive detector (lock-in amplifier).

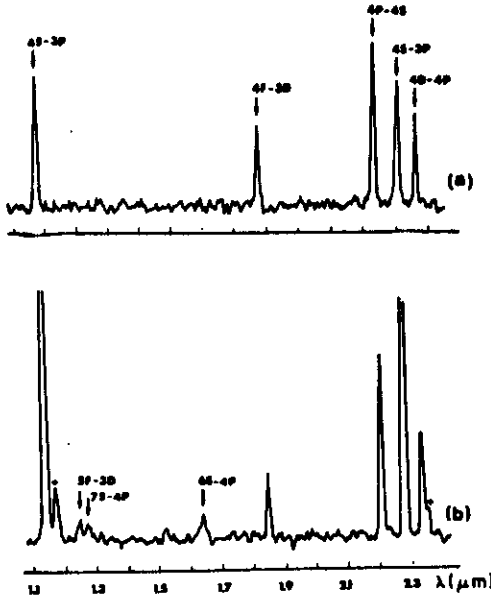

FIG. 3. Na fluorescence spectrum, uncorrected for the apparatus response. The laser power is ~100 mW; spectrum (a) is from a cell containing pure sodium at $T = 260$°C while spectrum (b) is from a cell containing sodium at $T = 260$°C plus 10 Torr of helium as buffer gas. The lines indicated with a + are due to potassium impurities in the cell.

dramatically with increasing temperature. However, this increase arises from contributions of processes other than energy pooling, processes which become important only at higher densities. In order to get a better signal-to-noise ratio at low temperatures, a further improvement of the apparatus was necessary. A second laser-beam chopper at a very low frequency (0.4 Hz) was used; a function generator drives this chopper and triggers a multichannel analyzer used for signal averaging. The statistical error is then reduced by the factor $1/\sqrt{N}$ where N is the number of averaging cycles of 5 sec duration each on the maximum of the fluorescence line. The signal is later on displayed on the analyzer and chart recorder.

The determination of $\sigma(4F)$ is obtained by observing the fluorescences $4F$-$3D$ at 1.84 μm and $4D$-$4P$ at 2.33 μm. It is sufficient to measure just the relative intensities because we only need the ratio $I(4F\text{-}3D)/I(4D\text{-}4P)$. In our experiment, laser intensity and fluorescence volume are the same for both $4F$ and $4D$ levels and radiation trapping is negligible for these high levels. In Fig. 4 the ratio of the two fluorescences of interest is plotted for a fixed temperature versus the laser power: It is clear that the variations are within 7%, which justifies our assumption. A first set of measurements was made with the cell containing pure sodium. The $4F$-$3D$ and $4D$-$4P$ fluorescences were recorded over $N = 2^6$ averaging cycles on the multichannel analyzer so that the statistical error was decreased by the factor $1/2^3$. By using the relation between the transition probabilities and the line intensities (see, for example, Ref. 9) the $N(4F)/N(4D)$ ratio of Eq. (6) can be written in terms of the fluorescence line intensities. Data have been fitted to this expression and the resulting best-fit parameters are

$$K(4F) = (5.6 \pm 2.2) \times 10^{-11} \text{ cm}^3 \text{sec}^{-1}$$

and

$$K \simeq (9.8 \pm 4.9) \times 10^{-9} \text{ cm}^3 \text{sec}^{-1} .$$

The best-fit curve for $Na(4F)/Na(4D)$ and the experimental values are reported versus temperature in Fig. 5.

The uncertainty in $K(4F)$ is slightly bigger than that in the absolute measurement of $K(5S)$ and $K(4D)$. The 50% indeterminacy of K shows that this experiment is not suitable for measuring the rate coefficient for the energy-transfer $4D$-$4F$ in sodium. If in the rate equations

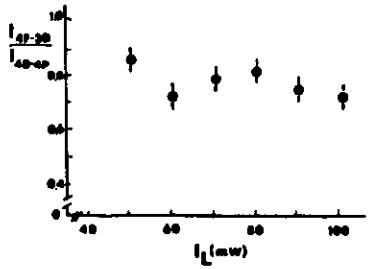

FIG. 4. Intensity ratio of the $4F$-$3D$ and $4D$-$4P$ fluorescences at $T = 260$°C vs laser power.

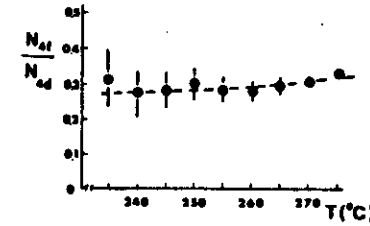

FIG. 5. Population ratio of the $4F$ and $4D$ levels. Dots represent the data and the dashed line the best-fit curve to Eq. (6).

(4) and (5) the term describing this transfer process is neglected and the data are fitted with the same procedure to the new expression for $N(4F)/N(4D)$, the result is

$$K(4F) = (6.0 \pm 2.4) \times 10^{-11} \text{ cm}^3 \text{sec}^{-1} .$$

Thus by neglecting the exchange $4D$-$4F$ process (3) the relative error introduced in the energy-pooling cross section $\sigma(4F)$ is only of order 5%, at least at the temperatures of our experiment. Since $\sigma(4D)$ is about one order of magnitude bigger than $\sigma(4F)$ the influence of the $4D$-$4F$ collisions (which were indeed neglected in both the experiments of Refs. 4 and 5) is even less important for the determination of $\sigma(4D)$.

As shown in Fig. 3(b) the emission spectrum recorded with a cell containing sodium plus a buffer gas also contains fluorescence lines originating from the $5F$, $6S$, and $7S$ levels. (For comparison, all observed lines are listed in Table I.) The presence of lines from such high states clearly shows that the buffer gas favors, in addition to energy pooling, other collisional processes. Earlier experiments in which visible fluorescence spectra resulting from laser irradiation of sodium vapor were obtained also showed that atomic levels lying higher than the $3P + 3P$ energy were produced.[10] The precise sequence of reac-

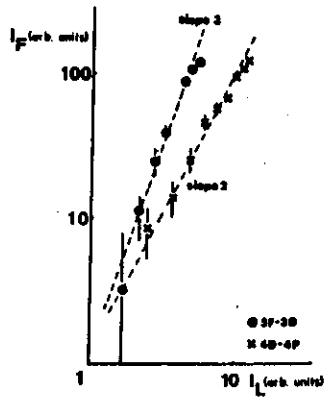

FIG. 6. Log plot of the fluorescence intensity for transitions from the $5F$ and $4D$ levels vs laser intensity.

tions that leads to the production of these states is quite complicated, involving superelastic electron collisions, secondary collisions of the atoms excited by primary energy pooling, and ionization mechanisms with subsequent electron-ion recombination. In this work we will concentrate only on the population mechanism of the $5F$ level. The dependence upon the laser power of the $5F$-$3D$ fluorescence intensity, compared to the $4F$-$3D$ line (see Fig. 6), gives direct evidence that the $5F$ and $4F$ levels are populated through different mechanisms. From our experiment it is not possible to determine the contribution to the population of the $5F$ level of each process taken into account in the rate equation (8). However, since in the full range of temperatures of our experiments emission from the $5F$ level has not been observed in the cell without buffer gas, we are able to place an upper limit on the cross section $\sigma(5F)$ of process (7). Measurement of the intensity of the $5F$-$3D$ line leads for this limit to $K(5F) < 10^{-13}$ cm sec^{-1}.

IV. THEORETICAL APPROACH

In this section a theoretical evaluation of the cross sections for the energy-transfer collisions (1) with $nL = 4D$ and $4F$ is given. To our knowledge this is the first calculation for $\sigma(4F)$, and the result is in good agreement with the measured value reported in Sec. III. For $\sigma(4D)$ we find a value that agrees better than other theoretical calculations[6] with the results of reliable experiments.[4,5]

The population of the highly excited atomic levels, due to energy-transfer collisions, can be looked at as resulting from transitions among different electronic molecular states connected to various dissociation limits and coupled by the total Hamiltonian. In our experiment the total averaged cross section is measured for a given set of initial and final atomic states; no other information is available about the collision process itself. Therefore, for a quantitative comparison between the theoretical predictions and the experimental results one should in principle include all the possible electronic states that dissociate into the product of the collisional process and solve the complete set of coupled equations for each possible value of the relative velocity and of the total angular momentum. The resulting values of σ should be averaged with statistical weights which depend on the distribution of the atomic fragments among the initial states.

In our specific case the classification of the electronic molecular states according to the projection Λ of the electronic angular momentum along the internuclear axis gives this set of initial states, connected to the $(3P+3P)$ dissociation limit,

$$({}^1\Sigma_g^+(2), {}^3\Sigma_g^-, {}^1\Pi_g, {}^3\Pi_g, {}^1\Delta_g)\,,$$
$$({}^3\Sigma_u^+(2), {}^1\Sigma_u^-, {}^3\Pi_u, {}^1\Pi_u, {}^3\Delta_u)\,, \tag{10}$$

and this set of final states, connected to the $(3S+4D)$ and $(3S+4F)$ dissociation limits,

$$({}^1\Sigma_{g/u}^+, {}^3\Sigma_{g/u}^+, {}^1\Pi_{g/u}, {}^3\Pi_{g/u}, {}^1\Delta_{g/u}, {}^3\Delta_{g/u})\,, \tag{11}$$

plus $({}^1\Phi_{g/u}, {}^3\Phi_{g/u})$ for the $(3S+4F)$ limit. Almost every pair of states having the same g/u and $+/-$ symmetry is coupled by some terms in the Hamiltonian: the derivatives of the radial internuclear distance for states with the same Λ and S, the Coriolis terms for states having the same S but $\Delta\Lambda = \pm 1$, the spin-orbit operator for states with different values of S, etc. Thus a complete *a priori* treatment of this problem is quite impractical considering also that the molecular states involved in this problem are highly excited electronic states. However, for obtaining an order of magnitude of the measured cross section and taking into account that we are dealing with slow (thermal) collisions, we have selected among all the states given in (10) one energetically favorable entry channel, that represented by the ${}^1\Sigma_g^+$ molecular states, and we have calculated the contributions to the measured cross section due to the transitions from these states to the other ${}^1\Sigma_g^+$ states that go to the $(3S+nL)$ dissociation limits. Because of the slow-velocity regime and since large interatomic distances ($R > 20$ a.u.) are important in the collisions between our excited atoms, it seems reasonable to disregard the centrifugal coupling with the Π states. Also, neglect of the spin-orbit coupling does not represent a crucial approximation in the case of sodium atoms. For these reasons we believe that significant comparisons can be made between the cross sections for the transition processes $(3P+3P) \rightarrow (3S+4D,\ 3S+4F)$ calculated using the subset of the ${}^1\Sigma_g^+$ electronic states and the experimental results valid at least as to order of magnitude.

In the following we describe briefly the method used to construct the electronic wave functions and to calculate the potential-energy curves as well as the coupling matrix elements between these wave functions. Finally, we describe the semiclassical procedure for evaluating the cross section for the $3P+3P$ collisions which populate the $4D$ and $4F$ levels, and we compare our results with the measured values.

A. Wave functions and electronic terms

We start from the solution of the electronic problem for the two separated atomic fragments. For each of them we construct a set of Hartree-Fock orbitals separately optimized for the various states, starting from the ground up to the $(4d)$ and $(4f)$ excited ones. Note that from now on we will identify each atomic state by using the quantum numbers n and l (lower case) of its valence electron in the independent particle description. The Hartree-Fock orbitals are used for constructing valence-bond wave functions, having ${}^1\Sigma_g^+$ symmetry and corresponding to the various dissociation limits of the Na_2 molecule: $(3s,nl)$ with $n = 3$, 4, and 5; $l = 0$, 1, 2, and 3; and $(3p,3p)$. Writing each electronic wave function as an antisymmetrized product of group functions, we give to each molecular state the representation

$$\psi(1',2',\ldots,N',1'',2'',\ldots,N'';1,2) = \hat{M}\hat{A}[\Phi_{CA}(1',2',\ldots,N') \times \Phi_{CB}(1'',2'',\ldots,N'')\Phi_\gamma(1,2)]\,, \tag{12}$$

where Φ_{CA} is the group function for the singlet ground state of the core electrons of the atom A having the following structure in terms of the atomic core orbital centered on A:

$$\Phi_{CA} = |\,1s_A\overline{1s}_A 2s_A\overline{2s}_A 2p_{zA}\overline{2p}_{zA}2p_{yA}\overline{2p}_{yA}2p_{xA}\overline{2p}_{xA}\,|\,. \tag{13}$$

Analogously, Φ_{CB} in (12) describes the core electrons of the atom B while Φ_γ is the group function for the valence electrons in the ${}^1\Sigma_g^+$ state with the following valence-bond structure [corresponding to the $(nl)(n'l')$ dissociation limit]:

$$\Phi_\gamma(1,2) = \tfrac{1}{2}M_\gamma(1+\hat{i})(1+\hat{\mathcal{P}})\phi_{nl_A}(1)\phi_{n'l'_B}(2)\frac{\alpha\beta-\beta\alpha}{\sqrt{2}}\,, \tag{14}$$

where α and β are the usual spin functions.

We notice that in (12) $\hat{A}$ is the total antiaymmetrizer and in (14) M_γ is a normalization constant, while $\hat{i}$ and $\hat{\mathcal{P}}$ are, respectively, the inversion and the permutation operators acting on the spatial electronic coordinates. We construct a set of such ${}^1\Sigma_g^+$ electronic molecular functions, starting from the lowest dissociation limit $(3s+3s)$ up to the $(3s+4f)$ one. At infinite internuclear distance these wave functions $\{\psi\}$ are automatically orthogonal, as are the orbitals used for their construction. Going to finite internuclear distances and keeping the same structure (14) for each valence group function, we allow free overlap between the two valence orbitals of each Φ_γ, while orthogonalizing them to the core orbitals and the core orbitals among themselves for each ψ. In such a way and without introducing any other configuration we can take into account the contributions due to the so-called ionic structures, which are essential for a complete description of the state, and we can also disregard the corrections due to the basis superposition errors.[11]

Following such a procedure we obtain at each internuclear distance a set of electronic wave functions that are weakly dependent on the internuclear distance because of their structure and whose orbitals maintain a well-defined atomic character. Such functions are coupled in practice only by the electronic Hamiltonian and can cross each other at finite internuclear distance: They therefore represent our diabatic reference states. Note that these wave functions are in general mutually nonorthogonal, but they can be easily orthogonalized without changing their main characteristics using the Löwdin procedure:[12]

$$\{\psi'\} = \{\psi\}\Delta^{-1/2}\,, \tag{15}$$

where Δ is the overlap matrix among $\{\psi\}$. The behavior of the potential-energy curves, obtained from $\{\psi'\}$, is shown in Fig. 7 for the states of interest.

This diabatic representation has a physical meaning at sufficiently large internuclear distances, where the Hund (d) coupling case is appropriate, while at smaller internuclear distances ($R < 20$ a.u.) the interatomic potential strongly mixes the atomic symmetries and an adiabatic representation becomes more physically significant. This change of representation can be readily achieved by diagonalizing the matrix representative of the electronic Hamiltonian in the diabatic

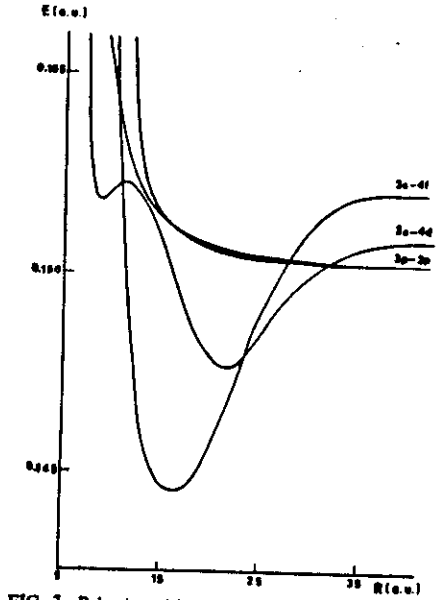

FIG. 7. Behavior with the internuclear distance R, given in atomic units (a.u.), of the four diabatic ${}^1\Sigma_g^+$ terms going to the $(3p+3p)$ and $(3s+4d),(3s+4f)$ dissociation limits. The energies are given in a.u. with respect to the $(3s+3s)$ dissociation limit.

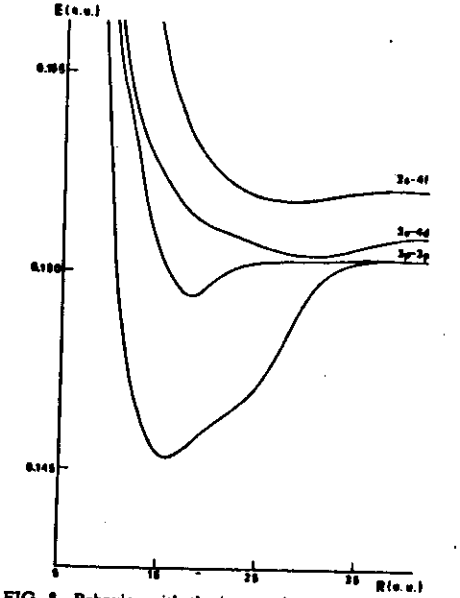

FIG. 8. Behavior with the internuclear distance R, given in atomic units (a.u.), of the four adiabatic ${}^1\Sigma_g^+$ terms going to the $(3p+3p)$ and $(3s+4d),(3s+4f)$ dissociation limits. The energies are given in a.u. with respect to the $(3s+3s)$ dissociation

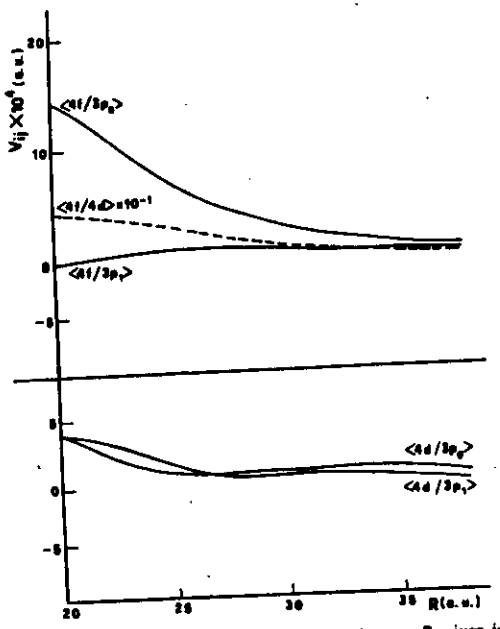

FIG. 9. Behavior with the internuclear distance R, given in atomic units (a.u.), of the coupling terms V_{ij}, given in a.u., between the various diabatic states of interest. The two $^1\Sigma_g^+$ states going to the $(3p+3p)$ dissociation limit are classified as $3P_0$ (the one higher in energy) and $3P_1$ (the lower one).

this matrix represent the adiabatic terms whose behavior as a function of the internuclear distance is shown in Fig. 8 for the states of interest. The eigenvectors give the expansion coefficients of the adiabatic many-determinant wave functions that are the solutions of the electronic problem for the various molecular states. These adiabatic wave functions are coupled by the radial derivatives of the internuclear distance whose matrix elements become relevant and change rapidly at the crossing points between the diabatic states.

In the following cross-section calculations we have utilized the adiabatic surfaces for treating the nuclear dynamic and the diabatic terms and wave functions to locate the transition points between the various surfaces and for evaluating the transition probabilities at internuclear distances $R \geq 20$ a.u. The behaviors of the coupling matrix elements between the diabatic states of interest are shown in Fig. 9.

Finally, we observe that from our variational calculations we get many-determinant wave functions for the valence electrons moving in an effective potential due to core electrons, which are described by the same Hartree-Fock single-determinant wave function for each state. The differences between the calculated and the experimental values of the energy defects between the various dissociation products are essentially due to the fact that we disregard the core-valence correlation energy and polarization effects which, however, should not influence to any large extent the coupling matrix elements between the various wave functions.

B. Cross sections

The calculation of the cross sections for the energy-transfer collisions (1) with $nl=4d$ and $4f$ has been carried out in a semiclassical way as a four-state problem involving the two $^1\Sigma_g^+$ adiabatic states that go to the $(3p+3p)$ dissociation limit and the two adiabatic states going to the $(3s+4d)$ and $(3s+4f)$ limits.

Following an approach suggested in Refs. 13 and 14 we have treated the four-state interaction as a sequence of two-state interactions by assuming that each transition between adiabatic curves is localized at their complex intersection point, with a local probability independent of all the other curves. Such an approach disregards second-order effects due to the interference with the other states, but the results are usually in excellent agreement with accurate quantum calculations.[14] The method used for the cross-section calculations is sketched in what follows.

The total cross section for an inelastic process connecting the (λ) and (μ) states depends on the square modulus of the (μ,λ) element of the S matrix, which can be written as

$$S_{\mu\lambda}=\sum_a P_a e^{i\varphi_a} . \tag{16}$$

In (16) the sum runs over all the classical trajectories starting on the curve (λ) and ending on curve (μ), while P_a is the product of all the probability factors for making or not a transition at each branch point of that trajectory and φ_a is the real phase accumulated along that trajectory. Looking at the scattering process as a series of local transitions between pairs of states, we can write the scattering matrix as a product of propagators along the adiabatic curves and propagators for each branch point of the trajectory. The matrix representation of the propagator along the internuclear coordinate from R_1 to R_2 in a region devoid of the intersection points is given by a diagonal matrix, whose jth element corresponding to the adiabatic curve $W_j(R)$ is

$$F_j^{\mp}(R_1,R_2)=\exp\left[\mp i\int_{R_1}^{R_2}k_j(R)dR\right] , \tag{17}$$

where $K_j(R)=[2m[E-W_j(R)]]^{1/2}$ and the upper (lower) sign corresponds to the incoming (outgoing) part of the trajectory. On the other hand, the matrix representation of the local propagator around the complex intersection point, for example, of W_1 and W_2, is given by

$$G_{1,2}^{\mp}=\begin{vmatrix} (1-p)^{1/2} & \mp p^{1/2}e^{\mp i\chi} & 0 & 0 \\ \pm p^{1/2}e^{\pm i\chi} & (1-p)^{1/2} & 0 & 0 \\ 0 & 0 & 1 & 0 \\ 0 & 0 & 0 & 1 \end{vmatrix} , \tag{18}$$

where p gives the transition probability from the adiabatic curve W_1 to the adiabatic curve W_2 and χ is a phase whose magnitude depends on the coupling strength between the two states.

Since in our problem the intersection points between the diabatic curves are well separated both reciprocally and with respect to the classical turning points, and furthermore, the diabatic curves are sufficiently linear and their coupling terms quite constant near the crossing points, we have used the Landau-Zener approximation for evaluating the transition probability p and the phase factor in (18). Thus we get

$$p=\exp\left[\frac{-2\pi|V_{12}(R_x)|^2}{v_0\left|\frac{d}{dR}[V_1(R)-V_2(R)]\right|_{R=R_x}}\right] , \tag{19}$$

$$\chi=\tfrac{1}{4}\pi , \tag{20}$$

where $V_1(R)$ and $V_2(R)$ are the diabatic terms which cross each other at $R=R_x$ and are coupled by $V_{12}(R)$, while $v_0=(1/2m)(K_1+K_2)|_{R=R_x}$ is the local velocity of the nuclear motion at R_x. In our calculations we have used the adiabatic curves shown in Fig. 8, implemented by the introduction of the centrifugal potential, and the intersection points between each pair of diabatic curves V_i and V_j have been derived from Fig. 7 and the coupling terms V_{ij} from Fig. 9. Finally, every element $S_{\mu\lambda}$ of the scattering matrix has been calculated as the product of the appropriate propagators for the ingoing and outgoing parts of the trajectory, with the proper boundary conditions imposed for the vanishing of the wave functions at each classical turning point.

The total cross section for the transition process $(\lambda\rightarrow\mu)$ has been calculated by integration of $|S_{\mu\lambda}|^2$ over the impact parameter and the result has been averaged over a Maxwellian distribution $f(v,T)$ of the relative velocity v of the atoms at various given temperatures T, according to the expression

$$\sigma_{\mu\leftarrow\lambda}(T)=2\pi\int_{v_{\min}}^{\infty}f(v,T)dv\int_0^{b_{\max}}|S_{\mu\lambda}(b,v)|^2 b\,db . \tag{21}$$

In (21), $v_{\min}$ represents the minimum relative velocity for covering the energy defect between the final and initial states and $b_{\max}$ the largest impact parameter for which the incoming particle can surmount the effective potential at the crossing point. Note that the presence of the centrifugal barrier is taken into account by a proper definition of $b_{\max}$,[15] which reduces the range of the integration over the impact parameter when the maximum of the centrifugal barrier lies outside the crossing points between the surfaces, thus practically eliminating problems arising from coalescence of the paths.

In Table II we report the results of our calculations of $\sigma(3p\rightarrow4d)$ and $\sigma(3p\rightarrow4f)$ for the two entry channels as the average of these values for each transition process, $T=500$ K, which is a value intermediate between the experimental ones. As can be seen from Table II, the order of magnitude of the calculated cross sections coincide with the experimental values for both $\sigma(4D)$ and $\sigma(4F)$ and, furthermore, the value of $\sigma(4F)$ lies within the range of the experimental error. Note that this calculation, unlike previous ones,[6] exploits the entire adiabatic energy surfaces for evaluating the cross sections, taking into account the interference effects between the various wave functions which have been derived variationally. More accurate predictions of the experimental results can be obtained by considering other electronic states both as entrance channels for the collision and in the expansion of the total wave function and by evaluating completely the correlation and polarization contributions for the various electronic terms.

V. CONCLUSIONS

A simple modification of the apparatus used for measurements of the energy-transfer cross sections in collisions between two $3P$ sodium atoms has allowed the direct observation of the population transfer to the $4F$ and $5F$ levels. Working in an atom density range where other processes should be negligible we have established that energy-pooling collisions are indeed the dominant mechanism which populates the $4F$ level and we have measured the relative cross section. A theoretical model based on the construction of the molecular potential curves connected to the atomic fragments involved in the collision has been developed. The cross section calculated considering the contribution only from the $^1\Sigma_g^+$ molecular state is in good agreement with the measured result.

With the same theoretical approach the cross section

TABLE II. Comparison between our experimental and theoretical determinations of the $4D$ and $4F$ energy-pooling cross sections. The states $(^1\Sigma_g^+)_1$ and $(^1\Sigma_g^+)_2$ refer, respectively, to the energetically lower and higher entry channels, and $\langle\sigma\rangle$ is the mean value of their contributions to the total cross section which must be compared with the experimental result.

	$\sigma(4D)$ (cm^2)	$\sigma(4F)$ (cm^2)	T (K)
Expt.	$(3.2\pm1.1)\times10^{-15}$		483
		$(5.7\pm2.3)\times10^{-16}$	523
Calc.: $\langle\sigma\rangle$	1.0×10^{-15}	6.8×10^{-16}	500
$(^1\Sigma_g^+)_1$	9.4×10^{-16}	3.5×10^{-16}	500
$(^1\Sigma_g^+)_2$	1.1×10^{-15}	1.0×10^{-15}	500

for the $4D$ state has also been evaluated. This result is slightly outside our measurement reported in a previous work.[5] We do not have a clear explanation for this fact; however, we note that the experiment was performed at $T=487$ K while the calculation was carried out at $T=500$ K. $\sigma(4D)$ apparently decreases with temperature and indeed the experimental value of Huennekens and Gallagher[4] obtained at $T=597$ K is closer to the theoretical evaluation.

ACKNOWLEDGMENTS

This work was supported by the Consiglio Nazionale delle Ricerche under U.S.—Italy Cooperative Program Grant No. 47923. The authors would like to thank Professor J. J. Leventhal and Professor T. Woodruff for a critical reading of the manuscript, Mr. M. Badalassi for the preparation of the glass cells, and Mr. F. Papucci for technical assistance.

[1]G. H. Bearman and J. J. Leventhal, Phys. Rev. Lett. **41**, 1227 (1978).

[2]K. S. Kushawaha and J. J. Leventhal, Phys. Rev. A **22**, 2468 (1980).

[3]M. Allegrini, C. Gabbanini, and L. Moi, J. Phys. (Paris) Colloq. **46**, C1-61 (1985).

[4]J. Huennekens and A. Galagher, Phys. Rev. A **27**, 771 (1983).

[5]M. Allegrini, P. Bicchi, and L. Moi, Phys. Rev. A **28**, 1338 (1983).

[6]P. Kowalczyk, Chem. Phys. Lett. **68**, 203 (1979); **74**, 80 (1980); J. Phys. B **17**, 817 (1984).

[7]See, for example, J. B. Hasted, *Physics of Atomic Collisions* (Butterworths, London, 1982).

[8]A. N. Nesmeyanov, *Vapor Pressure of the Chemical Elements* (Elsevier, Amsterdam, 1963).

[9]W. L. Wiese, M. W. Smith, and B. M. Miles, *Atomic Transition Probabilities*, Natl. Bur. Stand. Ref. Data Ser., Natl. Bur. Stand. (U.S.) Circ. No. 22 (U.S. GPO, Washington, D.C., 1969), p. 4.

[10]M. Allegrini, G. Alzetta, K. Kopystyńska, L. Moi, and G. Orriols, Opt. Commun. **19**, 96 (1976); **22**, 329 (1977).

[11]P. Cremaschi, G. Morosi, M. Raimondi, and M. Simonetta, Mol. Phys. **34**, 1483 (1979).

[12]P.-O. Löwdin, J. Chem. Phys. **18**, 365 (1950).

[13]J. Laing and T. F. George, Phys. Rev. A **16**, 1082 (1977).

[14]W. H. Miller and T. F. George, J. Chem. Phys. **56**, 5637 (1972).

[15]A. M. Chang and D. E. Pritchard, J. Chem. Phys. **70**, 4524 (1979).